

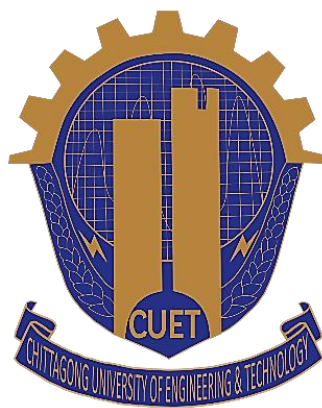
**Computational Modeling of Crack Detection for a Beam using
the Finite Element Method**

By

Rajib Karmaker

**A thesis submitted in partial fulfillment of the requirement for the
degree of**

MASTER OF PHILOSOPHY IN MATHEMATICS



Department of Mathematics

CHITTAGONG UNIVERSITY OF ENGINEERING AND TECHNOLOGY

2021

CERTIFICATION

The thesis titled “**Computational Modeling of Crack Detection for a Beam using the Finite Element Method**” submitted by Rajib Karmaker, Roll No.: 16MMATH001P, Session: 2016-2017 has been accepted as satisfactory in partial fulfillment of the requirement for the degree of Master of Philosophy in Mathematics on January 25, 2021.

BOARD OF EXAMINERS

- | | | |
|----|--|-------------------|
| 1. | Supervisor
Dr. Ujjwal Kumar Deb
Professor, Department of Mathematics
Chittagong University of Engineering & Technology | Chairman |
| 2. | Head
Dr. Ujjwal Kumar Deb
Professor, Department of Mathematics
Chittagong University of Engineering & Technology | Member |
| 3. | Dr. Ashutose Saha
Professor, Department of Mathematics
Chittagong University of Engineering & Technology | Member |
| 4. | Dr. Md. Aman Ullah
Professor, Department of Mathematics
University of Chittagong | Member (External) |

CANDIDATE'S DECLARATION

It is hereby declared that this thesis or any part of it has not been submitted elsewhere for the award of any degree or diploma.

Signature of the Candidate

.....
(Rajib Karmaker)

**Dedicated
To
My Parents**

CONTENTS

	Page
Candidate's Declaration	i
Dedication	ii
List of Tables and Figures	vii-ix
Nomenclature	x
Acknowledgement	xi
Abstract	xii
 CHAPTER I	 1-7
INTRODUCTION	
1.1 General Overview	1
1.1.1 Manual Inspection/ Destructive Testing	2
1.1.2 Automated Inspection/ Non-Destructive Testing	3
1.2 Scope of studies	4
1.3 Objectives	5
1.4 Organization of the Thesis	6
References	7
 CHAPTER II	 8-59
LITERATURE REVIEW	
2.1 General Overview	8
2.2 Crack	9
2.3 Causes of Cracking in Concrete Structures	10
2.4 Effects of Cracks	11
2.5 Physical parameters affecting dynamic characteristics of cracked structures	11
2.6 Modes of Fracture	12
2.6.1 Mode-I	12

2.6.2 Mode-II	12
2.6.3 Mode-III	12
2.7 Classification of Cracks	13
2.7.1 Macro Defects	13
2.7.2 Micro Defects	13
2.8 Special types of Cracks in Concrete	14
2.9 Different types of Cracks in Hypothetical Concrete Structure	15
2.9.1 Plastic Shrinkage Concrete Cracks	17
2.9.2 Expansion Concrete Cracks	17
2.9.3 Heaving Concrete Cracks	17
2.9.4 Settling Concrete Cracks	18
2.9.5 Concrete cracks caused by Overloading the Slab	18
2.10 Crack Detection Method by Non-Destructive Testing:	18
2.10.1 Ultrasonic Method	19
2.10.2 Acoustic Emission Method	19
2.10.3 Vibration Inspection Methods	20
2.11 Importance of Detecting Crack	21
2.12 Some Important Definitions	22
2.12.1 Stress and Strain	22
2.12.1.1 Tensile Stress	22
2.12.1.2 Compressive Stress	22
2.12.2 Young's modulus	23
2.12.3 The Poisson's ratio	24
2.12.4 Tensor	24
2.12.5 Rate of Deformation	25
2.12.6 Torsion	26
2.12.7 Deflection of Beams	27
2.12.8 Shear Forces (SF) and Bending Moment (BM)	28
2.13 Castigliano's Theorem	29
2.13.1 Castigliano's Theorem for Beam Deflection	29
2.14 Euler-Bernoulli Beam theory	29
2.14.1 Euler- Bernoulli Assumptions	30

2.14.2 The Euler- Bernoulli Beam Equation	31
2.15 Timoshenko Beam Theory	31
2.16 Numerical Methods for Computation	34
2.16.1 Finite Difference Method	34
2.16.2 Finite Volume Method	34
2.16.3 Boundary Element Method	35
2.16.4 Finite Element Method	35
2.16.4.1 Types of analysis done by Finite Element Method	36
2.16.4.2 History of Finite Element Method	36
2.16.4.3 Role of Finite Element Method	37
2.17 Computational Modelling	38
2.17.1 Modelling	38
2.17.2 Simulation	38
2.17.3 Steps of Computational Modelling by Finite Element Method	39
2.18 Method for Simulation using COMSOL Multiphysics	40
2.19 Previous Studies	41
References	49

CHAPTER III 60-82

COMPUTATIONAL MODELING OF A CRACKED BEAM WITH DIFFERENT LOCATION

3.1 Introduction	60
3.2 Stiffness Matrix	61
3.3 Beam Stiffness	61
3.4 Beam Stiffness Matrix Based on Euler-Bernoulli Beam theory	63
3.5 Mathematical Model	66
3.6 Finite Element Approximation	68
3.6.1 String beam theory	73
3.6.2 Elemental Stiffness matrix for Uncracked Beam	74
3.6.3 Elemental Mass matrix for Uncracked beam	75

3.6.4	Stiffness Matrix for a Cracked Beam Element	76
3.6.5	Flexibility matrix C_{intact} of the intact beam element	79
3.6.6	Total flexibility matrix C_{tot} of the cracked beam element	79
3.7	Conclusion	80
	References	82

CHAPTER IV **83-105**

NUMERICAL SIMULATION, RESULTS AND DISCUSSION

4.1	Introduction	83
4.2	Mathematical Modelling	84
4.2.1	Equation of free vibration	87
4.2.2	Boundary Conditions	87
4.3	Computational Domain and Mesh Design	87
4.4	Simulation Results	89
4.5	Numerical results and Discussions	91
4.6	Validation of the study	102
4.7	Conclusion	103
	References	105

CHAPTER V **106-108**

CONCLUSIONS 106

SUGGESTIONS FOR FUTURE WORKS 109

OUTPUT FROM THIS RESEARCH WORK 110

APPENDIX 111-119

List of Tables and Figures

List of Tables

Table 2.1: Location of different cracks in hypothetical concrete structure	15
Table 3.1: System Topology of elements	69
Table 4.1: Mesh Properties of the computational domain	90
Table 4.2: Properties of the simulation of computational domain	90
Table 4.3: Properties of Domain	91
Table 4.4: Properties of Materials	91
Table 4.5: Comparison among Priyadarshini ,Kisa and Present Analysis	102

List of Figures

Figure 1.1: Manual Inspection Methods	3
Figure 1.2: Non-Destructive Testing Methods	4
Figure 2.1: Sample images with cracks	9
Figure 2.2: Sample images without cracks	9
Figure 2.3: Modes of Fracture	12
Figure 2.4: Types of Cracks	14
Figure 2.5: Different types of cracks inside the wall	14
Figure 2.6: Examples of Intrinsic cracks in hypothetical concrete structure	16
Figure 2.7: Most Common types of Concrete Cracks	16
Figure 2.8: Types of Non-Destructive Testing	18
Figure 2.9: Ultrasonic Method	19
Figure 2.10: Acoustic Emission Method	20
Figure 2.11: Torsion of a square section bar	26
Figure 2.12: Deflection of Beams	27
Figure 2.13: Shear Forces (SF) and Bending Moment (BM) for various types of loads	28
Figure 2.14: The Plane Sections Remain Plane Assumption	30
Figure 2.15: Deformation of a Timoshenko beam (blue) compared with that	32

of an Euler-Bernoulli beam (red).

Figure 2.16: Steps of Computational Modelling	39
Figure 3.1: Beam theory sign conventions for shear forces and bending Moments	62
Figure 3.2: Beam element with positive nodal displacement, rotations, forces and moments	62
Figure 3.3: Beam under distributed load	63
Figure 3.4: Deflected curve of beam	65
Figure 3.5: Beam element with positive nodal displacement, rotations, forces and moments	68
Figure 3.6: Two noded beam with 3 elements with two degree of freedom	68
Figure 3.7: Beam segment (a) before deformation and (b) after deformation; (c) Angle of rotation of cross section ABCD	72
Figure 3.8: Load and diffusion of beam by applying Beam Theory and Stiffness Method	73
Figure 3.9: Typical Cracked beam element subject to shearing force and bending moment.	76
Figure 4.1(a): The geometry of the cracked computational domain	88
Figure 4.1(b): The geometry of the uncracked computational domain	88
Figure 4.2: Mesh design of The Computational Domain	89
Figure 4.3: Applying load on the crown edge of the computational domain	92
Figure 4.4: Deflection of the computational domain after applying load	92
Figure 4.5: Load absorbs and Frequency gained in the respective crack position	93
Figure 4.6: Load distributions and Line graph of the computational domain where the position of first crack is at 0.01m and second crack is at 0.06 m	95
Figure 4.7: Load distributions and Line graph of the computational domain where the position of first crack is at 0.02m and second crack is at 0.07 m	96
Figure 4.8: Load distributions and Line graph of the computational domain where the position of first crack is at 0.03m and second crack is at 0.08 m	97
Figure 4.9: Load distributions and Line graph of the computational domain where the position of first crack is at 0.04m and second crack is at 0.09 m	98
Figure 4.10: Load distributions and Line graph of the computational domain where the position of first crack is at 0.05m and second crack is at 0.10m	99
Figure 4.11: Load distributions and Line graph of the computational domain where the position of first crack is at 0.06m and second crack is at 0.11m	100
Figure 4.12: Line curve of Frequency vs Load	101

Figure 4.13: A Comparison of the frequencies in different positions of the crack of present analysis with Priyadarshini A and Kisa et al. experiments.	102
Figure i: Geometry of Computational domain	111
Figure ii: - Internal Geometry of Computational Domain	111
Figure iii: Internal Geometry of Computational Domain	112
Figure iv: Inlet layer of Computational Domain	112
Figure v: Selection of crown edge of Computational Domain	113
Figure vi: Selction of elastic layer in Computational Domain	113
Figure vii: Meshing	114
Figure viii: Selection of Eigen frequency	114
Figure ix: Selection of Eigan frequency modal	115
Figure x: Time selection of simulation	115
Figure xi: Line graph of the relative position of crack v/s Frequency	116
Figure xii: Contour Graph	116
Figure xiii: Load on Horizontal Crack	117
Figure xiv: Load on Vertical Crack	117
Figure xv: Deformation of Domain after applying transverse load	118
Figure xvi: Deflection of beam with load absorbtion	118
Figure xvii: Cross section of the load distributions at different position of the domain	119
Figure xviii: Slices of the load distributions at different position of crack	119

Nomenclature

σ	Stress
ε	Strain
ν	Poisson's ratio
ε_{trans}	Transverse strain
ε_{axial}	Axial strain
T	Torsion
τ	Maximum shear stress at outer surface
J_T	Torsion constant
Φ	Angle of twist in radians
G	Modulus of rigidity
W_i	Work done by internal force
U	Strain energy
δ	Deflection
θ	Rotation at the point of application
E	Young's modulus
I	Moment of inertia
κ	Timoshenko Shear coefficient
\mathbf{K}	Bending stiffness matrix
v_i	Transverse nodal displacements
\mathbf{M}	Consistent mass matrix
\mathbf{K}_g	Geometric stiffness matrix
\mathbf{q}	Displacement vector
\mathbf{P}	External force vector
\mathbf{P}_s	Static portion of force vector
P_t	Amplitude of the dynamic portion of P
Ω	Frequency of excitation
N_i	Shape function for a beam
A	Cross-sectional area of beam element
C_{ovl}	Overall additional flexibility matrix
C_{tot}	Total flexibility matrix
$F_i(s)$	Correction factors for stress intensity factors

Acknowledgement

First of all, I would like to express my gratitude to God, the Almighty and the most beneficent, for enabling me to complete this thesis work.

I would like to acknowledge with heartiest gratitude and deep sense of respect to my supervisor **Dr. Ujjwal Kumar Deb**, Professor and Head, Department of Mathematics, Chittagong University of Engineering and Technology (CUET) for his kind support, motivating discussion and constant help that I have received through the research work and introduced me such an interesting field of research.

I wish to express my cordial thanks to all of my teachers of the Department of Mathematics, CUET for their valuable suggestion and excellent support during this work.

I acknowledge and express my gratitude through my respected supervisor to the Centre of Excellence in Mathematics, Mahidol University, Bangkok, Thailand and also to the Simulation Lab, Department of Mathematics, CUET for the technical supports to complete this research.

I am grateful to the authority of Chittagong University of Engineering and Technology (CUET) for all kind of supports during this period.

Last, but not the least I would like to thank my closest family, my colleagues, relatives, friends and well wishers for their constant support and encouragement.

Abstract

Nowadays the presence of crack in different engineering structures becomes a serious threat to performance. Since most of the civil and mechanical structures may be damaged due to material fatigue, mechanical vibration, environmental attack and long-term service. Cracks in structural bodies lead to local changes in their stiffness, flexibility and consequently their static and dynamic behavior is affected. Moreover, dynamical systems of a beam usually possess non-linear characteristics, which causes practical difficulties on the model-based damage detection techniques. So it becomes essential to study the dynamic response characteristics in order to avoid any catastrophic failures and to follow structural integrity and performance. In the present study, a numerical simulation using the Finite Element Method (FEM) is carried out on a simply supported concrete beam of length 0.12m and width 0.015m with two open transverse cracks, to analyze the response characteristics for which the parameters considered are crack depth and its location. Its natural frequency and mode shapes are determined by applying suitable boundary conditions. A vibration-based model is employed to simulate the results by using COMSOL Multiphysics. By performing the computational analysis it is observed that, after applying load the frequencies of the cracked beam changes with the variation of the location of the crack for the all modes of vibration. It also found that frequencies are proportional to the increase in load and maximum frequency (around 2304.3 Hz) reserved at the cracked stage. Finally, it also revealed that the effects of crack are closer to the fixed end than at the free end, and by following this approach, very small sizes of crack (near 0.05 mm) can be identified in any structural beam.

CHAPTER I

INTRODUCTION

CHAPTER I

INTRODUCTION

1.1 General Overview

Structural Health Monitoring (SHM) refers to the process of implementing a damage detection and characterization strategy for engineering structures such as bridges and buildings. Here the damage is defined as changes to the material and/or geometric properties of a structural system, including changes to the boundary conditions and system connectivity, which adversely affect the system's performance. SHM provides a useful tool for ensuring integrity and safety, detecting the evolution of damage, and estimating performance deterioration of civil infrastructures. After extreme events, such as earthquakes or blast loading, it is used for rapid condition screening and aims to provide, in near real time, reliable information regarding the integrity of the structure [1]. The most important aspect of structural health monitoring is that the technique provides information on the life expectancy of structures, simultaneously detects and locates structural damage. This needs an idea of the model of structures in great detail, which is always not possible.

Damage detection and location, and condition assessment of engineering structures like concrete surface, beams have always been important subjects [2]. Cracks, deflection, mode shape is like damages in the structural body that lead to local changes in their stiffness, flexibility and consequently their static and dynamic behavior is affected. The influence of cracks on dynamic characteristics like natural frequencies, modes of vibration of structures has been the subject of many investigations. Cracks present a serious threat to the performance of structures since most of the structural failures are due to material fatigue.

The presence of a crack in structure changes its dynamic characteristics. The change is characterized by changes in modal parameters like modal frequencies, modal value and mode shapes associated with each modal frequency. It also alters the structural parameters like mass, damping matrix, stiffness matrix and flexibility matrix of the structure. The vibration technique utilizes one or more of these parameters for crack detection [3, 4]. The frequency reduction in a cracked beam is not due to the removal of mass from a beam, indeed the reduction in mass would increase natural frequency. The effect is due to the removal of material that carries significant stresses when defect is a narrow crack [5]. The results of local stiffness and natural frequency of structure gradually decrease [4, 6]. Due to presence of a crack there is local influence which results from reduction and second moment of area of cross-section where it is located. For this reason, in the last two decades methods of early detection and localization of cracks have been the subject of intensive investigation. As a result, a variety of analytical, numerical and experimental investigations now exist.

The crack detection can be done using two ways:

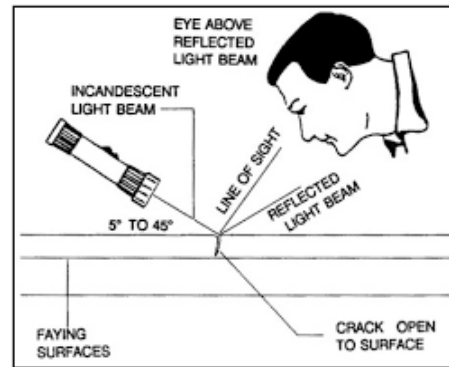
- Manual Inspection/ Destructive Testing
- Automated Inspection/ Non-Destructive Testing

1.1.1 Manual Inspection/ Destructive Testing

In conventional methods, manual inspection was done by set of skilled inspectors with the help of surveying instruments and visual examination to detect the irregularities and defects in the structure. However, this method has certain drawbacks, as it is impossible for a crew to detect the cracks in inaccessible areas such as large dams, monuments, buildings, etc. and also the estimation of size, length and width of the crack.



Crack on concrete structure



Visual inspection of crack

Figure 1.1: Manual Inspection Methods

1.1.2 Automated Inspection/ Non-Destructive Testing

Non-Destructive Testing (NDT) is mainly concerned with the evaluation of flaws in materials which are in the form of cracks and which might lead to loss of strength in a concrete structure. Structural health monitoring by NDT like rebound hammer and Ultrasonic Pulse Velocity (UPV) test becomes very useful for the prediction of the service life of structure [7].

There are different methods in Non-Destructive test. But most popular and common methods are mentioned in below:

- Ultrasonic Pulse Velocity Test
- Rebound Hammer Test
- Cover Meter Test



Figure 1.2: Non-Destructive Testing Methods

The main advantages of Non-Destructive Testing are listed below:

- The probe test produces variable results and offers the fastest means of verifying concrete maturity and consistency.
- Schmidt hammer test provides a simple, quick and inexpensive method of obtaining the indication of the strength of concrete with an accuracy of 15 to 20%.
- Pull-out assessments provide details about growth and maturity.
- UPV method is the most ideal tool for determining whether concrete is uniform or not.
- Radioactive equipment testing is very simple, and the running cost is less, although the initial price might be very high.

1.2 Scope of Studies

This research offers a new technique of crack detection to detect cracks based on load and frequency. Recent research demonstrates the mathematical model of crack detection using various non-destructive concrete structure approaches, column beams, reinforced concrete beams, etc. These models clarify physical behavior, but we need more clarification to the research element to element properties. The flow of load on different geometries of the computational domain and different types of linear or non-linear cracks can be studied using the model. For this, one should

concentrate on vibration based method to detect the damage in a specific computational domain. For this we need a suitable mathematical model of crack detection based on numerical technique, which will significantly reduce the cost of computing crack detection and establish an effective method of pavement condition assessment. The key benefits of this research that it will provide a better interface to recognize the hidden or visible crack in concrete construction, sustainability and structural condition of beam. It may create an opportunity to diagnose any types of fault/fatigue in any construction field, according to the sequence of this research. It can help to save a lot of time and money to assess infrastructural conditions.

1.3 Objectives

The effect of single crack on the dynamics of structures has been studied by most researchers in recent years, and various mathematical models have been developed to detect and unwanted behavior of various structural bodies. There are some limitations and in some cases, the outcome is not satisfactory in reality. The primary objective of our research is to establish a mathematical model by using a vibration-based approach to detect different size cracks in different locations and structural behaviors. Therefore, attempts have been made to systematically monitor the complex behavior of simple crack systems. Vibration analysis is conducted here on a cantilever beam with and without cracking. The results are collected analytically and then compared to the results of the simulation. The existence of crack also decreases the rigidity of the derived structures.

The detailed analyses of crack modeling and stiffness matrices will be developed by using the Finite Element Method. The Euler-Bernoulli beam theory is used for dynamic characteristics of beams with transverse cracks. Modified boundary conditions due to presence of crack have been used to find out the theoretical expressions for natural frequencies and mode shape for the beams. The Vibration Based Inspection (VBI) method has emerged as a promising tool for monitoring and classification of faults in machine and equipment. This technique is well prepared for solving inverse variational problems in the context of monitoring

and fault detection because of its pattern recognition and interpolation capabilities. The VBI method also successfully approach and classify the problems associated with nonlinearities, provided they are well represented by input patterns, and also can avoid the complexity introduced by conventional computational methods.

1.4 Organization of the Thesis

The continuation of the study is coordinated as follows. Chapter II describes an overview of various types of crack and methods of detecting crack and structural health monitoring. This chapter also contains the available numerical techniques together with the Finite Element Method that are used to model and analyze the computational domain's behavior. In this chapter, we will also briefly discuss the literature reviews which are relevant to our thesis.

Chapter III presents the development of a mathematical model for a cracked concrete beam. The Numerical approximation of the model is done on the base of Finite Element Method precisely using the vibration based method. The governing equations for detecting crack and some basic terminologies related to this work are given here. The Euler-Bernoulli beam and string theory is also discussed in this section which is used for phase and dynamic behavior of the computational domain.

Chapter IV is the main chapter of our thesis where the numerical simulation of a cracked concrete beam model is performed. We have considered the concrete beam and slice of iron for our simulation. The COMSOL Multiphysics Software has been used to find the simulation results. The deflection, shear rate, load distribution, damage location and thickness of the cracks are observed and results are compared. A detailed description of the results is also discussed in this chapter.

Finally, Chapter V includes a conclusion of our entire work and findings of the research, along with potential recommendations for future work that may contribute to the further development of this research in this field.

References

- [1] Structural health monitoring From Wikipedia, the free encyclopedia.
- [2] Behera R.K., “Vibration Analysis of multi cracked structure”, PhD Thesis.
- [3] Rubio L., “An Efficient Method for Crack Identification in Simply Supported Euler–Bernoulli Beams”, *ASME Journal of Vibration and Acoustics*, Vol. 131, pp. 051001-6, October 2009.
- [4] Taylor S.G. and Zimmerman D.C., “Improved Experimental Ritz Vector Extraction with Application to Damage Detection”, *ASME Journal of Vibration and Acoustics*, pp. 011010-12 , February 2010.
- [5] Seo Y. H., Lee C.W. and Park K. C., “Crack Identification in a Rotating Shaft via the Reverse Directional Frequency Response Functions”, *ASME Journal of Vibration and Acoustics*, Vol. 131, pp. 011012-12 , February. 2009.
- [6] Karthikeyan M., Tiwaril R. and Talukdar S., “Development of a Technique to Locate and Quantify a Crack in a Beam Based on Modal Parameters”, *Journal of Vibration and Acoustics*, Vol. 129, pp. 395-401, June 2007.
- [7] Kumavat R, Patel V, Tapkire G and Patil R, “Utilization of Combined NDT in the Concrete Strength Evaluation of Concrete Specimen from existing building”, *International Journal of Innovative Research In Science Engineering and Technology*, Vol.6(1), pp. 556-562 , 2017.

CHAPTER II

LITERATURE REVIEW

CHAPTER II

LITERATURE REVIEW

2.1 General Overview

A beam is a structural element that primarily resists loads applied transversely to the beam's axis. Its mode of deflection is primarily by bending. The loads applied to the beam result in reaction forces at the beam's support points. The Beam structures are widely used in many applications, such as automotive, aerospace, and civil engineering [1–4]. Many beam structures are subjected to cyclic loading, which results in fatigue cracks [5, 6].

Cracks are formed in the structures due to various aspects in due course of time. The formation of cracks does not lead to immediate failure of the structure, it effects gradually. The presence of a crack in a structural component leads to a local reduction in stiffness and an increase in damping which will affect its vibration response. They may cause serious damage or injury; therefore detecting damage in structural components at the earliest possible stage has become an important aspect in today's engineering. Sometimes cracks cannot be detected with the naked eye hence non-destructive methods of detection of cracks are applied. There are various techniques in crack detection. One of the techniques in non-destructive detection and locating of cracks is the use of vibration response of the structures.

Crack detection through vibration measurements has attracted much interest over the years. A substantial amount of work has been conducted on natural frequency and mode shape based damage detection methods in the past. The presence of a crack in a structural component leads to a local reduction in stiffness and an increase in damping which will affect its vibration response. Mostly modal frequencies are used for monitoring the crack because modal frequencies are the main properties of the whole component. The natural frequency of the component

decreases as a result of the crack. Many methods have been developed to detect and locate the crack by measuring the change in the natural frequencies of the component due to the crack.

2.2 Crack

Cracks are a potential source of catastrophic failure in mechanical engineering, civil structures and aerospace engineering. Generally Structural cracks are those which result from incorrect design, faulty construction or overloading and these may endanger the safety of a building and their inmates. Cracks in any structural systems are very common due to various effects with respect to time, due to natural calamities (such as Earthquake, cyclone; etc.), construction defects, shrinkage of concrete, chemical reactions in concrete etc.



Figure 2.1: Sample images with cracks



Figure 2.2: Sample images without cracks [7]

2.3 Causes of Cracking in Concrete Structures

There are different reasons for creating a crack. Such as, the cracking of joints, especially knuckles, was long believed to lead to arthritis and other joint problems. The cracking mechanism and the resulting sound is caused by carbon dioxide cavitation bubbles suddenly partially collapsing inside the joints. Cracks in concrete occur mostly due to premature drying, inappropriate design and construction practices. There are two common types of cracks brought on by premature drying-

- i) Cracking cracks and
- ii) Crusting cracks.

When a concrete slab (or its top layer, to be specific) loses moisture quickly, which can lead to cracks. Cracking cracks appear when the top layer of the slab quickly loses moisture naturally, resembling a spider-web. Crusting cracks appear during the stamping process when the top layer is dried for embedding patterns [8]. Both these types might look unappealing, but they are largely harmless for the structural strength of the slab. Understanding the specific types allows us to identify the root cause behind these cracks and take appropriate steps.

In summary a list of some factors causing crack are as follows:

- Poor quality of concrete-too high a water content and use of excessively high cement contents.
- Poor structural design.
- The development of differential thermal stresses due to the high heat of hydration.
- Because of restricted thermal expansion and contraction from temperature changes, and subsequent dimensional changes as a result of diurnal and seasonal temperature cycles, the tensile stresses formed.
- Dimensional expansion and contraction caused by cycles of wetting and drying.
- Errors, negligence or bad workmanship.

- Corrosion of steel by chloride ions or carbonation of concrete.
- Rapid evaporation of moisture due to dry, hot and windy conditions prevailing at the time of placing.
- Improper compaction of earth or subgrade.
- Excessive addition of water in concrete or using a high slump.
- Improper finishing of concrete.
- Inadequate, improper or no curing of concrete.

2.4 Effects of Cracks

Generally structures are not collapsed on initial growth of cracks. A crack must be detected in the early state, as it may cause serious failure of the structures with due course of time. However, it is difficult to recognize a crack by visual inspection techniques, when it is too tiny and small. Hence non-destructive testing such as vibration technique is used for crack detection. It is essential to study the behavior of structure having cracks.

2.5 Physical parameters affecting dynamic characteristics of cracked structures

The dynamic response of a structure is normally determined by the physical properties, boundary conditions and the material properties. The changes in dynamic characteristics of structures are caused by their variations. The presence of a crack in structures also modifies its dynamic behavior.

The following properties of the crack influence the dynamic response of the structure.

- The depth of crack
- The location of crack
- The orientation of crack
- The number of cracks

2.6 Modes of Fracture

The crack experiences three specific types of loading which are-

2.6.1 Mode-I

Mode-I represents the opening mode. In this opening mode the crack faces separates in a direction perpendicular to the plane of the crack and the respective displacements of crack walls are symmetric with respect to the crack front. Loading is perpendicular to the crack plane, and has the tendency to open the crack. Generally Mode I is considered the most risky loading condition.

2.6.2 Mode-II

Represents the in-plane shear loading. In this one the crack face appears to slide compared to the other (shearing mode). Here the stress is parallel to the direction of crack formation.

2.6.3 Mode-III

Represents the out-of-plane shear loading. Here the crack faces are sheared parallel to the crack front.

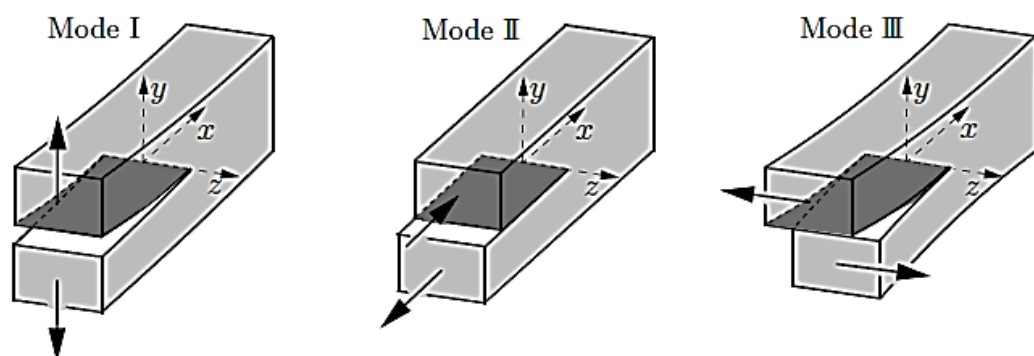


Figure 2.3: Modes of Fracture

2.7 Classification of Cracks

Structural cracks are caused by a lack construction sites, saturated soil, weak bearing or overloading of soil. Other symptoms of foundation problems, such as sticking doors and windows, slanted doors, sloping floors and gaps in porches, typically follow these cracks. Concrete, once cured, is solid but still has weight limits. Crazy cracks will form if the top of the concrete slab dries too quickly. There are very tiny cracks on the surface that look like spider webs or broken glass. Cracking cracks may be unsightly, but they are not a structural issue. So different types and sizes of crack can be formed by different incidents. On the basis of geometry, cracks can be broadly classified into two categories-

2.7.1 Macro Defects

Concrete has low strength if these defects are present and can deteriorate rapidly due to easy penetration of water and other chemicals. The structure would typically need repairs within a few years of its construction. Causes will have to be analyzed and defects removed before doing any additional protective treatment.

2.7.2 Micro Defects

These defects are not visible to the naked eye. They are usually very fine voids caused by large capillary pores resulting from the use of low grades (strength) of concrete with high water to cement ratio.

It is not possible to prevent cracks completely in concrete. However cracks can be minimized by adapting good concrete practices. Some of guidelines to prevent or minimize cracking are as follows: Subgrade and Formwork, Concrete, Finishing Concrete Surface, Curing of Concrete, Joints in Concrete, Cover over Reinforcement etc. It's often difficult to determine exactly what caused a particular crack. Proper site preparation, a quality mix, and good concrete finishing practices

can go a long way towards minimizing the appearance of cracks and producing a more aesthetically pleasing concrete project [9].

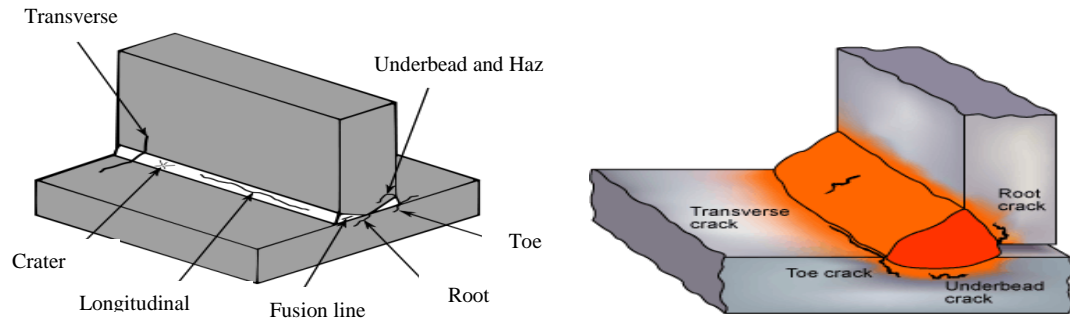
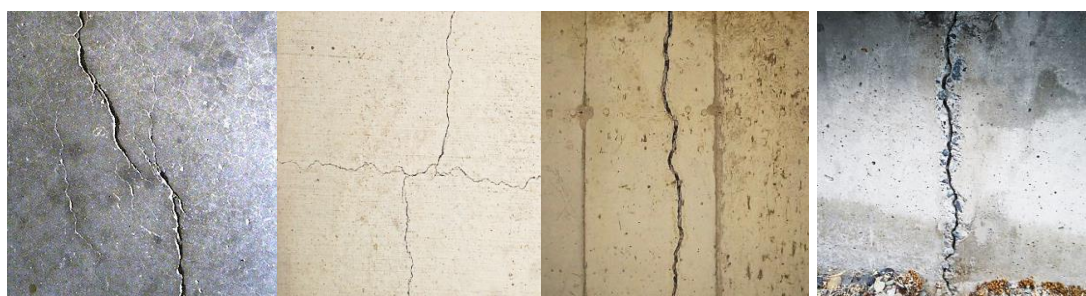


Figure 2.4: Types of Cracks

2.8 Special types of Cracks in Concrete

Cracks that appear in early age of concrete are not very critical. These cracks appear in later stages are critical and may affect structural integrity, strength or service life of the concrete structure. These crack creates new cracks due to freeze and thaw cycles and due to settlement etc. These cracks lead to deterioration of the concrete structure. Tremendous forces can build up inside the wall due to any causes of cracks [10]. Different types of cracks may create inside the wall as follows-



(a) Shrinkage Crack

(b) Hairline Crack

(c) Settlement Crack

(d) Vertical Crack

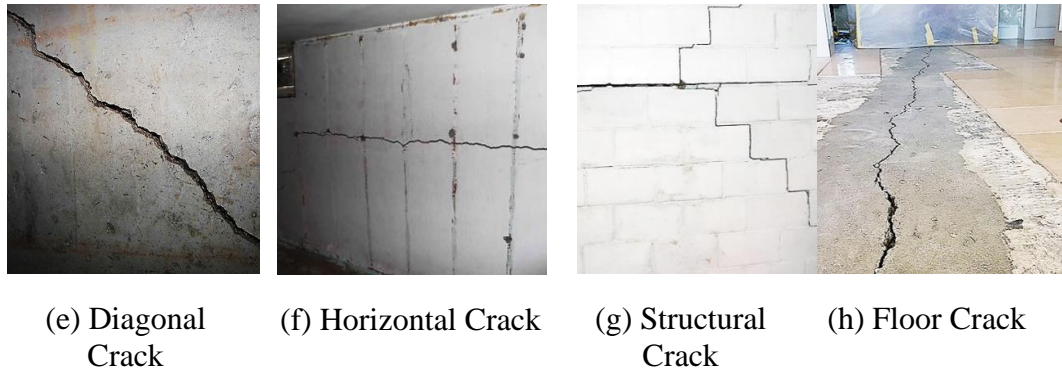


Figure 2.5: Different types of cracks inside the wall

2.9 Different types of Cracks in Hypothetical Concrete Structure

Concrete expands and contracts as other construction materials do whenever there is change in temperature or moisture. Concrete also deflects due to imposed or self-load and support conditions. Cracks in concrete appear when these movements are restricted and no provisions are made to accommodate these movements.

The following figure shows various types of cracks in concrete beams due to shear stress known as shear crack, reinforcement corrosion, inadequate rebar cover, bending stress and compression failure.

Table 2.1: Location of different cracks in hypothetical concrete structure

Types of Cracking	Designation	Time of occurrence
Plastic settlement	A,B,C	Ten minutes to three hours
Plastics Shrinkage	D,E,F	Thirty minutes to six hours
Early thermal Contraction	G,H	One day to two to three weeks
Long-term drying shrinkage	I	Several weeks or months
Crazing	J,K	One to seven days-sometimes much later
Corrosion of reinforcement	L,M	Several years, but may be sooner
Alkali-aggregate reaction	N	More than five years

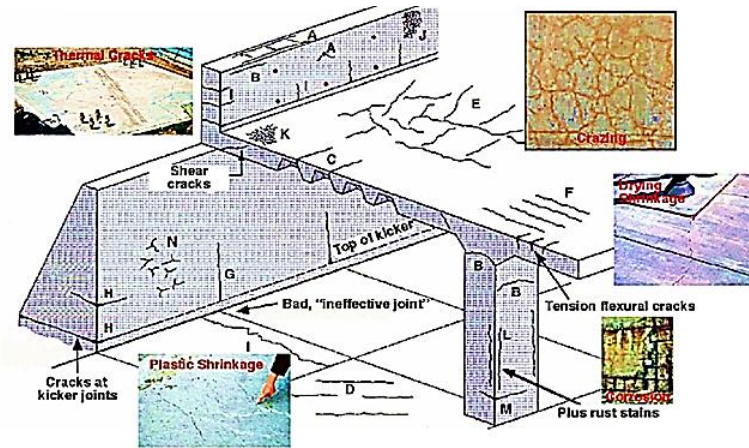


Figure 2.6: Examples of Intrinsic cracks in hypothetical concrete structure

Generally there are five of the most common types of concrete cracks below-

- Plastic shrinkage concrete cracks.
- Expansion concrete cracks.
- Heaving concrete cracks.
- Settling concrete cracks.
- Concrete cracks caused by overloading the slab



(a) Shrinkage cracks originating at re-entrant corners



(b) Expansion Concrete Cracks



(c) Heaving concrete cracks



(d) Settling Concrete Cracks



(e) Large Weights can Crack a Slab

Figure 2.7: Most Common types of Concrete Cracks

2.9.1 Plastic Shrinkage Concrete Cracks

When concrete is still in its plastic state (before hardening), it is full of water. When that water eventually leaves the slab, it leaves behind large voids between the solid particles. These empty spaces make the concrete weaker and more prone to cracking. This type of cracking happens frequently and is referred to as “Plastic Shrinkage Cracking”. While plastic shrinkage cracks can happen anywhere in a slab or wall, they almost always happen at reentrant corners (corners that point into the slab) or with circular objects in the middle of a slab. Since concrete cannot shrink around a corner, stress will cause the concrete to crack from the point of that corner. Plastic shrinkage cracks are typically very narrow in width and barely visible. While nearly invisible, it is important to remember that plastic shrinkage cracks don’t just exist on the surface, they extend throughout the entire thickness of the slab.

2.9.2 Expansion Concrete Cracks

Just like a balloon, heat causes concrete to expand. When concrete expands, it pushes against anything in its way (a brick wall or adjacent slab for example). When neither the ability to flex, the expanding force has can be enough to cause concrete to crack. Expansion joints are used as a point of separation (or isolation), between other static surfaces. Typically made of a compressible material like asphalt, rubber, or lumber, expansion joints must act as shock absorbers to relieve the stress that expansion puts on concrete and prevent cracking.

2.9.3 Heaving Concrete Cracks

When the ground freezes, it can sometimes lift many inches before thawing and settling back down. This ground movement brought on by the freezing and thawing cycle is a huge factor contributing to concrete cracking. If the slab is not free to move with the ground, the slab will crack. Large tree roots can have the same effect on a slab. If a tree is located too close to a slab, the growing roots can lift and crack the concrete surface.

2.9.4 Settling Concrete Cracks

On the other hand, ground settling below a concrete slab can also cause cracking. Settling cracks typically occur in situations where a void is created in the ground below the concrete surface. Think about when a large tree is removed from nearby and the roots begin to decompose or when a utility company digs a trench for their lines, pipes, etc. and don't compact the soil when they refill it—these are examples of instances where settling cracks are likely to happen.

2.9.5 Concrete cracks caused by Overloading the Slab

Although concrete is a very strong building material, it does have its limits. Placing excessive amounts of weight on top of a concrete slab can cause cracking. When concrete mix has a strength of 2000, 3000, 4000, or 5000+ PSI (Pounds per Square Inch), it is referring to the pounds per square inch it would take to crush that concrete slab. When it comes to residential concrete slabs, overload of the actual slab isn't all that common. Instead, what is more likely to occur is excess overload on the ground below the slab. After a heavy rain or snowmelt when the ground below is soft and wet, excessive weight on the slab can press the concrete down and result in cracks.

2.10 Crack Detection Method by Non-Destructive Testing

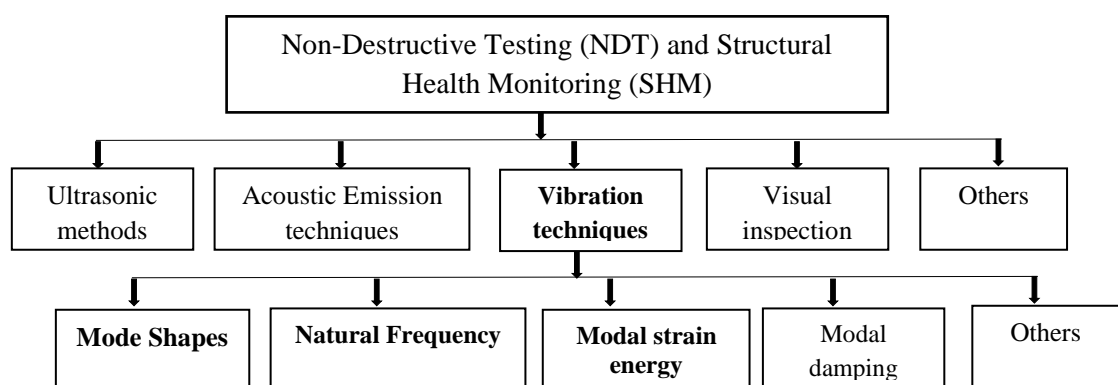


Figure 2.8: Types of Non-Destructive Testing

2.10.1 Ultrasonic Method

Ultrasonic methods of NDT use beams of mechanical waves (vibrations) of short wavelength and high-frequency, transmitted from a small probe and detected by the same or other probes. In high quality metal, such mechanical waves can travel wide distances in the form of a differing wave with progressive attenuation. The frequency is in the range 0.1 to 20 MHz and the wavelength in the range 1 to 10 mm. The velocity depends on the material and is in the range 1000-6000 m/s. The technique detects internal, secret discontinuities below the surface that may be deep. To generate waves of several kinds, including longitudinal, shear, and surface waves, transducers and coupling wedges are available.

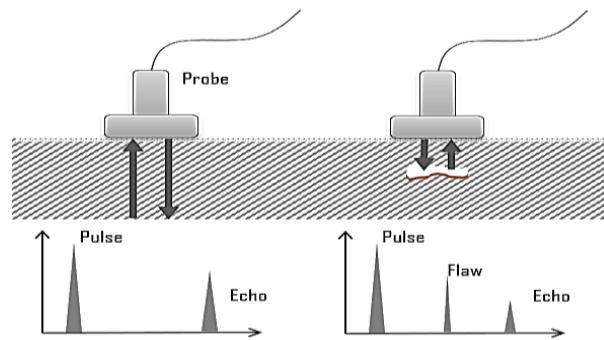


Figure 2.9: Ultrasonic Method

2.10.2 Acoustic Emission Method

Acoustic Emission (AE) refers to the generation of transient elastic waves produced by a sudden redistribution of stress in a material. When a structure is subjected to an external stimulus (change in pressure, load, or temperature), localized sources trigger the release of energy, in the form of stress waves, which propagate to the surface and are recorded by sensors. With the right equipment and setup, motions on the order of picometers (10^{-12} m) can be identified. Detection and analysis of AE signals can supply valuable information regarding the origin and importance of a discontinuity in a material. Because of the versatility of Acoustic Emission Testing (AET), it has many industrial applications and is used extensively as a research tool. The advantages of AET include fast and complete volumetric

inspection using multiple sensors, permanent sensor mounting for process control, and no need to disassemble and clean a specimen. Drawback of AE stems from loud service environments which contribute extraneous noise to the signals. For successful applications, signal discrimination and noise reduction are essential.

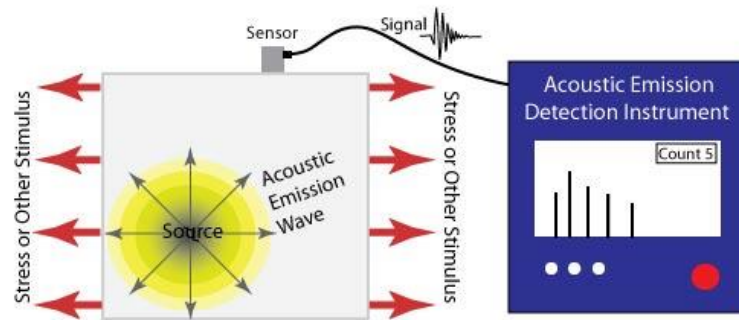


Figure 2.10: Acoustic Emission Method

2.10.3 Vibration Inspection Method

Vibration Based Inspection Methods (VBI) are common due to the convenience of modal parameter measurement and selection. The global presence of the parameters (such as natural frequencies) ensures that experiments can be conducted at virtually arbitrary points. A prior knowledge of the location of the damage is not required [11]. VBI techniques also define a hidden injury that is usually difficult to reach. This skill has drawn the attention of mathematicians and engineers over the past decade. For numerical simulation, it is necessary to model the crack beam. The modeling of the cracked beam portion will assist in hairline crack modeling using the methods of linear invoice mechanics [12]. For crack detection in cantilever beams [13], an analytical as well as experimental approach is used. In order to relate the crack position and depth, the intersection of contours with the constant modal natural frequency planes is used [14].

Non-Destructive error detection suggests that if dynamic response of structure is monitored. Variation in monitored signatures is indication of error and it can be located [15]. The equivalent stiffness may be computed from the crack strain energy function [16, 17]. The expression for the spring stiffness represent a crack

depth ratio is presented [18, 19]. The damage detection in composites is done by measurement of natural frequency.

2.11 Importance of Detecting Crack

Identification of structural crack location has become an intensely investigated subject due to its practical importance since the unpredicted structural failure may cause catastrophic, economic, and life loss. It becomes a crucial task in monitoring structural health and ensuring structural safety [20-23]. In the recent years, with the advancement of Science and technology, the study of detecting of crack has been increasing among researchers. Being very commonly used in steel construction and machinery industries, health monitoring and the analysis of damage in the form of crack in Beam structures poses a vital role.

Particularly for concrete elements, cracks create access to harmful and corrosive chemicals to penetrate into the structure, which consequently damage their integrity as well as esthetics. Normally Cracks that appear in early age of concrete are not very critical. Cracks that appear in later stages are critical and may affect structural integrity, strength or service life of the concrete structure [24]. The presence of the crack not only changes the regional stress and strain fields of the crack tip but also affects structural dynamics [25]. If these fatigue cracks cannot be timely detected and repaired, the subsequent fracture can bring catastrophic failure to the beam structures [26]. Cracks in concrete can be reduced by ensuring the following:

- Concrete structure should be designed properly for all type of anticipated loads,
- Provide shrinkage and insulation joints properly,
- Proper sub grade for slab on grade should be developed,
- Concrete should be correctly installed and finished,
- Concrete should be cured properly.

It is not possible to prevent cracks completely in concrete. However cracks can be minimized by adapting good concrete practices. In this work we choose Concrete beam to detect crack. Because Concrete beams are the choice shape for structural builds because of their high functionality. The shape of concrete beams makes them excellent for unidirectional bending parallel to the web.

2.12 Some Important Definitions

2.12.1 Stress and Strain

When a body is subjected to a deforming force, a restoring force occurs in the body which is equal in magnitude but opposite in direction to the applied force. This restoring force per unit area is known as stress. We can also refer to stress as a measure of the internal force experienced by an object per unit of cross-sectional area.

When the force applied to an elastic body, the body deforms and the deformation depends upon the force applied to it. Stress is the force per unit area upon which it acts.

$$\text{Stress, } \sigma = \frac{\text{Force}}{\text{Area}}$$

Stress applied to a material can be of two types- **i)** Tensile and **ii)** Compressive

2.12.1.1 Tensile Stress

It is the force applied per unit area which results in the increase in length (or area) of a body. Objects under tensile stress become thinner and longer.

2.12.1.2 Compressive Stress

It is the force applied per unit area which results in the decrease in length (or area) of a body. The object under compressive stress becomes thicker and shorter.

According to the strain definition, it is defined as the amount of deformation experienced by the body in the direction of force applied, divided by initial dimensions of the body. Strain is the relative internal change in shape of an infinitesimally small cube of material and can be expressed as a non-dimensional change in length or angle of distortion of the cube. Shortly it is the deformation per unit of its original length. The relation for deformation in terms of length of a solid is given below,

$$\text{Strain, } s = \frac{dL}{L}$$

2.12.2 Young's modulus

Young modulus or the modulus of elasticity in tension, is a mechanical property that measures the tensile stiffness of a solid material. It quantifies the relationship between tensile stress σ (force per unit area) and axial strain ϵ (proportional deformation) in the linear elastic region of a material and is determined using the formula [27],

$$E = \frac{\sigma}{\epsilon}$$

Young's moduli are typically so large that they are expressed not in Pascal but in Giga-Pascals (GPa).

Young's modulus enables the calculation of the change in the dimension of a bar made of an isotropic elastic material under tensile or compressive loads. For instance, it predicts how much a material sample extends under tension or shortens under compression. The Young's modulus directly applies to cases of uniaxial stress, that is tensile or compressive stress in one direction and no stress in the other directions. Young's modulus is also used in order to predict the deflection that will occur in a statically determinate beam when a load is applied at a point in between the beam's supports.

2.12.3 The Poisson's ratio

In materials science and solid mechanics, Poisson's ratio ν is a measure of the Poisson effect, the deformation (expansion or contraction) of a material in directions perpendicular to the direction of loading. The value of Poisson's ratio is the negative of the ratio of transverse strain to axial strain. For small values of these changes, ν is the amount of transversal elongation divided by the amount of axial compression. The ratio is form as,

$$\nu = -\frac{d\varepsilon_{trans}}{d\varepsilon_{axial}}$$

Where,

ν = the resulting Poisson's ratio,

ε_{trans} = transverse strain (negative for axial tension (stretching), positive for axial compression)

ε_{axial} = axial strain (positive for axial tension, negative for axial compression).

Most materials have Poisson's ratio values ranging between 0.0 and 0.5. Nearly incompressible materials, such as rubber, have a ratio near 0.5. The Poisson's ratio of a stable, isotropic, linear elastic material must be between -1.0 and $+0.5$ because of the requirement for Young's modulus, the shear modulus and bulk modulus to have positive values [28]. A perfectly incompressible isotropic material deformed elastically at small strains would have a Poisson's ratio of exactly 0.5. Most steels and rigid polymers when used within their design limits (before yield) exhibit values of about 0.3, increasing to 0.5 for post-yield deformation which occurs largely at constant volume [29].

2.12.4 Tensor

A tensor is a concept from mathematical physics that can be thought of as a generalization of a vector and is a geometric objects that describe linear relations between geometric vectors, scalars and matrices. While tensors can be defined in a

purely mathematical sense, they are most useful in connection with vectors in physics. Euclidean vectors, often used in physics and engineering applications, and scalars themselves are also tensors. A linear map is represented by a matrix (a 2-dimensional array) in a basis, and therefore is a 2nd-order tensor. A vector is represented as a 1-dimensional array in a basis, and is a 1st-order tensor. Scalars are single numbers and are thus 0th-order tensors.

Tensors are useful when trying to understand how a given system reacts to directional forces. They are simply a mathematical tool used by scientists and engineers to describe and understand how a system is affected when these forces, usually represented by vectors (which have both magnitude and direction) change when acted upon by other forces.

2.12.5 Rate of Deformation

The strain rate tensor or the deformation rate is a physical quantity that describes the rate of change of the deformation of a material in the neighborhood of a certain point, at a certain moment of time. Stress tensor is a second order tensor named after Augustin-Louis Cauchy. The stress at a point in a solid body needs nine components to be completely specified, since each component of the stress must be defined not only by the direction in which it acts but also the orientation of the surface upon which it is acting.

In engineering, deformation refers to the change in size or shape of an object. Displacements are the absolute change in position of a point on the object. Strains are related to the forces acting on the cube, which are known as stress, by a stress-strain curve. The relationship between stress and strain is generally linear and reversible up until the yield point and the deformation is elastic. [30]. Above the yield point, some degree of permanent distortion remains after unloading and is termed plastic deformation.

2.12.6 Torsion

In the field of solid mechanics, torsion is the twisting of an object due to an applied torque. Unlike axial loads which produce a uniform, or average, stress over the cross section of the object, a torque creates a distribution of stress over the cross section. When a torque is applied to the structure, it will twist along the long axis of the rod, and its cross section remains circular. Torsion is expressed in either the Pascal (Pa), an SI unit for Nm^{-2} , or in pounds per square inch (psi) while torque is expressed in Newton-Meters (N·m) or foot-pound force (ft·lbf). In sections perpendicular to the torque axis, the resultant shear stress in this section is perpendicular to the radius.

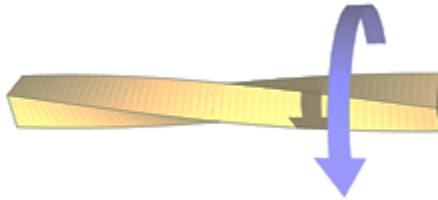


Figure 2.11: Torsion of a square section bar

In non-circular cross-sections, twisting is accompanied by a distortion called warping, in which transverse sections do not remain plane. For shafts of uniform cross-section unrestrained against warping, the torsion is:

$$T = \frac{J_T}{r} \tau = \frac{J_T}{l} G \phi$$

Where,

T = applied torque or moment of torsion in Nm.

τ = maximum shear stress at the outer surface

J_T = torsion constant for the section.

r = perpendicular distance between the rotational axis and the farthest point in the section (at the outer surface).

l = length of the object to or over which the torque is being applied.

ϕ = angle of twist in radians.

G = shear modulus, also called the modulus of rigidity, and is usually given in Giga-Pascal (GPa), lbf/in² (psi), or lbf/ft² or in ISO units N/mm².

The product $J_T G$ is called the torsional rigidity w_T .

2.12.7 Deflection of Beams

Deflection, in structural engineering terms, refers to the movement of a beam or node from its original position due to the forces and loads (due to its deformation) being applied to the domain. Deflection, also known as displacement or may refer to an angle, can occur from external applied loads or from the weight of the structure itself, and the force of gravity in which this applies. It can occur in beams, trusses, frames and basically any other structure. The deflection distance of a member under a load can be calculated by integrating the function that mathematically describes the slope of the deflected shape of the member under that load. Standard formulas exist for the deflection of common beam configurations and load cases at discrete locations. Otherwise methods such as virtual work, direct integration, Castigliano's method, Macaulay's method or the direct stiffness method are used. An example of the use of deflection is in building construction. Architects and Engineers select materials for various applications. The deformation of a beam is usually expressed in terms of its deflection from its original unloaded position. The configuration assumed by the deformed neutral surface is known as the elastic curve of the beam.

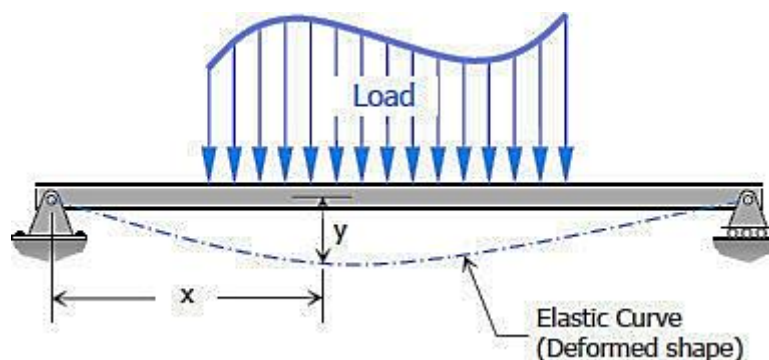


Figure 2.12: Deflection of Beams

2.12.8 Shear Forces (SF) and Bending Moment (BM)

Shear Forces occurs when two parallel forces act out of alignment with each other. Bending Moments are rotational forces within the beam that cause bending. At any point within a beam, the Bending Moment is the sum of each external force multiplied by the distance that is perpendicular to the direction of the force. In a cantilever beam, shear force at any section is equal to the sum of the loads between the sections and the free end. Bending moment at a given section is equal to the sum of the moments about the section of all the loads between the section and the free end of the cantilever. Shear Force (SF) at any cross-section of the beam is the algebraic sum of all vertical forces on the beam, acting on the right or left side of the domain. Sagging from both sides i.e. Left or Right; upward force will produce positive BM.

Shear and bending moment diagrams are analytical tools used in conjunction with structural analysis to help perform structural design by determining the value of shear force and bending moment at a given point of a structural element such as a beam.

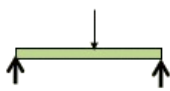
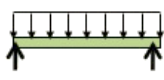
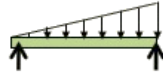






Load			
	P	Constant	Linear
Shear			
	Constant	Linear	Parabolic
Moment			
	Linear	Parabolic	Cubic

Figure 2.13: Shear Forces (SF) and Bending Moment (BM) for various types of loads

2.13 Castigliano's Theorem

Italian engineer Alberto Castigliano (1847 – 1884) developed a method of determining deflection of structures by Strain Energy Method (SEM). His theorem of the derivatives of internal work of deformation extended its application to the calculation of relative rotations and displacements between points in the structure and to the study of beams in flexure. Energy of structure is its capacity of doing work and strain energy is the internal energy in the structure because of its deformation [31]. By the principle of conservation of energy,

$$U = W_i$$

Where, U denotes the strain energy and W_i represents the work done by internal forces. The expression of strain energy depends therefore on the internal forces that can develop in the member due to applied external forces.

2.13.1 Castigliano's Theorem for Beam Deflection

For linearly elastic structures, the partial derivative of the strain energy with respect to an applied force (or couple) is equal to the displacement (or rotation) of the force (or couple) along its line of action. When a body is elastically deflected by any combination of loads, the deflection at any point and in any direction is equal to the partial derivative of strain energy (computed with all loads acting) with respect to a load located at that point and acting in that direction.

$$\delta = \frac{\delta U}{\delta P} \quad \text{or} \quad \theta = \frac{\delta U}{\delta \bar{M}}$$

Where δ is the deflection at the point of application of force P in the direction of P , θ is the rotation at the point of application of the couple \bar{M} in the direction of \bar{M} , and U is the strain energy.

2.14 Euler–Bernoulli Beam theory

The Euler- Bernoulli beam theory is a model of how beams behave under axial forces and bending. (It is also known as engineer's beam theory or classical beam theory) [32] which is a simplification of the linear theory of elasticity which

provides a means of calculating the load-carrying and deflection characteristics of beams. It covers the case for small deflections of a beam that are subjected to lateral loads only.

This theory relies on a couple major assumptions. Of course, there are other more complex models that exist (such as the Timoshenko beam theory); however, the Euler- Bernoulli assumptions typically provide answers that are 'good enough' for design in most cases. It was first enunciated circa 1750, but was not applied on a large scale until the development of the Eiffel Tower and the Ferris wheel in the late 19th century [33]. Following these successful demonstrations, it quickly became a cornerstone of engineering and an enabler of the Second Industrial Revolution.

2.14.1 Euler- Bernoulli Assumptions

The two primary assumptions made by the Euler- Bernoulli beam theory are that “Plane Sections Remain Plane” and that deformed beam angles (slopes) are small. The plane sections remain plane assumption is illustrated in Figure 2.14. It assumes that any section of a beam (i.e. a cut through the beam at some point along its length) that was a flat plane before the beam deforms will remain a flat plane after the beam deforms. This assumption is generally relatively valid for bending beams unless the beam experiences significant shear or torsional stresses relative to the bending (axial) stresses. Shear stresses in beams may become large relative to the bending stresses in cases where a beam is very deep and short in length [34].

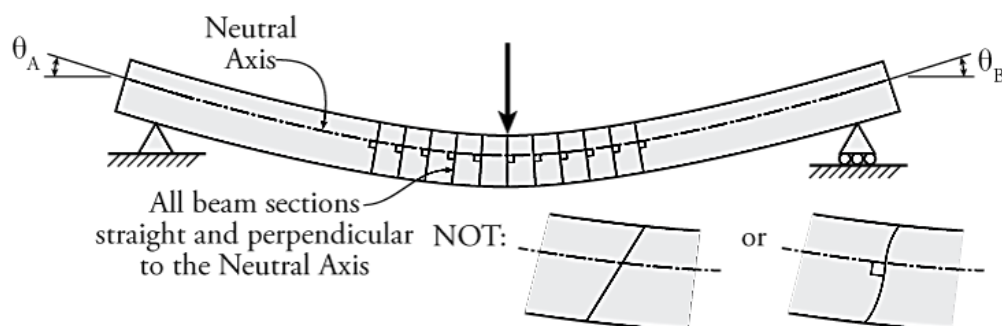


Figure 2.14: The Plane Sections Remain Plane Assumption

The plane sections remain plane assumption also assumes that any section of a beam that was perpendicular to the neutral axis before the beam deforms will remain perpendicular to the neutral axis after the beam deforms.

2.14.2 The Euler- Bernoulli Beam Equation

The out-of-plane displacement w of a beam is governed by the Euler-Bernoulli Beam Equation,

$$\frac{d^2}{dx^2} \left[EI \frac{d^2 w}{dx^2} \right] = p$$

Where, p is the distributed loading (force per unit length) acting in the same direction as y (and w), E is the Young's modulus of the beam, and I is the area moment of inertia of the beam's cross section.

If E and I do not vary with x along the length of the beam, then the beam equation simplifies to,

$$EI \frac{d^4 w}{dx^4} = p$$

2.15 Timoshenko Beam Theory

Timoshenko beam theory is one of several classical structural models in solid mechanics. It was first developed in 1921, and was refined in 1922 by Timoshenko [35, 36]. Since then, it has been revised and extended for broad applications in vibration analysis of beam-like structures of homogeneous, composite, and functionally graded materials [37]. Since Timoshenko beam theory actually accounts for the first order shear deformation in an average sense [38], the First-Order Shear Deformation Theory (FSDT) is also included as a generalization of Timoshenko theory. In recent years, the Timoshenko theory has been modified to an on local theory for vibration analysis of Micro-and Nano-structures [39].

The model takes into account shear deformation and rotational bending effects, making it suitable for describing the behavior of thick beams, sandwich composite beams, or beams subject to high-frequency excitation when the wavelength approaches the thickness of the beam. The resulting equation is of fourth order but, unlike Euler–Bernoulli beam theory, there is also a second-order partial derivative present. Physically, taking into account the added mechanisms of deformation effectively lowers the stiffness of the beam, while the result is a larger deflection under a static load and lower predicted Eigen frequencies for a given set of boundary conditions [40].

Timoshenko beam theory is a simple extension to Euler-Bernoulli Beam theory. Shear deformations, which are absent in Euler-Bernoulli beam theory, are included in Timoshenko beam theory.

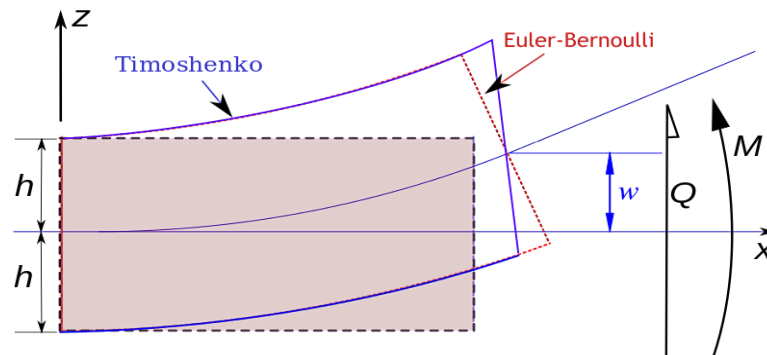


Figure 2.15: Deformation of a Timoshenko beam (blue) compared with that of an Euler-Bernoulli beam (red).

In static Timoshenko beam theory without axial effects, the displacements of the beam are assumed to be given by,

$$u_x(x, y, z) = -z \varphi(x) ; u_y(x, y, z) = 0 ; u_z(x, y) = \omega(x)$$

where (x, y, z) are the coordinates of a point in the beam, u_x , u_y , u_z are the components of the displacement vector in the three coordinate directions, φ is the angle of rotation of the normal to the mid-surface of the beam, and ω is the displacement of the mid-surface in the z -direction.

The governing equations are the following coupled system of ordinary differential equations:

$$\frac{d^2}{dx^2} \left(EI \frac{d\varphi}{dx} \right) = q(x)$$

$$\frac{d\omega}{dx} = \varphi - \frac{1}{\kappa AG} \frac{d}{dx} \left(EI \frac{d\varphi}{dx} \right)$$

The Timoshenko beam theory for the static case is equivalent to the Euler-Bernoulli theory when the last term above is neglected, an approximation that is valid when

$$\frac{1}{\kappa L^2 AG} \ll 1$$

Where,

L = length of the beam.

A = cross section area.

E = elastic modulus.

G = shear modulus.

I = second moment of area.

κ , called the Timoshenko shear coefficient, depends on the geometry. Normally, $\kappa = 5/6$ for a rectangular section.

$q(x)$ = distributed load (force per length).

Combining the two equations gives, for a homogeneous beam of constant cross-section,

$$EI \frac{d^4 \omega}{dx^4} = q(x) - \frac{EI}{\kappa AG} \frac{d^2 q}{dx^2}$$

The bending moment M_{xx} and the shear force Q_x in the beam are related to the displacement ω and the rotation φ . These relations, for a linear elastic Timoshenko beam, are-

$$M_{xx} = -EI \frac{\delta \varphi}{\delta x} \quad \text{and} \quad Q_x = \kappa AG \left(-\varphi + \frac{\delta \omega}{\delta x} \right)$$

2.16 Numerical Methods for Computation

Computational Numerical methods is the branch of numerical analysis that studies the numerical solution of partial differential equations (PDEs).

Some Numerical methods for Computation mentioned below-

- i. Finite Difference Method
- ii. Finite Volume Method
- iii. Boundary Element Method
- iv. Finite Element Method

2.16.1 Finite Difference Method

In numerical analysis, Finite Difference Methods (FDM) are a class of numerical techniques for solving partial differential equations (PDE) by approximating derivatives with finite differences. It has been used to solve a wide range of problems. The application of FDM is not difficult as it involves only simple arithmetic in the derivation of the discretization equations and in writing the corresponding programs [41]. Finite difference methods convert ordinary differential equations (ODE) or partial differential equations (PDE), which may be nonlinear, into a system of linear equations that can be solved by matrix algebra techniques, and the value of the solution is approximated by solving algebraic equations containing finite differences and values from nearby points. Today, FDM are one of the most common approaches to the numerical solution of PDE, along with Finite Element Methods [42].

2.16.2 Finite Volume Method

The Finite Volume Method (FVM) is also a method for representing and evaluating partial differential equations in the form of algebraic equations. Similar to the finite difference method or finite element method, values are calculated at discrete places on a meshed geometry. "Finite volume" refers to the small volume surrounding each node point on a mesh. In the finite volume method, volume

integrals in a partial differential equation that contain a divergence term are converted to surface integrals, using the divergence theorem. These terms are then evaluated as fluxes at the surfaces of each finite volume. Because the flux entering a given volume is identical to that leaving the adjacent volume, these methods are conservative. Another advantage of the finite volume method is that it is easily formulated to allow for unstructured meshes. The method is used in many computational fluid dynamics packages [43].

2.16.3 Boundary Element Method

The Boundary Element Method (BEM) is another numerical computational method of solving linear partial differential equations which have been formulated as integral equations (i.e. in boundary integral form) including fluid mechanics, acoustics, electromagnetics (Method of Moments), fracture mechanics and contact mechanics. The boundary element method is well suited for analyzing cracks in solids. There are several boundary element approaches for crack problems. The boundary element method is derived through the discretization of an integral equation that is mathematically equivalent to the original partial differential equation. The essential reformulation of the PDE that underlies the BEM consists of an integral equation that is defined on the boundary of the domain. The former is termed a Boundary Integral Equation (BIE) and the BEM is often referred to as the Boundary Integral Equation Method or Boundary Integral Method [44].

2.16.4 Finite Element Method

The Finite Element Method (FEM) is the most widely used method for solving problems of engineering and mathematical models. Typical problem areas of interest include the traditional fields of structural analysis, heat transfer, fluid flow, mass transport, and electromagnetic potential. The FEM is a particular numerical method for solving partial differential equations in two or three space variables (i.e., some boundary value problems). To solve a problem, the FEM subdivides a large system into smaller, simpler parts that are called finite elements. This is achieved by

a particular space discretization in the space dimensions, which is implemented by the construction of a mesh of the object: the numerical domain for the solution, which has a finite number of points. The Finite Element Method formulation of a boundary value problem finally results in a system of algebraic equations. The method approximates the unknown function over the domain. The simple equations that model these finite elements are then assembled into a larger system of equations that models the entire problem. FEA is a good choice for analyzing problems over complicated domains, when the domain changes (as during a solid-state reaction with a moving boundary), when the desired precision varies over the entire domain, or when the solution lacks smoothness. FEA simulations provide a valuable resource as they remove multiple instances of creation and testing of hard prototypes for various high fidelity situations [45].

2.16.4.1 Types of analysis done by Finite Element Method

- Structural Analysis
- Vibrational Analysis
- Fatigue Analysis
- Heat Transfer Analysis

2.16.4.2 History of Finite Element Method

Finite Element Analysis simulation concept developed from the theoretical basis established by the finite element method (FEM), which was founded with the publication of a set of scientific papers in the 1940s. Created as numerical techniques for finding approximate solutions to boundary value problems for partial differential equations, FEM software is based on a problem domain's subdivision into simpler parts called finite elements, and on the calculus of variational methods to minimize an associated error function.

The scientific pillars of the finite element method are a direct result of the need to solve complex elasticity and structural analysis problems in civil and aeronautical engineering. The first development can be traced back to the work of A. Hrennikoff in 1941 [46] and R. Courant in 1943 [47]. Although these pioneers used

different perspectives in their finite element approaches, they each identified the one common and essential characteristic: mesh discretization of a continuous domain into a set of discrete sub-domains, usually called elements. Another fundamental mathematical contribution to the FEM is represented by the book “An Analysis of the Finite Element Method” by Gilbert Strang and George Fix, first published in 1973 [48]. Since then, FEM has been generalized for the numerical modeling of physical systems in many engineering disciplines including electromagnetism, heat transfer, and fluid dynamics. Benefits of the Finite Element Method (FEM). Many specializations under the umbrella of mechanical engineering, such as the aeronautical, biomechanical, and automotive industries, are commonly using integrated FEM in product design and development. Several modern FEM packages include specific components such as thermal, electromagnetic, fluid, and structural working environments. For example, in a structural simulation, the FEM helps in “producing stiffness and strength visualizations and also in minimizing weight, materials, and costs” [49]. The main capability of FEM is its detailed visualization of bending and twisting places for a structure, indicating stresses and displacement distribution. Modern FEM applications software offer a variety of simulation options for modeling and analysis.

Over the course of modern engineering history, FEM algorithms were embedded in many powerful design tools, contributing to raising the standards of engineering and significantly improving the design process. Using FEM algorithms integrated into FEA applications, any engineering structure design can be developed, tested, and modified in advance, long before the manufacturing of product prototypes.

2.16.4.3 Role of Finite Element Method

FEM helps the designer know all the theoretical stresses within the structure by showing all the problem areas in detail and thus helping the designer to predict the failure of the structure. It is an economic method of determining the causes of failure and the way the failures can be avoided. In our study we are analyzing the

cracked beam in the FEM method by using a software known as COMSOL. It has several application in mechanical event simulation and computation.

There are various types of numerical method to solve computational problem. We use the Finite Element Method (FEM) instead of the Finite Difference Method (FDM), Boundary Element Method (BEM) and Finite Volume Method (FVM) from various numerical techniques. In general, the Finite Difference Method (FDM) applies only to simple geometry problems. In addition, the Boundary Element Method is a more efficient and precise method that reduces the problem's dimensionality by one and requires a unique solution to the problem. The Finite Element Method thus provides a better approximation for complex geometries compared to other numerical approaches.

2.17 Computational Modelling

2.17.1 Modelling

Modelling is the process of representing a model which includes its construction and working. This model is similar to a real system, which helps the analyst predict the effect of changes to the system. In other words, modelling is creating a model which represents a system including their properties. It is an act of building a model.

2.17.2 Simulation

Simulation of a system is the operation of a model in terms of time or space, which helps analyze the performance of an existing or a proposed system. In other words, simulation is the process of using a model to study the performance of a system. It is an act of using a model for simulation [50].

2.17.3 Steps of Computational Modelling by Finite Element Method

There are some important steps in the computational modelling of any physical process:

- (i) Problem definition,
- (ii) Mathematical Modelling,
- (iii) Computer Simulation, and
- (iv) Result and Decision.

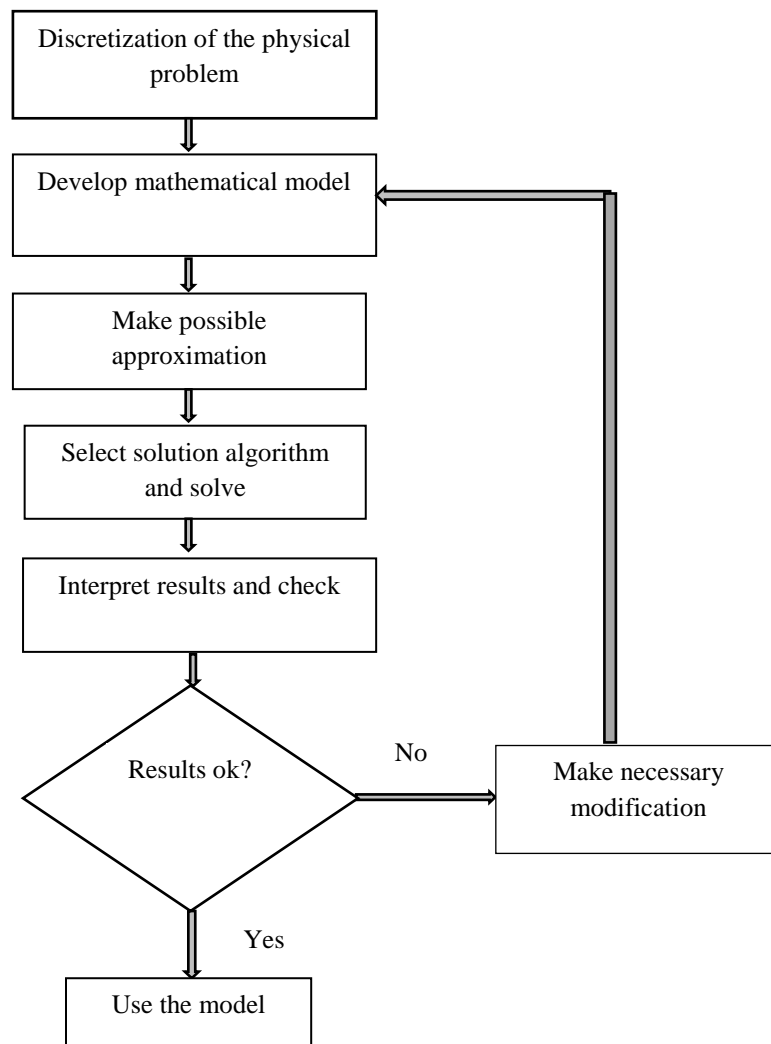


Figure 2.16: Steps of Computational Modelling

2.18 Method for Simulation using COMSOL Multiphysics

The simulation of computers has become an important part of science and engineering. A model is constructed for a real or theoretical physical structure in this discipline of design, implementing the model and analyzing the execution performance. Researchers today use everything from the standard programming language to sophisticated approaches in high-level packages.

COMSOL Multiphysics is such like a solver and simulation software package based on Finite Element Analysis used for different physics and engineering applications, particularly in combined phenomena or multiphysics. In addition to traditional user interfaces focused on physics, COMSOL Multiphysics also enables Partial Differential Equations (PDEs) combined systems to be implemented. One can access the partial differential equations directly or using the theoretical basis.

COMSOL Multiphysics is a versatile framework that enables users to design all the physical aspects of their models that are important. In order to develop optimal protection applicable to their particular situations, experienced users should go wider and use their expertise. COMSOL provides the assurance to construct the model with real world accuracy with this kind of complete modeling environment [51]. There are some task oriented advantages of COMSOL Multiphysics. Using COMSOL at the beginning of a new project allows the user to understand this concept. Different geometric and physical features of a model may be evaluated, thereby improving the user's major structural challenges. By optimizing every element of our model, we can carry our simulation to the production level. So it can be say that, COMSOL is a total problem solving method.

In this work we choose COMSOL Multiphysics Software to simulate the concrete beam to detect crack in different location, deflection and others requirements of computation.

2.19 Previous Studies

Many extensive researches on crack detection in different method have been performed theoretically and experimentally till today.

Kim and Zhao [52] studied a very distinctive crack detection technique employing a harmonic response, where the displacement and slope modes of a cracked cantilever beam are thought of 1st, that the approximate formula for displacement and slope response under single-point harmonic excitation comes. They conclude that the slope response incorporates a pointy amendment with the crack location and additionally the depth of the crack.

A new idea has developed by Lee and Chung [53] that how to look out the lowest four natural frequencies of the cracked structure by FEM and additionally the approximate crack location is obtained by exploitation. Later, Owolabi et al. [54] have experimentally investigated of the possessions of cracks and damages on the dependability of structures.

An analytical and experimental approach for the damage detection in cantilever beams like structure by vibration analysis has developed by Nahvi [55]. Presently numerous analytical, numerical and experimental techniques are in use for crack detection throughout a fiber-reinforced composite, laminated composites and non-composite structures for its vibration analysis.

In the same case I. Goda [56], has applied numerical study exploitation finite parts is performed to research the free vibration response of laminated composite beams. They had a tendency to perform dynamic modeling of the laminated beams by associate eigenvalue analysis, exploitation associate eight-node bedded shell part to simulate the free vibrations. The major importance of their study was for the mechanical designer to conceive and optimize composite structures subjected to dynamic loadings.

Prasad et al. [57] discussed the effect of location of crack from the free end to the fixed end on crack growth rate along vibrating cantilever beam and a

mathematical model was developed using dimensional analysis to find out the value of the crack growth rate along vibrating cantilever beam.

Rizos et al. [58] suggested a method for using measured amplitudes at two points of a cantilever beam vibrating at one of its natural modes to identify crack location and depth. They investigated the flexural vibrations of a cantilever beam with a rectangular cross-section having a transverse surface crack which is modeled as a mass less rotational spring. They also assumed that the crack is fully open and has uniform depth. As an experimental study, they forced the beam by a harmonic exciter to vibrate at one of the natural modes of vibration and measured the amplitudes at two positions.

Lee [59] presented a method to detect a crack in a beam. The crack was not modeled as a massless rotational spring, and the forward problem was solved for the natural frequencies using the boundary element method. The inverse problem was solved iteratively for the crack location and the crack size by the Newton-Raphson method. The present crack identification procedure was applied to the simulation cases which use the experimentally measured natural frequencies as inputs, and the detected crack parameters are in good agreements with the actual ones. The present method enables one to detect a crack in a beam without the help of the massless rotational spring model.

Owolabi et al. [60] used natural frequency as the basic criterion for crack detection in simply supported and fixed beams. The method suggested has been extended to cantilever beams to check the capability and efficiency. There is need to see if this approach can be used for fixed-free beams.

The research group of Kisa [61] analyzed the vibrational characteristics of a cracked Timoshenko beam. The study integrates the FEM and component mode synthesis. The beam divided into two components related by a flexibility matrix which incorporates the interaction forces. The forces were derived from fracture mechanics expressions as the inverse of the compliance matrix is calculated using stress intensity factors and strain energy release rate expressions.

Ratcliffe [62] also developed a technique for identifying the location of structural damage in a beam using a 1D FEA. A finite difference approximation called Laplace's differential operator was applied to the mode shapes to identify the location of the damage.

Sadettin and Murat [63] assumed an exponential stress distribution in the vicinity of the crack and applied a variational principle to study the dynamic behavior of the system. If the stress distribution be known, it would have made this method very rational. The exponential approximation is valid only for notches and the exponent is estimated experimentally.

The research group of Shayanfar [64] used time-domain responses for damage detection of a bridge structure. The method proposed by them include, measuring acceleration responses of the time-domain and also creating a finite element model of the structure, based on the equations of motion of the bridge under a moving load. Afterwards, an objective function for solving the inverse problem of damage detection was defined; and by using ECBO algorithm, the problem was solved.

In the study of Sabuncu et al. [65], the effects of number of stories, static and dynamic load parameters, crack depth and crack location, on the in-plane static and dynamic stability of cracked multi-storey frame structures subjected to periodic loading, were investigated numerically using the Finite Element Method.

Dharmaraju et al.[66] considered Euler-Bernoulli beam element in the finite element analysis. In this the transverse surface crack is considered to remain open. A local compliance matrix of four degrees of freedom is considered for the modeling of a crack. This compliance matrix contains diagonal and off-diagonal terms. A harmonic force of given amplitude and frequency is used to excite dynamically the beam.

Sekhar [67] has presented a review work on multi-crack identification techniques in structures such as beams, rotors, pipes. Cahsalevris and Papadopoulos [68] have studied the dynamic behavior of a cracked beam with two transverse

surface cracks. Each crack was characterized by its depth, position, and relative angle. The compliance matrix was calculated for all angles of rotation.

Singh and Tiwari [69] have developed a two-step multi-crack identification algorithm which was based on forced responses from a non-rotating shaft, the Timoshenko beam theory is used to model the shaft by using the finite element method. The methodology identifies very well the presence of cracks and also estimates quite accurately the location and the size of cracks on the shaft.

Most recently, Al-Shudeifat and Butcher [70] have proposed an accurate mechanism for breathing crack model. A new time-varying function of the breathing crack model was introduced. They applied this new model using the FEM, and formed an actual periodically time-varying stiffness matrix for a breathing crack and then merged it into the stiffness matrix of the global system matrix. This model drew on the principle of reducing second moment of area locally, which proposed by Mayes and Davis in 1984 [71].

Machorro, Adams et al [72] have identified damaged shafts by using active sensing simulation and experimentation, which were based on Timoshenko beam theory. Various kinds of defects such as transverse cracks, imbalance, misalignment, bent shafts and a combination of them were considered.

Chondros et al. [73] developed a continuous cracked beam theory for free vibration analysis; their basic assumption was that the crack caused a continuous change in flexibility in its neighborhood which they modelled by incorporating a consistent displacement field with singularity. A different but related approach in which a crack in rotational shaft is replaced by a mass-less spring-link located at the crack position became popular due to much effort by Dimarogonas and Papadopolous [74].

Aktas and Sumer [75] modelled pre-damaged Reinforced Concrete (RC) beams in finite element program and indicated that inclusion of pre-damage levels by means of cracks into the cross sections have significant effect on beams moment capacity.

Gerist et al. [76] presented a new method to detect the structural damages. In this method, the sensitivity matrices of structural responses with respect to elemental damages were evaluated by finite difference method with various finite difference increments. Then, various systems of equations were formed for the structure and solved by BP.

Shakti et al. [77]. They investigated the influence of parameters like crack depth and crack inclination angles, on the dynamic behaviour of deteriorated structures excited by time-varying mass. Analysis of the structure was carried out at constant transit mass and speed.

Ryu et al [78] conducted fire tests and residual strength tests on Reinforced concrete (RC) beams having different fire exposure time periods and sustained load levels. To detect the automated cracks, surface images of the fire damaged beam surfaces are taken with digital cameras and an automatic crack detection method is developed using a Convolutional Neural Network (CNN). They found that the quantity of the automatically detected cracks is numerically related to the temperatures inside the beams as well as the stiffnesses obtained from the residual strength tests.

Al-Saffar et al [79] tried to discover the variations of depth, shapes and locations of the crack on the natural frequency of thirty-two cracked Aluminium shafts have 25 mm diameter and 45 mm length cantilever circular shaft with 1,2,4,5 mm crack depths and different positions on the beam. The results showed that increasing the depth of crack reduces the frequency of shaft for same mode number. While, at the small crack depth, there is no influence of crack position on the first and second modes of frequencies.

Sahu and Rohini [80] considered a square area of mild steel specimen to examine the act of cracks on the free vibration of cantilever shaft. FEM in MATLAB environment was used and from theory of linear elastic fracture, a local flexibility matrix was added to the total flexibility matrix. In the study of Liu et al [81], they detect crack by the analysis of the measured tensile strain profiles is in excellent agreement with the visually observable cracks mapped during the test. A Distributed

Optical Fiber (DOF) sensing system with Rayleigh Optical Frequency Domain Reflectometry (OFDR) technique was deployed to a member of RC structure in a full-scale laboratory experiment, which was subjected to a monotonic lateral load. This confirms the ability of the optical fiber inside of RC members to capture cracks on concrete surface.

Chaudhari et al [82] has studies on modal parameters like natural frequency, damping and mode shape. In their work, cantilever beam having line crack with changing depth and changing crack position is compared with non-defective beam. The vibration signals from defect-free and line crack beam were equated in the frequency domain with the help of Fast Fourier Transform in Lab-View.

Saleh et al [83] presents the use of Frequency Response Functions (FRFs) to determine damage index and crack damage in reinforced concrete beam structures using vibration signals based on the Mode Shape Curvature Square (MSCS) method. The damage index and crack detection based on the numerical computation were determined by subtracting the MSCS between undamaged to damaged beams. The resulting accuracy of the damage index used to define the level of damage and damage location was absolutely achieved by comparing the numerical and observed experimental results.

Long et al [84] is presents a new model which is established by the finite element displacement method for studying the effects of crack parameters on the dynamics of a cracked beam structure. The stiffness matrix of the cracked beam element is firstly derived by the displacement method. Starting with a finite element model of cracked beam element, the equation of strain energy of a cracked beam element is formed by the displacement method combined with the linear fracture mechanics. Their results shows that the dynamic model discovers the internal relation between the dynamic characteristics of cracked beam structure and structural parameters, material parameters, and crack parameters.

Jiang et al [85] presented an overview of a stress wave-based active sensing method to detect the crack in FRP (Fiber Reinforced Polymer) reinforced concrete beams. The embedded Smart Aggregates (SAs), which utilize Lead Zirconate

Titanate (PZT) as transducers, are employed in this research to generate and sense the stress wave. Signals received by the SA sensors are analyzed in both time domain and frequency domain. Experimental results show the test specimens experience crushing failure when the concrete compression exceeds its compressive strength. Increasing the contact area between FRP bar and concrete can effectively improve the cracking load of the FRP-reinforced concrete beam and reduce the cracking speed and depth of FRP-reinforced concrete beam.

A special reinforced concrete beam structure was designed by Zhang et al [86] for crack detection under load. Four continuous distributed optical fibers are fixed on the steel skeleton, which is located within the reinforced concrete beam. Three Fiber Bragg Grating (FBG) sensors are fixed on the lower surface of the beam, near its center. By analyzing the sensor data, it can be found that the Brillouin Optical Frequency Domain Analysis (BOFDA) -distributed fiber can be used to detect internal cracking before surface cracking, and the difference between scans can be used to judge the time of onset of internal cracking.

This chapter provides a summary of the possibility of cracks, crack forms, and the complex behavior of structural and industrial bodies when cracks occur. The types of non-destructive crack identification techniques are classified and introduced, especially the vibration-based techniques that are specifically identified and demonstrated because of the important role of these techniques in structural system crack investigations. A comprehensive review on the approaches, techniques and models that researchers have developed for the identification of cracks in concrete structural systems. All studies suggest that the region of crack identification in shafts is active and desperately needs more expertise to establish accurate techniques, despite the great advances that researchers have made in crack identification, because there is no accepted (or reliable) model or technique that can be used to identify all different types of cracks in mechanical shafts. Furthermore, the literature shows that more studies are required for modelling aspects of crack propagation and residual life estimation. Several investigations have been presented

using only numerical simulations which require to be validated experimentally.

Despite so much advancement in vibration based techniques, new and reliable fault diagnostics need to be developed in simulation tools. Investigations are required on the crack sensitivity variables for condition monitoring. Studies are needed to model a crack under the influence of the interaction of impact forces and surface friction due to the closing and opening of cracks during movement.

References

- [1] Liu W. and Barkey M. E, “Nonlinear vibrational response of a single edge cracked beam”, *Journal of Mechanical Science and Technology*, Vol. 31(11), pp. 5231–5243, 2017.
- [2] Zarfam R. and Khaloo A. R., “Vibration control of beams on elastic foundation under a moving vehicle and random lateral excitations,” *Journal of Sound and Vibration*, Vol. 331(6), pp. 1217–1232, 2012.
- [3] Li X. F., “Free vibration of axially loaded shear beams carrying elastically restrained lumped-tip masses via asymptotic Timoshenko beam theory,” *Journal of Engineering Mechanics*, Vol. 139(4), pp. 418–428, 2013.
- [4] Lee J. W. and Lee J. Y., “In-plane bending vibration analysis of a rotating beam with multiple edge cracks by using the transfer matrix method,” *Meccanica*, Vol. 52(4-5), pp. 1143–1157, 2016.
- [5] Nguyen S. H. and Chelidze D., “Dynamic Model for fatigue evolution in a cracked beam subjected to irregular loading,” *Journal of Vibration and Acoustics*, Vol. 139(1) , 2016.
- [6] Bovsunovsky A. P. and Matveev V. V., “Analytical approach to the determination of dynamic characteristics of a beam with a closing crack,” *Journal of Sound and Vibration*, Vol. 235(3), pp. 415–434, 2000.
- [7] <https://towardsdatascience.com/detection-of-surface-cracks-in-concrete-structures-using-deep-learning-f8f85cd8ac8b>, Date-12.11.2020.
- [8] <https://www.reocrete.com.au/6-different-types-of-cracks-in-concrete/12.11.2020>.
- [9] <https://concretesupplyco.com/6-concrete-cracks/>: Date-12.11.2020.

- [10] https://www.flexomeric.com/Types-of-Cracks-in-Concrete_ep_50.html, Date-12.11.2020.
- [11] Ruotolo R., Surace C., Crespo P., Storer D., “Harmonic analysis of the vibrations of a cantilevered beam with a closing crack”. *Computers and structures* , Vol. 61, pp 1057- 1074, 1996.
- [12] Owolabi G.M., Swamidas A. S.J. and Seshadri R., “Crack detection in beams using changes in frequencies and amplitudes of frequency response functions” *Journal of sound and vibration* , Vol. 265, pp.1-22, 2003.
- [13] Nahvi H., Jabbari M., “Crack detection in beams using experimental modal data and finite element model”, *International Journal of Mechanical Science* Vol. 47, pp. 1477-1497, 2005.
- [14] Chinchalkar S., “Determination of crack location in beams using natural frequencies”, *Journal of Sound and vibration*, Vol. 247(3), pp. 417-429, 2001.
- [15] Lawrence W.T., “Damage Assessment based on structural response function”, *Experimental Mechanics, Springer*, pp. 34-37, 1998.
- [16] Christides, S. and Barr, A.D.S., “One dimensional theory of cracked Bernoulli Euler beams”, *International Journal of Mechanical Science*, Vol. 26(11/12), pp. 639-648, 1984.
- [17] Chondros, T.G. and Demarogonas, A.D., “Identification of cracks in welded joints of complex structures”, *Journal of Sound and Vibration*, Vol. 69 (4), pp. 530-538 , 1980.

- [18] Ostachowicz W.M. and Krawczok M., “Analysis of the effect of cracks on the natural frequencies of cantilever beam”, *Journal of Sound and Vibration*, Vol. 150, pp. 191-201, 1991.
- [19] Adams R.D. and Cawley P. A, “Vibration technique for non-destructively assessing the integrity of structures”, *Journal of Mechanical Engineering Science*, Vol. 20(2), 93-100, 1978.
- [20] Liang, R.Y. and Choy, F.K., “Detection of cracks in beam structures using measurement of natural frequencies”, *Journal of Franklin Institute*, Vol. 328(4), pp. 505-518 , 1991.
- [21] Pandey A.K. and Biswas M., “Damage detection from changes in curvature mode shapes”, *Journal of Sound and Vibration*, Vol. 145(2), pp. 321-332, 1991.
- [22] Kam T.Y. and Lee T.V, “Detection of cracks in structures using modal test data”, *Engineering Fracture Mechanics*, Vol. 42 (2), pp. 381-38, 1991.
- [23] Chondros T.G. and Demarogonas A.D., “Vibration of a cracked cantilever beam”, *Journal of vibration and Acoustic*, Vol.120, pp. 742-746, 1998.
- [24] Sinou J. J., “Experimental Study on the Nonlinear Vibrations and nX Amplitudes of a Rotor with a Transverse Crack”, *ASME Journal of Vibration and Acoustics*, Vol. 131, pp. 041008-6, August 2009.
- [25] Dimarogonas A. D., “Vibration of cracked structures: a state of the art review,” *Engineering Fracture Mechanics*, Vol. 55(5), pp. 831–857, 1996.
- [26] Yang D. L., Yiu Y. L., Li S. B, et. al., “Fatigue crack growth prediction of 7075 aluminum alloy based on the GMSVR model optimized by the artificial

- bee colony algorithm,” *Engineering Computations*, Vol. 34(1), pp.1–14, 2017.
- [27] Jastrzebski, D. “Nature and Properties of Engineering Materials”, *John Wiley and Sons, Inc*, 1959.
- [28] Gercek H., "Poisson's ratio values for rocks", *International Journal of Rock Mechanics and Mining Sciences*. Vol. 44 (1), pp. 1–13, January 2007.
- [29] Park, RJT. Seismic Performance of Steel-Encased Concrete Piles
- [30] [https://en.wikipedia.org/wiki/Deformation_\(engineering\)](https://en.wikipedia.org/wiki/Deformation_(engineering)), Date-12.11.2020.
- [31] Ueda J., Asada H., “Castigliano Theorem: Modeling of cellular actuators”, ScienceDirect, 2017.
- [32] Timoshenko S., “History of strength of materials”, McGraw-Hill New York, 1953.
- [33] Truesdell, C., “The rational mechanics of flexible or elastic bodies Venditioni Exponunt Orell Fussli Turici”, pp. 1638–1788, 1960.
- [34] <https://learnaboutstructures.com/Bernoulli-Euler-Beam-Theory>, Date-15.11.2020.
- [35] Timoshenko S.P., “On the correction for shear of the differential equation for transverse vibrations of prismatic bars”, *Phil. Mag. Series*, Vol. 6(41) pp. 744–746, 1921.
- [36] Timoshenko S.P., “On the transverse vibrations of bars of uniform cross sections”, *Phil. Mag.Series* Vol. 6(43) pp. 125–131, 1922.

- [37] Li X.F., “A unified approach for analyzing static and dynamic behavior of functionally graded Timoshenko and Euler–Bernoulli beams”, *J. Sound Vib.* Vol. 318, pp. 1210–1229, 2008.
- [38] Tessler A., DiSciuva M. , Gherlone M., “Refinement of Timoshenko beam theory for composite and sandwich beams using zigzag kinematics”. *NASA/TP-2007-215086*, 2007.
- [39] Arash B., Wang Q., “A review on the application of nonlocal elastic models in modeling of carbon nanotubes and graphenes”, *Comput. Mater. Sci.* Vol. 51, pp. 303–313, 2012.
- [40] Elishakoff I., “Handbook on Timoshenko-Ehrenfest Beam and Uflyand-Mindlin Plate Theories”, *World Scientific, Singapore*, ISBN 978-981-3236- Vol. 51(6), 2020.
- [41] Binns K.J., Lawrenson P.J., “Analysis and Computation of Electric and Magnetic Field Problems” *Pergamon Press*, 1973.
- [42] Grossmann C., Roos H. G., Stynes M., “Numerical Treatment of Partial Differential Equations”, *Springer Science and Business Media*. pp.23. ISBN 978-3-540-71584-9, 2007.
- [43] Bruch E.K. “Introduction to the Boundary Element Method. In: The Boundary Element Method for Groundwater Flow”. *Springer, Berlin, Heidelberg*. Vol. 70, 1991.
- [44] https://en.wikipedia.org/wiki/Finite_element_method-Date-12.11.2020.
- [45] Shukla A., Singh A. K., Singh P., “A Comparative Study of Finite Volume Method and Finite Difference Method for Convection-Diffusion Problem”,

American Journal of Computational and Applied Mathematics ,Vol. 1(2), pp. 67-73, 2011.

- [46] Hrennikoff, A., “Solution of problems of elasticity by the framework method”. *Journal of applied mechanics* , Vol. 8(4), pp. 169–175, 1941
- [47] Courant, R., “Variational methods for the solution of problems of equilibrium and vibrations”, *Bulletin of the American Mathematical Society*, Vol.49, pp. 1–23, 1943.
- [48] Strang, G., “An Analysis of the Finite Element Method”, *Prentice Hall*, 1973.
- [49] Kiritsis, Eemmanouilidis D. , Koronios C., Mathew A. J., “Engineering Asset Management” , *Proceedings of the 4th World Congress on Engineering Asset Management (WCEAM)*, pp. 591-592, 2009.
- [50] https://www.tutorialspoint.com/modelling_and_simulation/modelling_and_simulation_quick_guide.htm
- [51] Introduction to COMSOL Multiphysics. U.S. Patents 7, 519, 518; 7, 596, 474 and 7, 623, 991. Patents Pending, *Version: COMSOL4.2a, 2011*, Part No. CM010004.
- [52] Kim M-B, Zhao M., “Study on crack detection of beam using harmonic responses”, *Proceedings of the 2004 International conference on Intelligent Mechatronics and Automation*, 26-31 August 2004, Chengdu, China, pp. 72–6, 2004.
- [53] Young, Myung S. L. and Chung J., “A study on crack detection using eigen frequency test data”, *Computers and Structures*, Vol. 77, pp. 327-342, 2000.

- [54] Owolabi , G. M., Swamidas, A. S. J., and Seshadri, R. “Crack detection in beams using changes in frequencies and amplitudes of frequency response functions”, *Journal of Sound and Vibration*, Vol. 265, pp. 1-22, 2003.
- [55] Nahvi H., Jabbari M., “Crack detection in beams using experimental modal data and finite element model”, *International Journal of Mechanical Sciences*, Vol. 47, pp. 1477–1497, 2005.
- [56] Goda I., Ganghoffer J.F., Aly M. F., “Parametric Study on the Free Vibration Response of Laminated Composite Beams, Mechanics of Nano, Micro and Macro Composite Structures”, *Politecnico di Torino*, pp.18- 20, 2012.
- [57] Prasad H. K., Kumar M. S., “Studies on Effect of Change in Dynamic Behavior of Crack using FEM”, *International Journal of Recent Trends in Engineering*, Vol. 1, pp. 137-141, 2009.
- [58] Rizos R.F., Aspragathos N., Dimarogonas A.D., “Identification of crack location and magnitude in a cantilever beam from the vibration modes”, *Journal of Sound and Vibration* , Vol. 138(3), pp. 381–388, 1990.
- [59] Lee J., “Identification of a crack in a beam by the boundary element method”, *Journal of Mechanical Science and Technology*, Vol. 24 (3), pp. 801-804, 2010.
- [60] Owolabi G.M., Swamidas A.S.J., R. Seshadri, “Crack detection in beams using changes in frequencies and amplitudes of frequency response functions”, *Journal of Sound and Vibration*, Vol. 265 (1), pp. 1–22, 2003.
- [61] Kisa M., Brandon J. and Topcu M., “Free vibration analysis of cracked beams by a combination of finite elements and component mode synthesis methods”, *Computers and Structures*, Vol. 67, pp. 215-223, 1998.

- [62] Ratcliffe, C.P., “Damage detection using a modified Laplacian operator on mode shape data”, *Journal of Sound and Vibration*, Vol. 204(3), pp. 505-517, 1997.
- [63] Çam E., Sadettin O. and Murat L., “An analysis of cracked beam structure using impact echo method”, *NDT and E International*, Vol. 38, pp.368–373, 2005.
- [64] Shayanfar M, et al. Damage detection of bridge structures in time domain via enhanced colliding bodies optimization, *International Journal Optimization of Civil Engineering* ,Vol. 6(2), pp. 211-26, 2016.
- [65] Sabuncu M, Ozturk H, Yashar A., “Static and dynamic stability of cracked multi-storey steel frames”, *Struct Eng Mech*, Vol. 58(1), pp. 103-19, 2016.
- [66] Dharmaraju N., Tiwari R. and Talukdar S., “Identification of an open crack model in a beam based on force–response measurement”, *Computers and Structures*, Vol. 82, pp.167–179, 2004.
- [67] Sekhar A.S., “Multiple cracks effects and identification”, *Mechanical Systems and Signal Processing*, Vol. 22, pp. 845-878, 2008.
- [68] Chasalevris A.C., Papadopoulos C.A., “Coupled horizontal and vertical bending vibrations of a stationary shaft with two cracks”, *Journal of Sound and Vibration*, Vol. 309, pp. 507-528, 2008.
- [69] Singh S.K., Tiwari R.,” Identification of a multi-crack in a shaft system using transverse frequency response functions”, *Mechanism and Machine Theory*, Vol. 45, pp. 1813-1827, 2010.

- [70] Al-Shudeifat M.A., “On the finite element modeling of the asymmetric cracked rotor”, *Journal of Sound and Vibration*, Vol. 332, pp. 2795-2807, 2013.
- [71] Mayes I. W., Davies W.G.R., “Analysis of the Response of a Multi-Rotor-Bearing System Containing a Transverse Crack in a Rotor”, *Journal of Vibration, Acoustics, Stress and Reliability in Design*, Vol. 106, pp. 139-145, 1984.
- [72] Machorro-López J.M., Adams D. E., Gómez-Mancilla J. C. and Gul K. A., “Identification of damaged shafts using active sensing-Simulation and experimentation”, *Journal of Sound and Vibration*, Vol. 327, pp. 368-390, 2009.
- [73] Chondros T.G., Dimarogonas A.D., Yao J., “A continuous cracked beam vibration theory”, *Journal of Sound Vibration*, Vol. 215(1), pp. 17-34, 1998.
- [74] Papadopoulos C.A. , Dimarogonas A.D., “Coupled longitudinal and bending vibrations of a rotating shaft with an open crack”, *Journal of Sound Vibration* Vol. 117(1), pp. 81-93,1987.
- [75] Aktas M, Sumer Y., “Nonlinear finite element analysis of damaged and strengthened reinforced concrete beams”, *Journal of Civil Engineering and Management* , Vol. 20(2), pp. 201-10, 2014.
- [76] Gerist S, Naserlavi S, Salajegheh E., “Basis pursuit based genetic algorithm for damage identification”, *International Journal of Optimization in Civil Engineering*, Vol. 2(2), pp.301-19, 2012.
- [77] Jena S.P., Parhi D.R., Mishra D., “Comparative study on cracked beam with different types of cracks carrying moving mass”, *Structural Engineering of Mechanical*, Vol. 56(5): pp. 797-811, 2015.

- [78] Ryu, E., Kang, J., Lee, J. et al., “Automated Detection of Surface Cracks and Numerical Correlation with Thermal-Structural Behaviors of Fire Damaged Concrete Beams”. *International Journal of Concrete Structural Mater* Vol. 14, pp. 12, 2020.
- [79] Saffar A. A. A., Neamah R.A., Luay S. A., “Numerical and Experimental Analysis of Cracked Cantilever Beam under Free Vibration”, *Journal of Mechanical Engineering Research and Developments (JERDFO)*, Vol. 43(5), pp. 415-427, 2020.
- [80] Sahu S., Rohini B., "Free Vibration Analysis of Cantilever Beams with Transvers Open Cracks". *Proceedings of National Conf. on Recent Innovations in Science Engineering and Technology*, 13th Sept, Bengaluru, India, pp. 23-25, 2015.
- [81] Liu T., Huang H., Yang Y., "Crack Detection of Reinforced Concrete Member Using Rayleigh-Based Distributed Optic Fiber Strain Sensing System", *Advances in Civil Engineering*, Vol. 2020, Article ID 8312487, 11 pages, 2020.
- [82] Chaudhari C. C., Gaikwad J. A., Bhanuse V. R. and Kulkarni J. V., "Experimental investigation of crack detection in cantilever beam using vibration analysis," *First International Conference on Networks and Soft Computing (ICNSC2014)*, Guntur, pp. 130-134, 2014.
- [83] Saleh F., Fragomeni S., Tran D., and Prayuda1 H., “Crack Detection in Reinforced Concrete Beam Structures Based on The Highest Mode Shapes Subjected to Incremental Loads”, *Geotechnique, International Journal of Construction Materials and Environment (GEOMATE)*, Vol. 17(64), pp. 85 – 92, December 2019.

- [84] Long H, Liu Y., Huang C. , Wu W. and Li Z., "Modelling a Cracked Beam Structure Using the Finite Element Displacement Method", *Shock and Vibration*, Vol. 2019, Article ID 7302057, 13 pages, 2019.

- [85] Jiang T., Hong Y., Zheng J., Wang L. and Gu H., ‘Crack Detection of FRP-Reinforced Concrete Beam Using Embedded Piezoceramic Smart Aggregates’ , *Journal ListSensors*, ,Vol. 19(9), pp. 1979, 2019.

- [86] Zhang, Qinghua and Xiong, Ziming., “Crack Detection of Reinforced Concrete Structures Based on BOFDA and FBG Sensors”. *Shock and Vibration*. Vol. 2018, pp. 1-10, 2018.

CHAPTER III

COMPUTATIONAL MODELING OF A CRACKED BEAM WITH DIFFERENT LOCATION

CHAPTER III

COMPUTATIONAL MODELING OF A CRACKED BEAM WITH DIFFERENT LOCATION

3.1 Introduction

Nowadays Concrete is used literally to develop the growing infrastructural, structural and in civil engineering industries [1]. But the presence of a crack indicate a serious threat to the performance of structures. A crack in an elastic structural element like concrete, steel, iron etc introduces considerable local flexibility due to the strain energy concentration in the vicinity of the crack tip under load [2]. Since most of the structural failures are due to presence of crack or material fatigue. For this reason, methods allowing early detection and localization of cracks have been the subject of intensive investigation. Coherent ultrasonic methods have been found ineffective in concrete due to its high concentration of scatterers and heterogeneous nature, so a different approach is needed [3]. So, as a promising tool Vibration analysis has been emerged for monitoring and classification of damage in machine and equipment. This technique is well prepared for solving inverse variational problems in the context of monitoring and crack detection because of their pattern recognition and interpolation capabilities. A crack in a structural member introduces local flexibility that would affect vibration response of the structure [5]. This property may be used to detect existence of a crack together its location and depth in the structural member.

Vibration analysis on a beam with and without crack is carried out in this work. These cracks introduce new boundary conditions for the structures at the location of the cracks. These boundary conditions are derived from strain energy equation using Castiligiano's theorem. Presence of crack also causes reduction of stiffness of the structures which has been derived from stiffness matrix [4]. Euler-Bernoulli beam theory is used for dynamic characteristics of beams with transverse

cracks. Modified boundary conditions due to presence of crack have been used to find out the theoretical expressions for natural frequencies and mode shape for the beams. It causes reduction in natural frequencies and changes in mode shapes of vibrations. Any analysis of these changes makes it possible to identify cracks.

The purpose of the present work is to establish a method for predicting the location and depth of a crack in a cantilever beam using experimental vibration data and to establish the mode shape curvatures behavior of a composite beam with a transverse open crack subjected to free vibration. We will follow the discussion with solutions of beam subjected to distribute loading and comparing finite element solution to an exact solution for a beam subjected to a distributed loading.

3.2 Stiffness Matrix

Familiarity with the stiffness matrix is essential to understanding the stiffness method. We define the stiffness matrix as follows: For an element, a stiffness matrix $[k]$ is a matrix such that

$$\{f\} = [k]\{d\}$$

Where $[k]$ relates nodal displacements $\{d\}$ to nodal forces $\{f\}$ of a single element, such as the spring. For a continuous medium or structure comprising a series of elements, stiffness matrix $[K]$ relates global coordinate (x,y,z) nodal displacements $\{d\}$ to global forces $\{F\}$ of the whole medium or structure, such that

$$\{F\} = [K]\{d\}$$

Where $[K]$ represents the stiffness matrix of the whole body assemblage.

3.3 Beam Stiffness

A beam is a long, slender structural member generally subjected to transverse loading that produces significant bending effects as opposed to twisting or axial

effects. This bending deformation is measured as a transverse displacement and a rotation.

Consider the beam element shown in the following Figure 3.1. The beam is of length L with axial local coordinate x and transverse local coordinate y . The local transverse nodal displacements are given by v_i and the rotations by θ_i . The local transverse nodal displacements are given by q_i and the bending moments by m_i as shown. We infinitely neglect all axial effects.

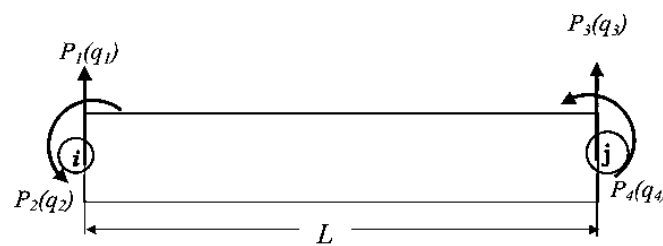


Figure 3.1: Beam theory sign conventions for shear forces and bending moments

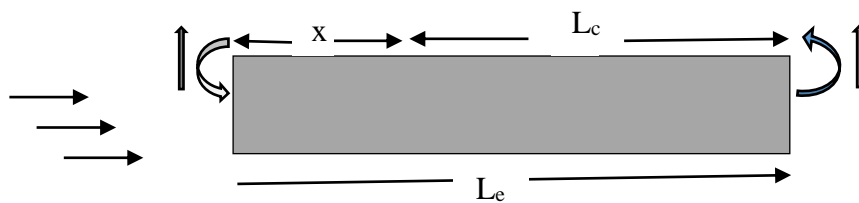


Figure 3.2: Beam element with positive nodal displacement, rotations, forces and moments

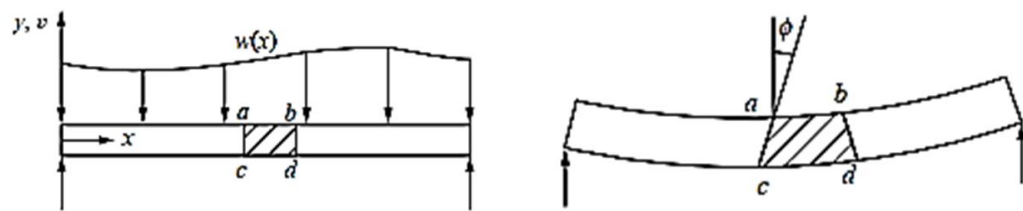
At all nodes, the following sign conventions are used:

1. Moments are positive in the counterclockwise direction.
2. Rotations are positive in the counterclockwise direction.
3. Forces are positive in the positive y direction
4. Displacements are positive in the positive y direction.

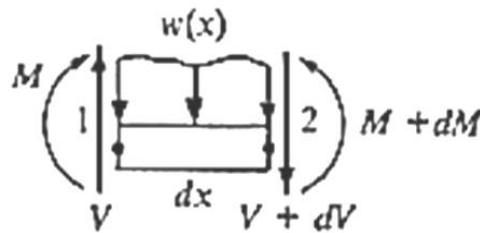
Figure 3.2 indicates the sign conventions used in simple beam theory for positive shear forces V and bending moments m .

3.4 Beam Stiffness Matrix Based on Euler-Bernoulli Beam theory

The differential equation governing elementary linear-elastic beam behavior which is called Euler-Bernoulli beam is based on plane cross sections perpendicular to the longitudinal centroidal axis of the beam before bending occurs remaining plane and perpendicular to the longitudinal axis after bending occurs. In the Figure 3.3 ,where a plane through vertical line a-c (Figure 3.3(a)) is perpendicular to the longitudinal x axis before bending, and this same plane through a-c (rotating through angle ϕ in Figure 3.3(b)) remains perpendicular to the bent x axis after bending. This occurs in practice only when a pure couple or constant moment exists in the beam. However it is a reasonable assumption that yields equations quite accurately predict beam behavior for most practical beams.



(a) Undeformed beam under load $w(x)$ (b) Deformed beam due to applied loading



(c) Differential beam element

Figure 3.3: Beam under distributed load

The different differential equation is derived as follows. Consider the beam shows in Figure 3.3 subjected to a distributed loading $\omega(x)$ (force/length). From the force and

moment equilibrium of a differential element of the beam, show in Figure 3.3(c) we have,

$$\sum F_y = 0: V - (V + dV) - \omega(x)dx = 0 \quad (3.1)$$

$$\text{Or, } -dV - \omega(x)dx = 0$$

$$\text{Or, } \omega(x) = -\frac{dV}{dx} \quad (3.2)$$

$$\sum M_2 = 0: -Vdx + dM + \omega(x)dx \frac{dx}{2} = 0$$

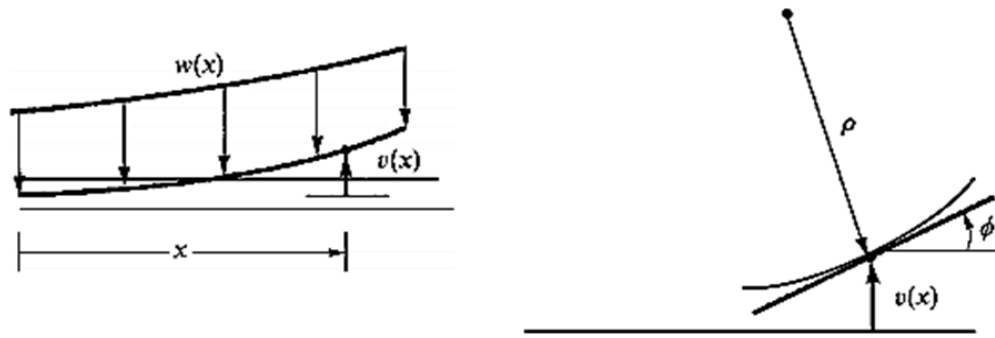
$$\text{Or, } V = \frac{dM}{dx} \quad (3.3)$$

The final form of equation (3.3) relating the shear force to the bending moment, is obtained by dividing the left equation by dx and then taking the limit of the equation as dx approaches 0. The $\omega(x)$ term then disappears.

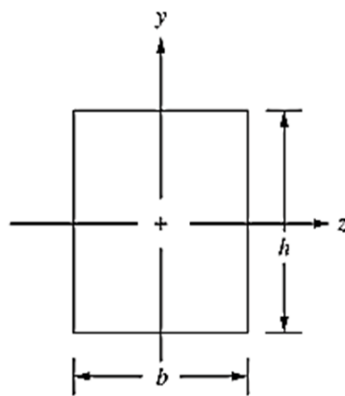
Also, the curvature κ of the beam is related to the moment by

$$\kappa = \frac{1}{\rho} = \frac{M}{EI} \quad (3.4)$$

Where ρ is the radius of the deflected curve shown in the Figure 3.4, v is the transverse displacement function in the y -direction, E is the modulus of elasticity and I is the principle moment of inertia about z -axis (where the z -axis is perpendicular to the x and y axes). ($I = \frac{bh^3}{12}$ for a rectangular cross section of base b and height h shown in Figure 3.4(c)).



(a) Portion of deflected curve of beam

(b) Radius of deflected curve at $v(x)$ 

(c) Typical rectangular cross section of beam

Figure 3.4: Deflected curve of beam

The curvature for small slope $\phi = \frac{dv}{dx}$ is given by

$$\kappa = \frac{d^2v}{dx^2} \quad (3.5)$$

Using equation (3.4) and (3.5) we obtain

$$\frac{d^2v}{dx^2} = \frac{M}{EI} \quad (3.6)$$

Solving equation (3.6) for M and substituting this result into (3.3) and (3.4) we obtain

$$\frac{d^2}{dx^2} \left[EI \frac{d^2 v}{dx^2} \right] = -\omega(x) \quad (3.7)$$

For constant EI and only nodal Forces and Moments equation (3.7) becomes

$$EI \frac{d^4 v}{dx^4} = 0 \quad (3.8)$$

We will now follow the steps to develop the stiffness matrix and equations for a beam element and then to illustrate complete solutions for beam.

3.5 Mathematical Model

The principle that certain variables can be tracked within a physical system is a fundamental instrument for deriving the equations of analytical mathematics and physics. Popular examples include mass, energy, and balance of strength or force conservation. We can now derive differential equations for detecting any failure in order to familiarize themselves with this way of thinking. The modeling of all these physical phenomena leads to the issue of the two-point boundary value, as we can see. Many physical phenomena are described by the same partial differential equations, and therefore the methods and mathematical theory can often be developed for certain model problems and still be applied to a wide range of different applications [6].

A mathematical model is developed on the basis of a unified boundary-integral approach for the main stages of the non-destructive process of deepened three-dimensional crack detection with arbitrary orientation in a homogeneous medium and horizontal interface cracks detection. The construction of source field asymptotics and the calculations of both load dissipation coefficient and deflection are described.

The equation of motion in matrix form for vibration of a beam under load is given by [11],

$$[M] \left\{ \frac{d^2 q(x)}{dx^2} \right\} + [K] - P[K_g] \{q\} = 0 \quad (3.9)$$

Where,

$[M]$ = Consistent mass matrix

$[K]$ = Bending stiffness matrix of the beam

$[K_g]$ = Geometric stiffness matrix

$\{q\}$ = Displacement vector

P = External force vector

For free vibration the forcing function $P = 0$. So the Equation (3.9) can be written as [11],

$$[M] \left\{ \frac{d^2 q(x)}{dx^2} \right\} + [K] \{q\} = 0 \quad (3.10)$$

In-plane, the load $P(t)$ can be expressed in the form as shown below,

$$P(t) = P_s + P_t \cos \Omega t \quad (3.11)$$

Where,

P_s = the static portion of P .

P_t = the amplitude of the dynamic portion of P and

Ω = the frequency of excitation.

Equation (3.10) represents an eigen value problem and the roots of the equation give rise to square of the natural frequency given by the equation,

$$[K] - (\omega_n)^2 [M] = 0 \quad (3.12)$$

3.6 Finite Element Approximation

We will now follow the steps to develop the stiffness matrix and equations for a beam element and then to illustrate complete solutions for beam.

Step-01: Discretization and Topology of Finite Element Mesh

In this analysis two noded beam elements with two degree of freedom (slope and deflection) per node is considered [7].

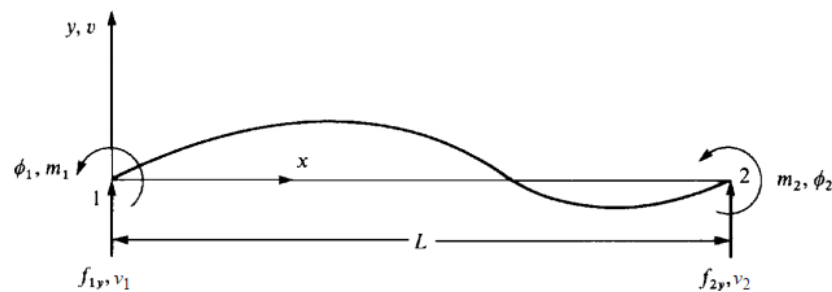


Figure 3.5: Beam element with positive nodal displacement, rotations, forces and moments

Suppose that we divide the beam into 3 equally spaced elements and represent the beam by labeling nodes at each end and in general by labeling the element number. Within each element, there are 2 nodes (left and right ends). Then, we design a global numbering scheme for the elements and nodes.

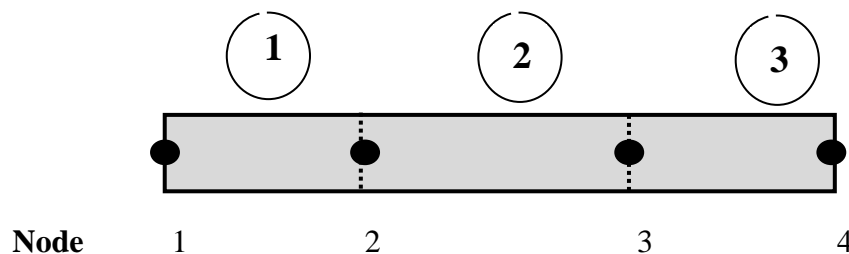


Figure 3.6: Two noded beam with 3 elements with two degree of freedom

Once the numbering scheme has been established for a finite element mesh, we must create the system's topology – the element definition. This topology tells how the elements are joined together. On the element level, the topology is simply the ordered numbering of the nodes. Table 3.1 illustrates the system topology that has been established for our model. This information can be easily stored into a two dimensional matrix with each row storing the topology of one element.

Table 3.1: System Topology of elements

Element	Numbering Scheme	
	Local	Global
1	i j	1 2
2	i j	2 3
3	i j	3 4

Step-02: Select a Displacement Function

The transverse displacement model taken as the polynomial as the polynomial which is itself a cubic equation

$$v(x) = a_1 x^3 + a_2 x^2 + a_3 x + a_4 \quad (3.13)$$

The complete cubic displacement function equation (3.13) is appropriate because there are four total degrees of freedom (a transverse displacement v_i and a small rotation ϕ_i at each node). The cubic function also satisfies the basic beam differential equation further justifying its selection. In addition, the cubic function also satisfies the conditions of displacement and slope continuity at nodes shared by two elements.

Using the same procedure, we can express v as a function of the nodal degrees of freedom v_1, v_2, φ_1 and φ_2 as follows:

$$\left. \begin{aligned} v(0) &= v_1 = a_4 \\ \frac{dv(0)}{dx} &= \varphi_1 = a_3 \\ v(L) &= v_2 = a_1 L^3 + a_2 L^2 + a_3 L + a_4 \\ \frac{dv(L)}{dx} &= \varphi_2 = 3a_1 L^2 + a_2 L + a_3 \end{aligned} \right\} \quad (3.14)$$

Where $\varphi = dv/dx$ for the assumed small rotation φ .

So we write it in the matrix form,

$$\begin{bmatrix} a_1 \\ a_2 \\ a_3 \\ a_4 \end{bmatrix} = \begin{bmatrix} \frac{2}{L^3} & \frac{1}{L^2} & \frac{-2}{L^3} & \frac{1}{L^2} \\ \frac{-3}{L^2} & \frac{-2}{L} & \frac{3}{L^2} & \frac{-1}{L} \\ 0 & 1 & 0 & 0 \\ 1 & 0 & 0 & 0 \end{bmatrix} \begin{bmatrix} v_1 \\ \varphi_1 \\ v_2 \\ \varphi_2 \end{bmatrix}$$

Solving equations (3.14) for a_1 through a_4 in terms of the nodal degrees of freedom and substituting into equation (3.13) we have,

$$v = \frac{2}{L^3}(v_1 - v_2) + \frac{1}{L^2}(\varphi_1 + \varphi_2)x^3 - \frac{3}{L^2}(v_1 - v_2) - \frac{1}{L}(2\varphi_1 + \varphi_2)x^2 + \varphi_1 x + v_1 \quad (3.15)$$

In matrix form we express equation (3.15) as,

$$v = [N] \times \{d\} \quad (3.16)$$

Where,

$$\{d\} = \begin{Bmatrix} v_1 \\ \varphi_1 \\ v_2 \\ \varphi_2 \end{Bmatrix} \quad (3.17)$$

$$\text{and } [N] = [N_1 \quad N_2 \quad N_3 \quad N_4] \quad (3.18)$$

So,

$$\left. \begin{aligned} [N_1] &= \frac{1}{L^3} (2x^3 - 3x^2L + L^3) \\ [N_2] &= \frac{1}{L^3} (x^3L - 2x^2L^2 + xL^3) \\ [N_3] &= \frac{1}{L^3} (-2x^3 + 3x^2L) \\ [N_4] &= \frac{1}{L^3} (x^3L - x^2L^2) \end{aligned} \right\} \quad (3.19)$$

N_1 , N_2 , N_3 and N_4 are called the shape function for a beam element. These cubic shape functions are known as Hermite cubic interpolation or cubic spline functions. For the element $N_1=1$ when evaluated at node 1 and $N_1=0$ when evaluated at node 2. Because N_2 is associated with ϕ_1 . We have from the second of equations (3.19), $\frac{dN_2}{dx} = 1$ when evaluated at node 1. Shape functions N_3 and N_4 have analogous results for node 2.

Step-03: Determination of Strain vs Displacement and Stress vs Displacement Relationships

Assume the following axial strain/displacement relationship to be valid:

$$\varepsilon_x(x, y) = \frac{du}{dx} \quad (3.20)$$

Where u is the axial displacement function.

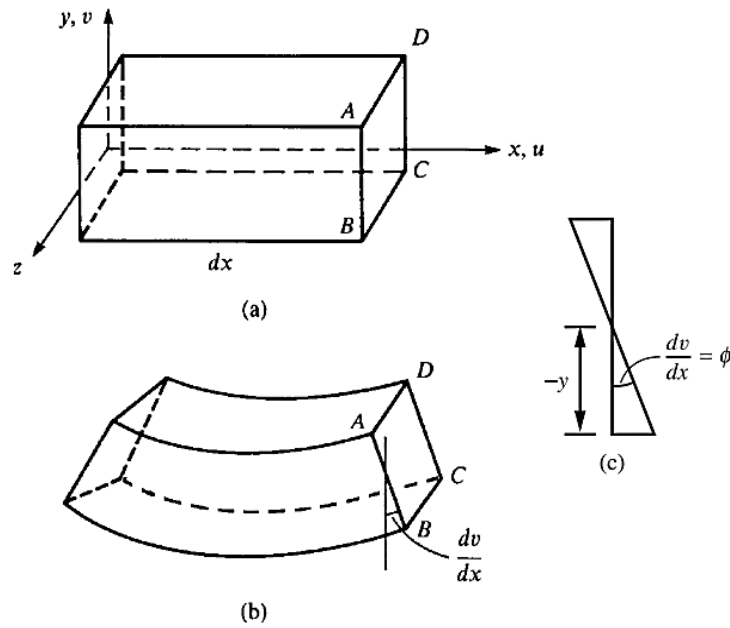


Figure 3.7: Beam segment (a) before deformation and (b) after deformation; (c) Angle of rotation of cross section ABCD

From the deformed configuration of the beam shown in Figure 3.7 we relate the axial displacement to the transverse displacement by,

$$u = -y \frac{dv}{dx} \quad (3.21)$$

Where we should recall from elementary beam theory [8] the basic assumption that cross sections of the beam that are planar before bending deformation remain planar and in general rotate through a small angle $\frac{dv}{dx}$. Using (3.20) and (3.21) we obtain,

$$\varepsilon_x(x, y) = -y \frac{d^2v}{dx^2} \quad (3.22)$$

Also using Hook's law ($\sigma_x = E\varepsilon_x$) and substituting $\frac{d^2v}{dx^2} = \frac{M}{EI}$ into equation (3.22), we obtain the beam flexure or bending stress formula as,

$$\sigma_x = \frac{-My}{I} \quad (3.23)$$

3.6.1 String beam theory

For elementary String beam theory, the bending moment and shear force are related to the transverse displacement function. This theory is useful to determine the force, moment, deflection and twist along the fifth metatarsal when it is subjected to both a point wise and a distributed load by using Young's Modulus and Moments of Inertia. Because we will use these relationships in the derivation of the beam element stiffness matrix, we now present them as,

$$m(x) = EI \frac{d^2 v}{dx^2} \quad \text{and} \quad V = EI \frac{d^3 v}{dx^3} \quad (3.24)$$

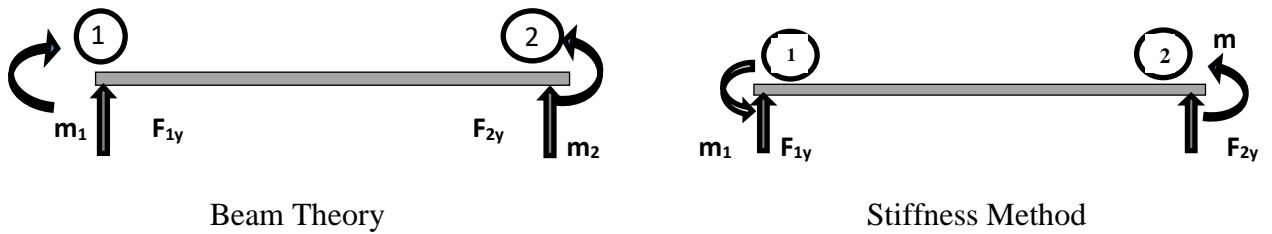


Figure 3.8: Load and diffusion of beam by applying Beam Theory and Stiffness Method

Step-04: Derivation of the Element Stiffness Matrix and Equations

At first we derive the element stiffness matrix and equations using a direct equilibrium approach. We now relate the nodal and beam theory sign conventions for shear forces and bending moments along with equation (3.15) and (3.24) to obtain,

$$\left. \begin{aligned}
 F_{1,y} = V(0) &= EI \frac{d^3 v(0)}{dx^3} = \frac{EI}{L^3} (12v_1 + 6L\phi_1 - 12v_2 + 6L\phi_2) \\
 m_1 = -m &= -EI \frac{d^2 v(0)}{dx^2} = \frac{EI}{L^3} (6Lv_1 + 4L^2\phi_1 - 6Lv_2 + 2L^2\phi_2) \\
 F_{2,y} = -V(0) &= -EI \frac{d^3 v(L)}{dx^3} = \frac{EI}{L^3} (12v_1 - 6L\phi_1 + 12v_2 - 6L\phi_2) \\
 m_2 = m &= EI \frac{d^2 v(L)}{dx^2} = \frac{EI}{L^3} (6Lv_1 + 2L^2\phi_1 - 6Lv_2 + 4L^2\phi_2)
 \end{aligned} \right\} \quad (3.25)$$

Where the minus signs in the second and third of equations (3.25) are the result of opposite nodal and beam theory positive bending moment conventions at node 1 and opposite nodal and beam theory positive shear force conventions at node 2. Equations (3.25) relate the nodal forces to the nodal displacements.

In matrix form equations (3.25) become

$$\begin{Bmatrix} F_{1,y} \\ m_1 \\ F_{2,y} \\ m_2 \end{Bmatrix} = \frac{EI}{L^3} \begin{bmatrix} 12 & 6L & -12 & 6L \\ 6L & 4L^2 & -6L & 2L^2 \\ -12 & -6L & 12 & -6L \\ 6L & 2L^2 & -6L & 4L^2 \end{bmatrix} \begin{Bmatrix} v_1 \\ \phi_1 \\ v_2 \\ \phi_2 \end{Bmatrix} \quad (3.26)$$

Where the Stiffness Matrix is then

$$[K^*] = \frac{EI}{L^3} \begin{bmatrix} 12 & 6L & -12 & 6L \\ 6L & 4L^2 & -6L & 2L^2 \\ -12 & -6L & 12 & -6L \\ 6L & 2L^2 & -6L & 4L^2 \end{bmatrix} \quad (3.27)$$

3.6.2 Elemental Stiffness matrix for Uncracked Beam

The stiffness matrix for 2 degree of freedom (v, θ) for bending in the xy -plane for a two-noded Timoshenko beam finite element with shear deformation is line with as [9],

$$[K] = \frac{EI}{L(L^2 + 12\beta)} \begin{bmatrix} 12 & 6L & -12 & 6L \\ 6L & 4L^2 + 12\beta & -6L & 2L^2 - 12\beta \\ -12 & -6L & 12 & -6L \\ 6L & 2L^2 - 12\beta & -6L & 4L^2 + 12\beta \end{bmatrix} \quad (3.28)$$

Where,

L = Length of the element

E = Young's modulus of elasticity

I = Moment of inertia of the section with respect to z-axis,

And,

$$\beta = \frac{EI}{\kappa GA}$$

Where,

κ = shear correction factor

G = the shear modulus

A = area of the cross - section of the element

For Free Vibration:

$$\alpha = 0, \beta = 0$$

Hence,

$$[K] = \frac{EI}{L^3} \begin{bmatrix} 12 & 6L & -12 & 6L \\ 6L & 4L^2 & -6L & 2L^2 \\ -12 & -6L & 12 & -6L \\ 6L & 2L^2 & -6L & 4L^2 \end{bmatrix} \quad (3.29)$$

3.6.3 Elemental Mass matrix for Uncracked beam

$$[M] = \int_0^L [N]^T [\rho A] [N] dx$$

$$\text{Or, } [M] = \frac{\rho A l}{420} \begin{bmatrix} 156 & 22l & 54 & -13l \\ 22l & 4l^2 & 13l & -3l^2 \\ 54 & 13l & 156 & -22l \\ -13l & -3l^2 & -22l & 4l^2 \end{bmatrix} \quad (3.30)$$

Where,

ρ = Mass density of the beam material

A = Cross-sectional area of the beam element

3.6.4 Stiffness Matrix for a Cracked Beam Element

The key problem in using FEM is how to accurately obtain the stiffness matrix for the cracked beam element. The most feasible method is to obtain the total flexibility matrix first and then take inverse of it. The total flexibility matrix of the cracked beam element includes two parts. The first part is original flexibility matrix of the intact beam. The second part is the additional flexibility matrix due to the existence of the crack, which leads to energy release and additional deformation of the structure. Elements of the overall additional flexibility matrix C_{ovl} .

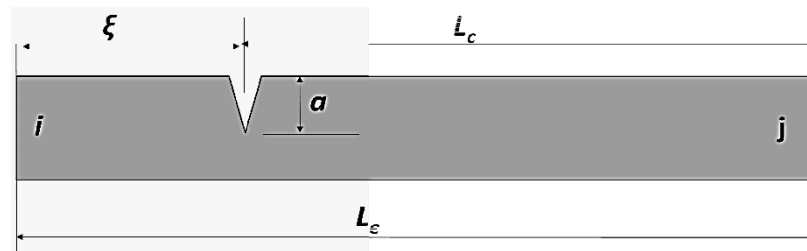


Figure 3.9: Typical Cracked beam element subject to shearing force and bending moment.

The above Figure 3.9 shows a typical cracked beam element with a rectangular cross section. Two side end node i and j is assumed to be fixed, while the middle portion is free.

b = Breath of the beam

h = Depth of the beam

a = crack depth

L_c = Distance between the right hand side end node j and the crack location

L_e = Length of the beam element

ξ = Distance of the crack from left hand side end node i

A = Cross-sectional area of the beam

I = Moment of inertia

According to Dimarogonas [10] the additional strain energy due to existence of crack can be expressed as,

$$\Pi_c = \int_A G dA_c \quad (3.31)$$

Where,

G = the strain energy release rate and

A_c = the effective cracked area.

$$G = \frac{1}{E'} \left[\left(\sum_{n=1}^2 K_{In} \right)^2 + \left(\sum_{n=1}^2 K_{IIIn} \right)^2 + k \left(\sum_{n=1}^2 K_{IIIIn} \right)^2 \right] \quad (3.32)$$

Where,

$E' = E$ for plane stress

$= \frac{E}{1-\nu^2}$ for plane strain

$k = 1 + \nu$

K_I , K_{II} and K_{III} = stress intensity factors for opening, sliding and tearing type cracks respectively.

$$G = \frac{1}{E'} \left[(K_{I1} + K_{I2})^2 + K_{III1}^2 \right] \quad (3.33)$$

The expressions for stress intensity factors from earlier studies are given by,

$$\left. \begin{aligned} K_{I1} &= \frac{6P_1 L_c}{bh^2} \sqrt{\pi \xi} F_1 \left(\frac{\xi}{h} \right) \\ K_{I2} &= \frac{6P_2}{bh^2} \sqrt{\pi \xi} F_1 \left(\frac{\xi}{h} \right) \\ K_{III1} &= \frac{P_2}{bh} \sqrt{\pi \xi} F_{II} \left(\frac{\xi}{h} \right) \end{aligned} \right\} \quad (3.34)$$

Where,

$$\left. \begin{aligned} F_I(s) &= \sqrt{\frac{\tan\left(\frac{\pi s}{2}\right)}{\left(\frac{\pi s}{2}\right)}} \left[\frac{0.923 + 0.199 \left(1 - \sin\left(\frac{\pi s}{2}\right)\right)^4}{\cos\left(\frac{\pi s}{2}\right)} \right] \\ F_{II}(s) &= \frac{1.122 - 0.561s + 0.085s^2 + 0.180s^3}{\sqrt{1-s}} \end{aligned} \right\} \quad (3.35)$$

Here, $S = \frac{\xi}{h}$ (crack depth during the process of penetrating from zero to final depth),

and $F_I(s)$ and $F_{II}(s)$ are the correction factors for stress intensity factors.

From definition, the elements of the overall additional flexibility matrix C_{ij} can be expressed as,

$$C_{ij} = \frac{\partial \delta_i}{\partial P_j} = \frac{\partial^2 \Pi_C}{\partial P_i \partial P_j} \quad (i, j=1, 2) \quad (3.36)$$

Substituting Equation (3.33) in Equation (3.34) and subsequently in Equation (3.31) we get,

$$C_{ij} = \frac{b}{E'} \frac{\partial^2}{\partial P_i \partial P_j} \int \left[\left\{ \frac{6P_1 L_C}{bh^2} \sqrt{\pi \xi} F_I\left(\frac{\xi}{h}\right) + \frac{6P_2}{bh^2} \sqrt{\pi \xi} F_I\left(\frac{\xi}{h}\right) \right\}^2 + \left\{ \frac{P_1}{bh} \sqrt{\pi \xi} F_{II}\left(\frac{\xi}{h}\right) \right\}^2 \right] d\xi \quad (3.37)$$

Substituting i, j (1,2) values, we get

$$\left. \begin{aligned} C_{11} &= \frac{2\pi}{E'b} \left[\frac{36L_C^2}{h^2} \int_0^{a/h} x F_1^2(x) dx + \int_0^{a/h} x F_{II}^2(x) dx \right] \\ C_{12} &= \frac{72\pi L_C}{E'bh^2} \left[\int_0^{a/h} x F_1^2(x) dx \right] = C_{21} \\ C_{22} &= \frac{72\pi}{E'bh^2} \left[\int_0^{a/h} x F_1^2(x) dx \right] \end{aligned} \right\} \quad (3.38)$$

Now, the overall flexibility matrix C_{ovl} is given by,

$$C_{ovl} = \begin{bmatrix} C_{11} & C_{12} \\ C_{21} & C_{22} \end{bmatrix} \quad (3.39)$$

3.6.5 Flexibility matrix C_{intact} of the intact beam element

$$C_{intact} = \begin{bmatrix} \frac{L_e^3}{3EI} & \frac{L_e^2}{2EI} \\ \frac{L_e^2}{2EI} & \frac{L_e}{EI} \end{bmatrix} \quad (3.40)$$

3.6.6 Total flexibility matrix C_{tot} of the cracked beam element

$$C_{total} = C_{intact} + C_{ovl} \quad (3.41)$$

$$C_{total} = \begin{bmatrix} \frac{L_e^3}{3EI} + C_{11} & \frac{L_e^2}{2EI} + C_{12} \\ \frac{L_e^2}{2EI} + C_{21} & \frac{L_e}{EI} + C_{22} \end{bmatrix}$$

ie. The Element stiffness matrix due to bending,

$$[K]_e = \int_0^L [B]^T [D][B] dx$$

$$\text{Or, } [K]_e = \frac{EI}{l^3} \begin{bmatrix} 12 & 6l & -12 & 6l \\ 6l & 4l^2 & -6l & 2l^2 \\ -12 & -6l & 12 & -6l \\ 6l & 2l^2 & -6l & 4l^2 \end{bmatrix} \quad (3.42)$$

The stiffness matrix K_{crack} or K_c of a cracked beam element: From equilibrium condition as in Figure 3.2.

Where,

$$L_e = \begin{pmatrix} -1 & 0 \\ L_e & -1 \\ 1 & 0 \\ 0 & 1 \end{pmatrix} \quad (3.43)$$

Hence the stiffness matrix K_{crack} or K_c of a cracked beam element can be obtained,

$$K_C = LC_{\text{total}}^{-1}L^T \quad (3.44)$$

The cracked element stiffness matrix becomes,

$$[K_e] = \frac{1}{C_{11}C_{22} - C_{12}C_{21}} \begin{bmatrix} C_{22} & (C_{22}L_e - C_{21}) & -C_{22} & C_{21} \\ (C_{22}L_e - C_{21}) & (C_{22}L_e^2 - C_{21}L_e - C_{12}L_e + C_{11}) & (-C_{22}L_e + C_{12}) & (-C_{21}L_e - C_{11}) \\ -C_{22} & (-C_{22}L_e + C_{21}) & C_{22} & -C_{21} \\ C_{12} & (C_{12}L_e - C_{11}) & -C_{12} & C_{11} \end{bmatrix} \quad (3.45)$$

Step-05: Introducing Boundary Conditions

Since two end sides of beam are fixed and no deformation will occur so $v_1 = \phi_1 = v_3 = \phi_3 = 0$. At that point there is no bending moment, shear force so the loading condition $F_1 = M_1 = F_3 = M_3 = 0$. We include a node at midlength because applied force and moment exist at the crown edge and at midlength. At this times, loads are assumed to be applied transversely at nodes. So, only the load applied in the middle portion and the bending moment M_2 and the cracked position of the beam will remain active. There are three faces present bounding the calculation domain which are thin Elastic Layer.

3.7 Conclusion

In this chapter we discussed the procedures of Finite Element Method for predicting the location and depth of a crack in a cantilever beam using experimental vibration data and to establish the mode shape curvatures. We began this chapter by developing the stiffness matrix for the bending of a beam element, the most common of all structural elements as evidenced by its prominence in constructional sector. The beam element is considered straight and have constant cross-sectional area. At first we derived the beam element stiffness matrix by using the principles that

developed for simple beam theory. Then we present simple beam element stiffness matrices and the solution of beam problems by the direct stiffness method. The solution of a beam problem illustrates that the degrees of freedom associated with a node are a transverse displacement and a rotation. We included the nodal shear forces and bending moments and the resulting shear forces and bending moment diagrams as part of the total solution. According to this procedures we get the global stiffness matrices for both cracked and uncracked beam. Finally, we discussed the procedure for handling distributed loading, because beams and frames are often subjected to distribute loading as well as concentrated nodal loading. The concepts presented in this chapter are prerequisite to understanding the concepts for frame analysis and simulation.

References

- [1] Kevin C. A., "Crack Depth Measurement In Reinforced Concrete Using Ultrasonic Techniques", Thesis Paper, *School of Civil and Environmental Engineering Georgia Institute of Technology*, May 2014.
- [2] Chondros ,T. G., Dimarogonas A. D., and J. Yao, "A continuous cracked beam vibration theory" , *Journal of Sound and Vibration* , Vol. 215(1), pp.17-34, 1998.
- [3] Rao S. D., Rao K.M., and Raju G.V., "Crack Identification on a Beam by Vibration Measurement And Wavelet Analysis", *International Journal of Engineering Science and Technology* , Vol. 2(5), pp. 907-912, 2010.
- [4] Ruotolo R, et al., "Harmonic analysis of the vibrations of a cantilevered beam with a closing crack", *Compute Struct*, Vol. 61(6), pp.1057–1074, 1996.
- [5] Sadettin O., "Analysis of free and forced vibration of a cracked cantilever beam", *NDT and E International*, Vol. 40, pp.43-450, 2007.
- [6] Larson M. G. and Bengzon F. "The Finite Element Method: Theory, Implementation and Practice " 2010, Cited by 46.
- [7] Liu W. and Barkey M. E., "Nonlinear vibrational response of a single edge cracked beam," *Journal of Mechanical Science and Technology*, Vol. 31, pp. 5231–5243, 2017.
- [8] Gere J.M. and Goodno B. J., *Mechanics of Materials*, 7th edition, Cengage Learning, OH, 2009.
- [9] Gounaris G., Papazoglou V. J., "Three-dimensional effects on the natural vibrations of cracked Timoshenko beams in water", *Computers and Structures*, Vol. 42(5), pp. 769-779, 1992.
- [10] Dimarogonas A.D., "Vibration of cracked structures: a state of the art review", *Engineering Fracture Mechanics*, Vol. 55, pp. 831-857, 1996
- [11] Priyadarshini A., "Identification of Cracks in Beams Using Vibrational Analysis", *Thesis Paper*, (2013), *Department of Civil Engineering*, National Institute of Technology, Rourkela.

CHAPTER IV

NUMERICAL SIMULATION, RESULTS AND DISCUSSION

CHAPTER IV

NUMERICAL SIMULATION, RESULTS AND DISCUSSION

4.1 Introduction

The concrete beam plays a vital role in real-world industrial construction and civil engineering activities. In many industrial and structural applications, crack is a normal phenomenon. Most of the structural failures are due to material fatigue, cracks present a significant challenge to the performance of structures. For this reason, in the last two decades, methods allowing early detection and localization of cracks have been the subject of intensive study [1]. In Chapter III, we presented a mathematical model based on the vibration-based approach approximation to get an in-depth understanding of vibration, beam deflection and their dynamic behavior.

Concrete structural components require an understanding of the responses to a number of loadings of these components. From both theoretical and computational approaches, there are a variety of methods to design concrete structures. Analysis of Finite Elements (FE) is a numerical analysis commonly applied to concrete structures focused on the use of materials' nonlinear behavior. FEA offers a method that can analyze the responses of concrete and pre-stressed concrete members and predict them [2].

The dynamics of the structure will change at each moment of passing the beam due to the position of the crack, which leads to the elements of both the mass and stiffness matrices being modified (or changed). However, when a crack is presented, the mass matrix elements will not be affected by the severity and location of the crack as much as the stiffness matrix elements will be affected at each time the location of the beam is changed. That is, in comparison to the stiffness matrix, which will be entirely different in its value when there is a crack or no crack, the mass

matrix will behave the same way if there is a crack or no crack during the crossing of the beam along the shaft.

In this chapter, we have analyzed the magnitude of frequencies, distribution of applied load, locations of crack and stress numerically. A numerical simulation using the Finite Element Method (FEM) has been done to determine the frequencies to detect the crack in the concrete beam. A vibration-based model is employed to simulate the results by using COMSOL Multiphysics. We also discussed about the deflection of the beams due to different amount of load.

4.2 Mathematical Modelling

During the last few decades vibration based crack detection methods are mostly used due to their simplicity for implementation. Most of the techniques are based on vibration measurement and analysis because the vibration based methods can offer an effective and convenient way to detect fatigue cracks in structures [3]. In this constant study we used vibration based method to identify crack in our considered domain. This approach is mainly based on changes in dynamic characteristics, such as natural frequency and crack position parameter.

The equation of motion in matrix form for vibration of a beam under load is given by [6],

$$[M] \left\{ \frac{d^2 q(x)}{dx^2} \right\} + [[K] - P[K_g]] \{q\} = 0 \quad (4.1)$$

Where,

$[M]$ = Consistent mass matrix

$[K]$ = Bending stiffness matrix of the beam

$[K_g]$ = Geometric stiffness matrix

$\{q\}$ = Displacement vector

P = External force vector

For free vibration the forcing function $P = 0$. So the Equation (4.1) can be written as,

$$[M] \left\{ \frac{d^2 q(x)}{dx^2} \right\} + [K] \{q\} = 0 \quad (4.2)$$

In-plane, the load $P(t)$ can be expressed in the form as shown below,

$$P(t) = P_s + P_t \cos \Omega t \quad (4.3)$$

Where,

P_s = the static portion of P .

P_t = the amplitude of the dynamic portion of P and

Ω = the frequency of excitation.

Equation (4.2) represents an eigen value problem and the roots of the equation give rise to square of the natural frequency given by the equation,

$$[K] - (\omega_n)^2 [M] = 0 \quad (4.4)$$

ie. The Element stiffness matrix due to bending,

$$[K]_e = \int_0^L [B]^T [D] [B] dx$$

$$[K]_e = \frac{EI}{l^3} \begin{bmatrix} 12 & 6l & -12 & 6l \\ 6l & 4l^2 & -6l & 2l^2 \\ -12 & -6l & 12 & -6l \\ 6l & 2l^2 & -6l & 4l^2 \end{bmatrix} \quad (4.5)$$

where,

$$L_e = \begin{pmatrix} -1 & 0 \\ L_e & -1 \\ 1 & 0 \\ 0 & 1 \end{pmatrix} \quad (4.6)$$

Hence the stiffness matrix K_{crack} or K_c of a cracked beam element can be obtained,

$$K_C = LC_{\text{total}}^{-1} L^T \quad (4.7)$$

The local stiffness matrix can be obtained by taking inverse of compliance matrix,
Defining the flexibility influence co-efficient C_{ij} per unit depth,

$$C_{ij} = \frac{\delta u_i}{\delta h} = \frac{\delta^2}{\delta P_i \delta P_i} \int_{-w/2}^{w/2} \int_0^{h_i} J_c(h) dh dz \quad (4.8)$$

where,

U_c = strain energy

$$J_c = \frac{\delta U_c}{\delta h} = \text{strain energy release rate.}$$

so that
$$u_i = \frac{\delta}{\delta P_i} \left[\int_0^{h_i} J_c(h) dh \right]$$

Using the value of strain energy release rate (J_c) we get,

$$C_{ij} = \frac{B}{E} = \frac{\delta^2}{\delta P_i \delta P_i} \int_0^{h_i} (K_{I1} + K_{I2})^2 dh$$

The local stiffness matrix can be obtained by taking inverse of compliance matrix,

$$[K] = \begin{bmatrix} K_{11} & K_{12} \\ K_{21} & K_{22} \end{bmatrix} = \begin{bmatrix} C_{11} & C_{12} \\ C_{21} & C_{22} \end{bmatrix}^{-1} \quad (4.9)$$

The stiffness matrix of first crack,
$$[K'] = \begin{bmatrix} C'_{11} & C'_{12} \\ C'_{21} & C'_{22} \end{bmatrix}^{-1} \quad (4.10)$$

The stiffness matrix of Second crack,
$$[K''] = \begin{bmatrix} C''_{22} & C''_{23} \\ C''_{32} & C''_{33} \end{bmatrix}^{-1} \quad (4.11)$$

The cracked element stiffness matrix becomes,

$$[K_e] = \frac{1}{C_{11}C_{22} - C_{12}C_{21}} \begin{bmatrix} C_{22} & (C_{22}L_e - C_{21}) & -C_{22} & C_{21} \\ (C_{22}L_e - C_{21}) & (C_{22}L_e^2 - C_{21}L_e - C_{12}L_e + C_{11}) & (-C_{22}L_e + C_{12}) & (-C_{21}L_e - C_{11}) \\ -C_{22} & (-C_{22}L_e + C_{21}) & C_{22} & -C_{21} \\ C_{12} & (C_{12}L_e - C_{11}) & -C_{12} & C_{11} \end{bmatrix} \quad (4.12)$$

4.2.1 Equation of free vibration

The natural frequency of the cracked beam can be evaluated using the crack model and boundary conditions. These equations can be written in compact form as,

$$[Q]\{A\} = \{0\} \quad (4.13)$$

Where $[Q]$ is the coefficient matrix defined in terms of the cracked beam parameters and A_i is the constants to be determined by the boundary conditions.

4.2.2 Boundary Conditions

Since two end sided of beam are fixed and no deformation will occur so $q_1 = \theta_1 = q_3 = \theta_3 = 0$. At that point there is no bending moment, shear force so the loading condition $F_1 = F_3 = M_1 = M_3 = 0$. Only the load applied in the middle portion, $F_2 = 500$ N and the bending moment M_2 and the cracked position of the beam will remain active.

There are three faces present bounding the calculation domain which are thin Elastic Layer (Boundary 6; see Appendix :Figure-iv).

$$\text{Symmetry thin Elastic Layer, } \mathbf{n} \cdot \mathbf{u} = 0 \quad (4.14)$$

$$\text{Outlet boundary, } -\rho\omega^2 u = \nabla \cdot \mathbf{S} + F_v e^{i\varphi} \quad (4.15)$$

4.3 Computational Domain and Mesh Design

A design of computational domain without crack and with crack are shown in Figure 4.1(a) and Figure 4.1(b). The computational domain is considered as a concrete beam with length 0.12m, width 0.015m and thickness 0.008m.

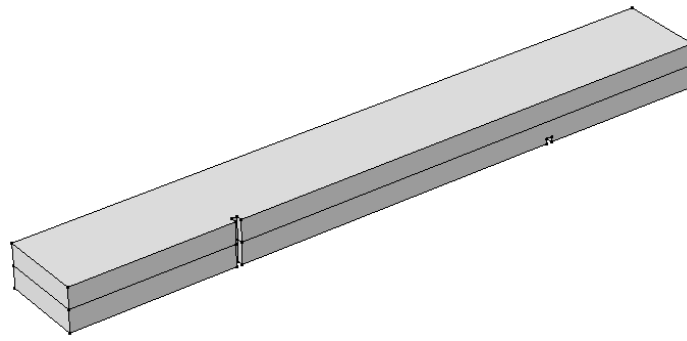


Figure 4.1(a): The geometry of the cracked computational domain

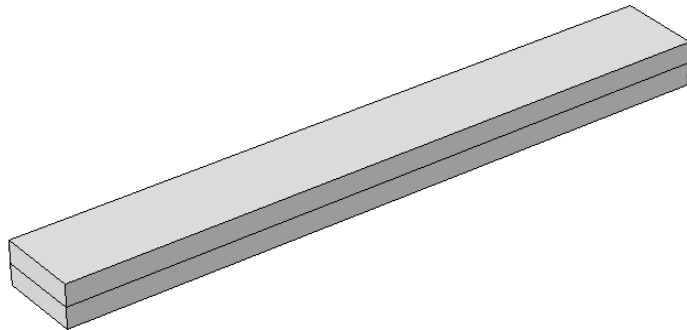
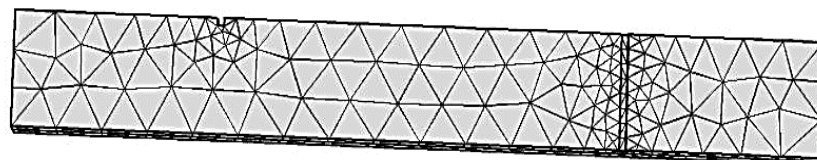
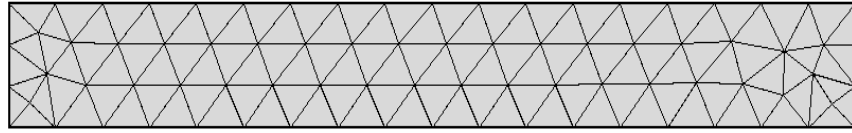


Figure 4.1(b): The geometry of the uncracked computational domain

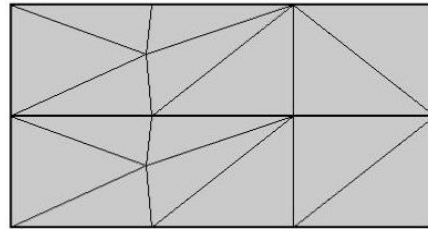
The geometry and a suitable mesh are generated by COMSOL Multiphysics Software are shown in Figure 4.2. To reach a satisfactory computational exactness we continually change the mesh design until the outcomes obtained. The Mesh element becomes higher near the cracked positions have shown in Figures 4.2 (a)-(c).



a) Along the cracked concrete beam



b) Along the uncracked concrete beam



c) Mesh design for the inlet boundary of the computational domain

Figure 4.2: Mesh design of The Computational Domain

The finite element mesh design for the computational domain (see Appendix Figure-vii) along the bar is shown in Figure 4.2 (a) and mesh design for inlet boundary is shown in Figure 4.2(b).

4.4 Simulation Results

The COMSOL Multiphysics has been used to simulate the load distribution and location of crack (see Appendix). We applied the load at the crown edge of the domain. Here concrete structural beam has been used to detect crack in its body. Because Concrete beams are the choice shape for structural builds because of their high functionality [4]. The shape of concrete beams makes them excellent for unidirectional bending parallel to the web. While the mesh and simulation properties of computational domain are shown in Table 4.1 and Table 4. 2.

Table 4.1: Mesh Properties of the computational domain

Description	Value
Minimum element quality	0.2093
Average element quality	0.6135
Tetrahedron	1424
Triangle	863
Edge element	232
Vertex element	32

Table 4.2: Properties of the simulation of computational domain

Description	Value
Number of degrees of freedom solved for	10093
Space dimension	3
Number of domains	1
Number of boundaries	23
Number of edges	52
Number of vertices	32
Space dimension	3

As our domain with defect is complicated thus computer processor capacity becomes a significant issue for the computational study. The finer mesh is used along the whole computational model for numerical simulation. We used 16 GB DDR3 RAM, Intel core i5 processor based computer for our simulation. The simulation was run for half an hour. We have analyzed the natural frequencies, stress, mode shape and the deformation of the body. In this part we also discuss about the deflection for different loads.

4.5. Numerical results and Discussions

In this study, we have investigated the frequency of the concrete beam containing double crack using Finite Element Method. For our simulation, we construct a solid concrete beam and have used different parameter values according to the Table 4.3 and Table 4.4.

Table 4.3: Properties of Domain

Description of Beam	Value
Length of the beam (L)	0.12m
Width of the beam (h)	0.015m
Thickness of the beam (H)	0.008m
Depth of First crack (D_1)	0.001m
Length of First crack (c_1l)	0.001m
Height of First crack (c_1h)	0.008m
Depth of the second crack (D_2)	0.017m
Length of second crack (c_2l)	0.001m
Height of second crack (c_2h)	0.001m

Table 4.4 Properties of Materials

Material Properties	Value
Density of concrete	1570 kg/m ³
Young's modulus	122.7 [GPa]
Poisson's ratio	0.2
Shear modulus	3.7 [GPa]
Tensile strength (σ)	2 – 5 Mpa
Shear strength (τ)	6 - 17 MPa

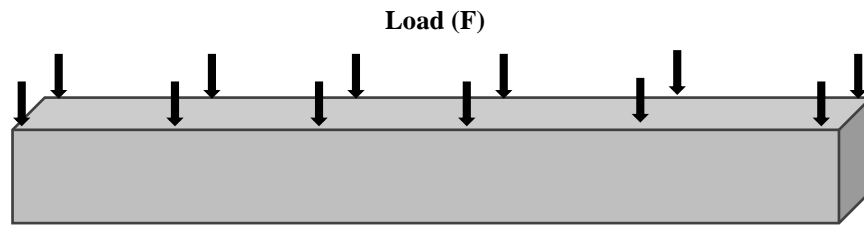


Figure 4.3: Applying load on the crown edge of the computational domain

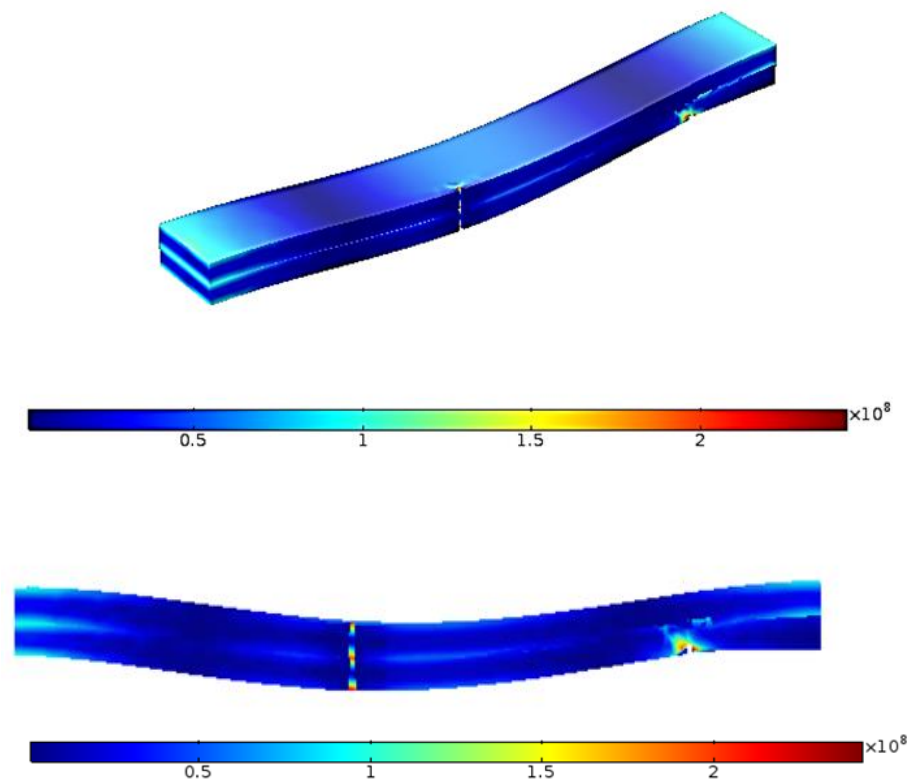
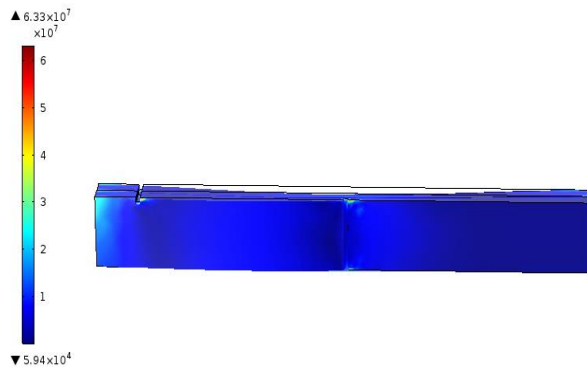
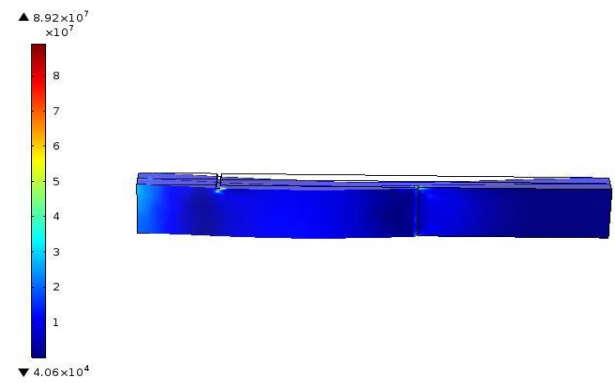


Figure 4.4: Deflection of the computational domain after applying load

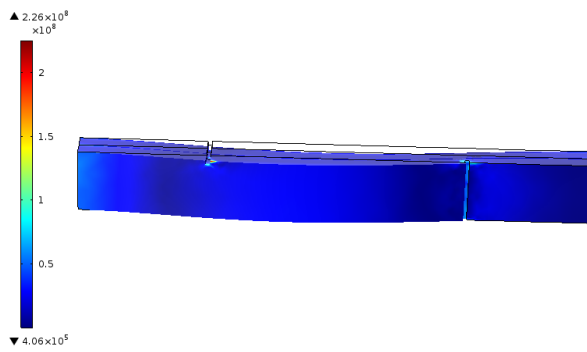
In Figure 4.3 it is shown that a load of 500 N is applied vertically on the top phase of the concrete beam. Figure 4.4 shows that the deflection and the phase of the computational domain after applying load. After applying the load, it is found that the load affects the body and frequency variability is observed essentially in the affected area [5].



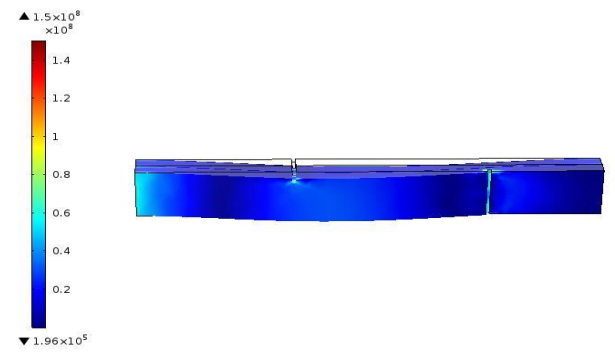
(a) The position of first crack is at 0.01m and second crack is at 0.06m



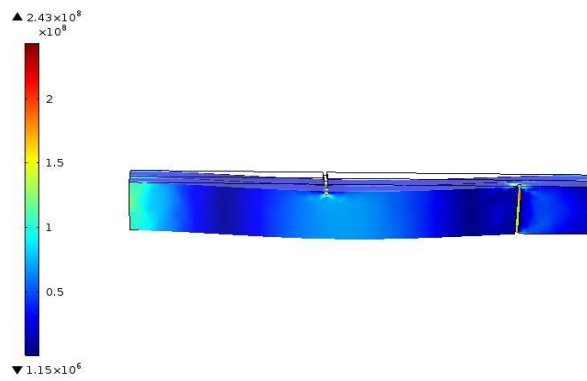
(b) The position of first crack is at 0.02m and second crack is at 0.07m



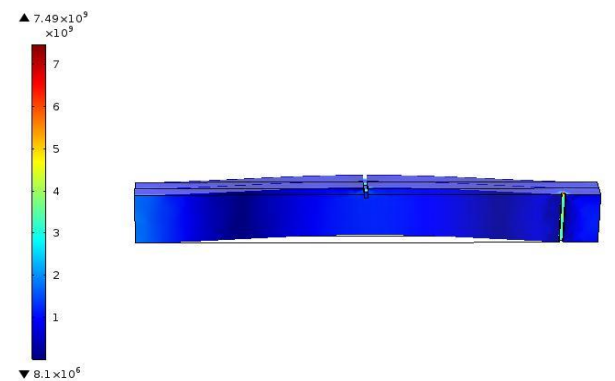
(c) The position of first crack is at 0.03m and second crack is at 0.08m



(d) The position of first crack is at 0.04m and second crack is at 0.09m



(e) The position of first crack is at 0.05m and second crack is at 0.10m

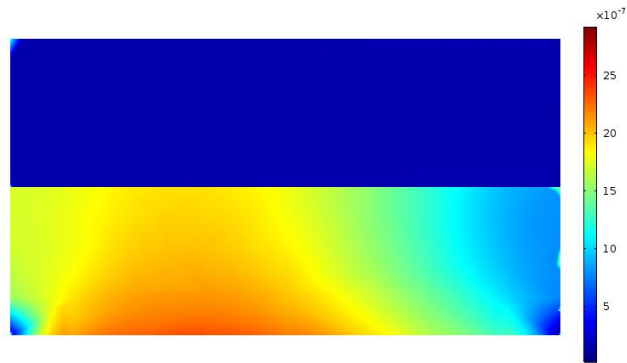


(f) The position of first crack is at 0.06m and second crack is at 0.11m

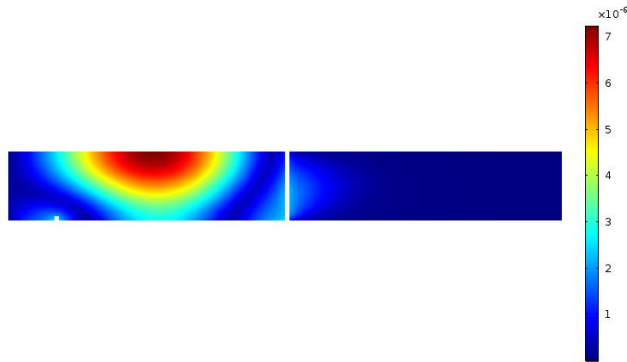
Figure 4.5: Load absorbs and Frequency gained in the respective crack position

The Figure 4.5 shown that different magnitudes of stress applied in the domain and corresponding deflection due to load. It is observed that, after applying load on the beam, a vibration on the structural body is created. The natural frequencies becomes maximum at the crack position due to the presence of vibration on that point. The maximum portion of load are absorbed in the middle part on the body, so there will be maximum absorption of load on that point. It is also noted that maximum load creates much vibration, which is the major causes to creating crack on any structural body.

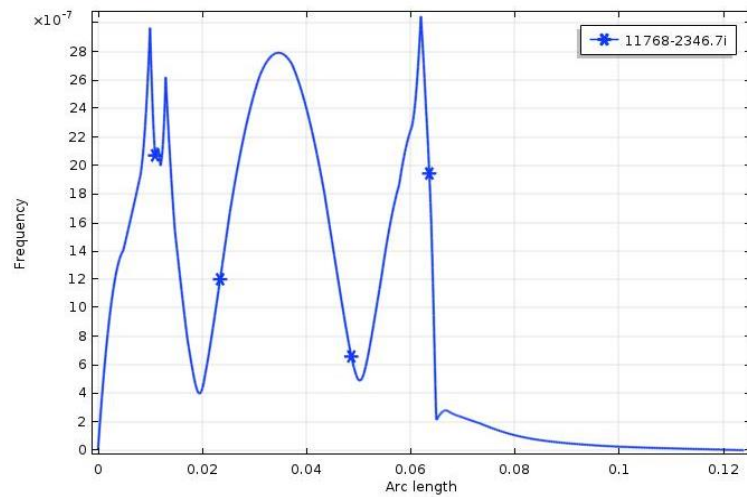
(i) The position of first crack is at 0.01m and second crack is at 0.06 m



(a) Slices of the load distributions at different position of crack



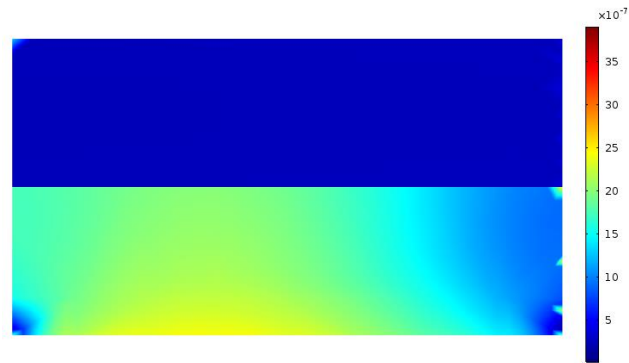
(b) Cross section of the load distributions at different position of the domain



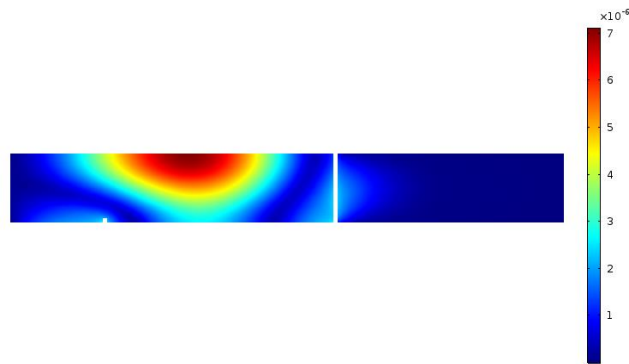
(c) Line graph of the relative position of crack v/s Frequency

Figure 4.6: Load distributions and Line graph of the computational domain where the position of first crack is at 0.01m and second crack is at 0.06 m

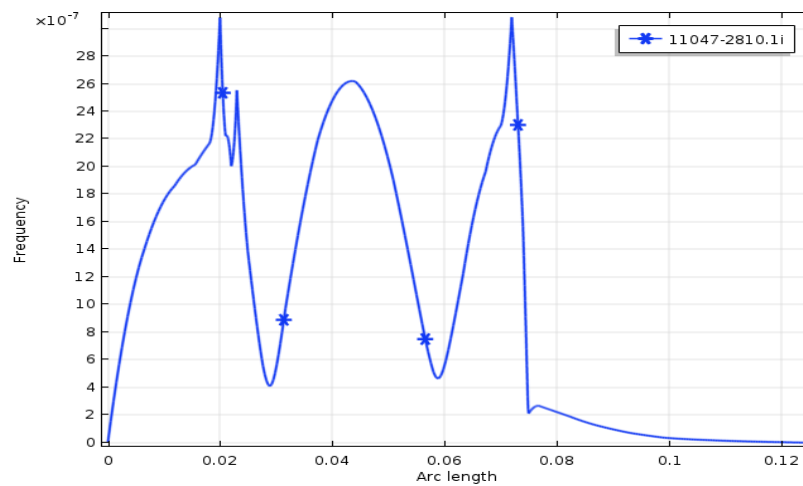
(ii) The position of first crack is at 0.02m and second crack is at 0.07 m



(a) Slices of the load distributions at different position of crack



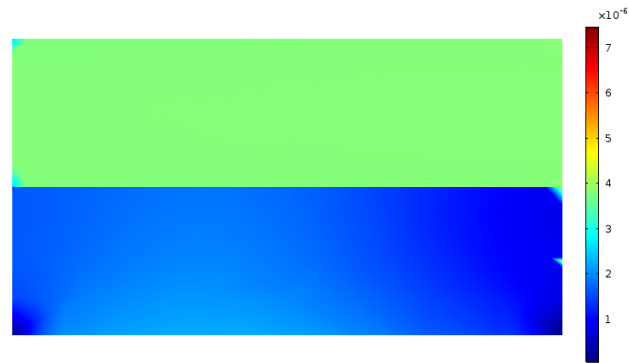
(b) Cross section of the load distributions at different position of the domain



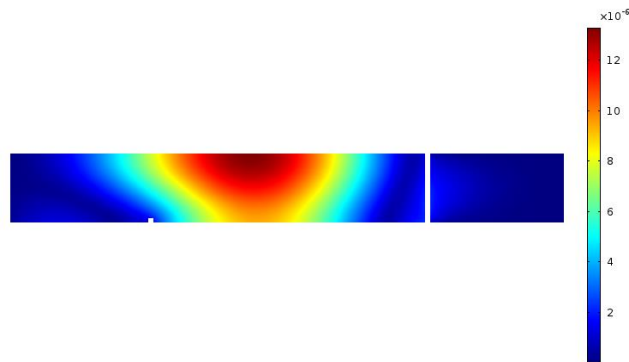
(c) Line graph of the relative position of crack v/s Frequency

Figure 4.7: Load distributions and Line graph of the computational domain where the position of first crack is at 0.02m and second crack is at 0.07 m

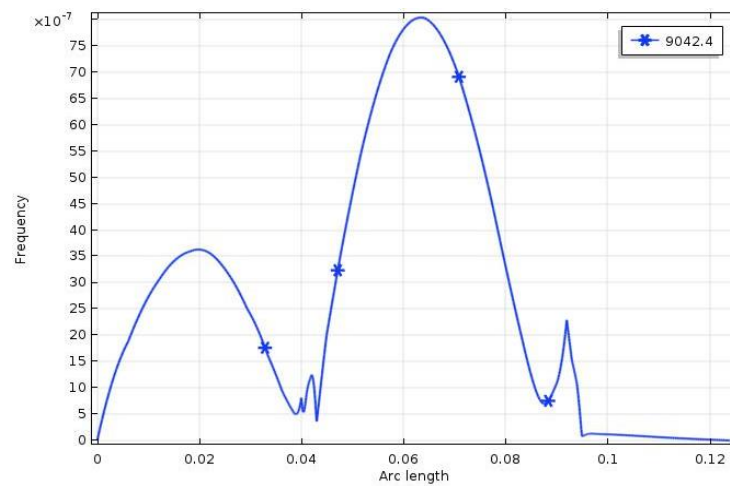
(iii) The position of first crack is at 0.03m and second crack is at 0.08 m



(a) Slices of the load distributions at different position of crack



(b) Cross section of the load distributions at different position of the domain



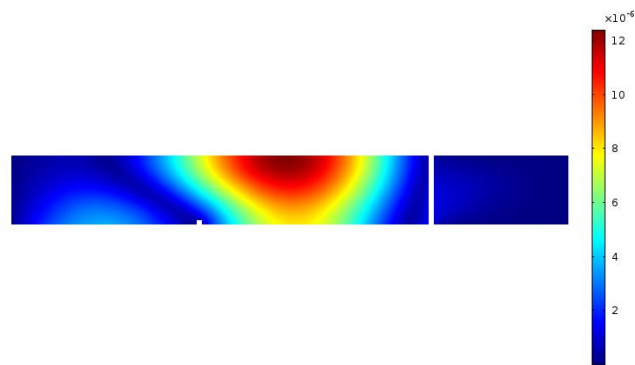
(c) Line graph of the relative position of crack v/s Frequency

Figure 4.8: Load distributions and Line graph of the computational domain where the position of first crack is at 0.03m and second crack is at 0.08 m

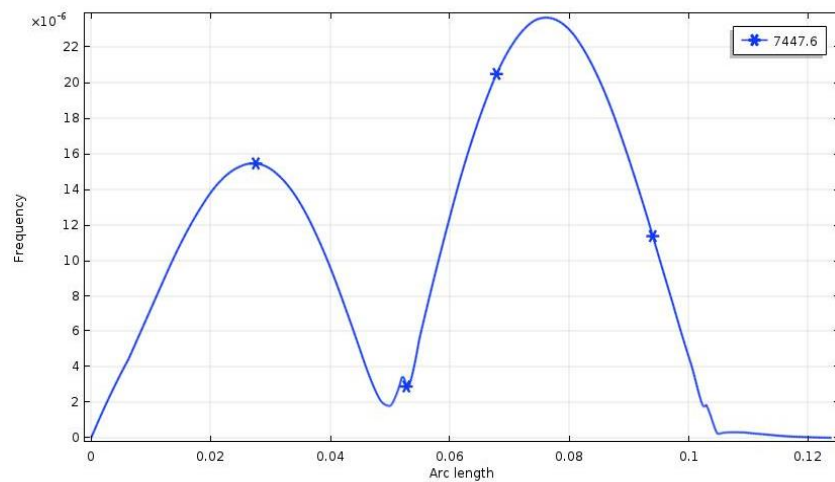
(iv) The position of first crack is at 0.04m and second crack is at 0.09 m



(a) Slices of the load distributions at different position of crack



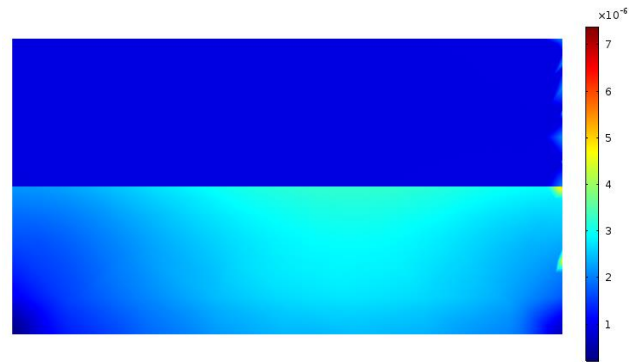
(b) Cross section of the load distributions at different position of the domain



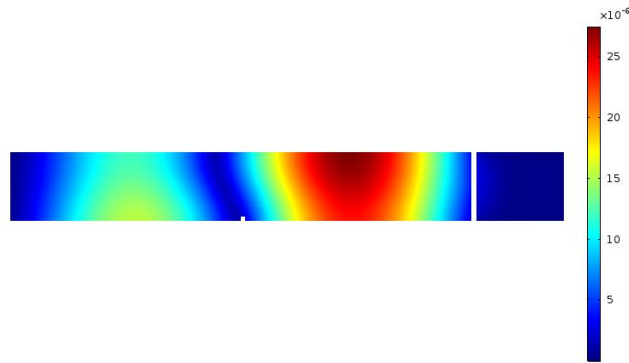
(c) Line graph of the relative position of crack v/s Frequency

Figure 4.9: Load distributions and Line graph of the computational domain where the position of first crack is at 0.04m and second crack is at 0.09 m

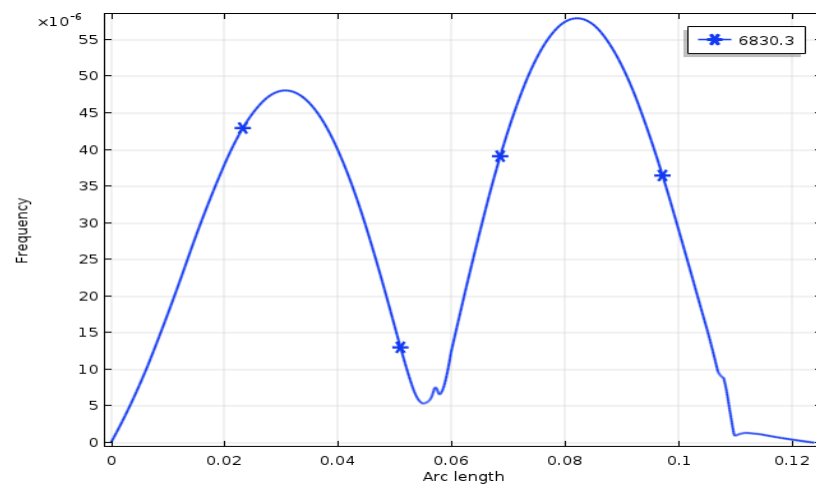
(v) The position of first crack is at 0.05m and second crack is at 0.10m



(a) Slices of the load distributions at different position of crack



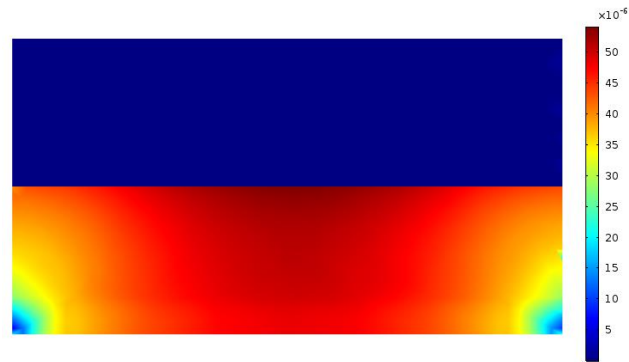
(b) Cross section of the load distributions at different position of the domain



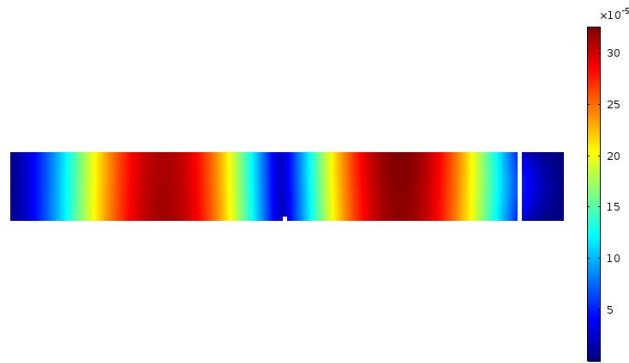
(c) Line graph of the relative position of crack v/s Frequency

Figure 4.10: Load distributions and Line graph of the computational domain where the position of first crack is at 0.05m and second crack is at 0.10m

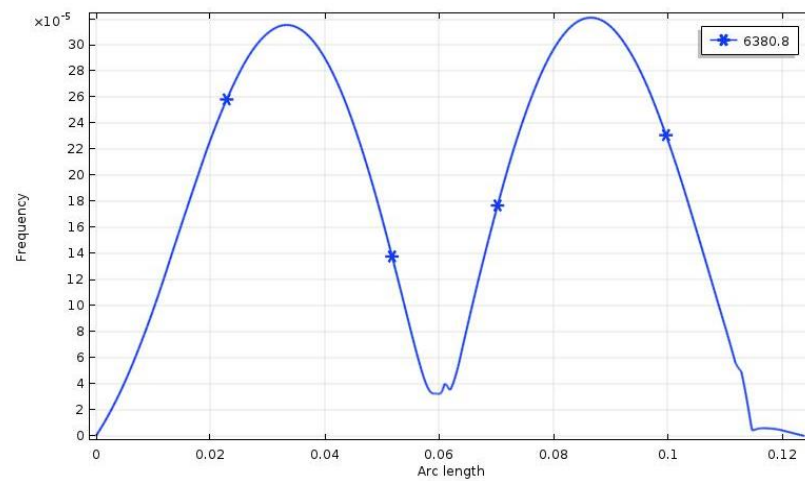
(vi) The position of first crack is at 0.06m and second crack is at 0.11m



(a) Slices of the load distributions at different position of crack



(b) Cross section of the load distributions at different position of the domain



(c) Line graph of the relative position of crack v/s Frequency

Figure 4.11: Load distributions and Line graph of the computational domain where the position of first crack is at 0.06m and second crack is at 0.11m

The Figure (4.6-4.11) shows that the slices and Cross section of the load distributions at different position of the domain and the line graph of frequency at the respective cracked position of crack.

We observed the load is maximum at the bottom of the domain. It is also found that the load was applied at the crown edge of the domain and distributed to bottom edge especially at the cracked position with high vibration and differs the frequency. But there is a difference is formed for the (f) that, after the load the beam distorted and deflected. So due to double deflection in this situation, the applied loads distributed into two end sides. Finally we observed that, at the cracked position vibration and frequencies are increased as the load increased and the presence of crack affects the natural frequency of the structure.

Comparing the frequency line graph at different position we observed that, the natural frequency graph shows irregularity at the crack positions. According to the graph Figure 4.6(c)-4.11(c) we found that, at the respective crack position the graph is fluctuated. So, we can say that at irregular of frequency curve identify the position of crack. It is also seen that as long as the crack changes its position (goes to end points) its frequencies are also increases gradually. Finally from the graph it is clear to us that natural frequencies of the beam is directly affected by the location of the cracks.

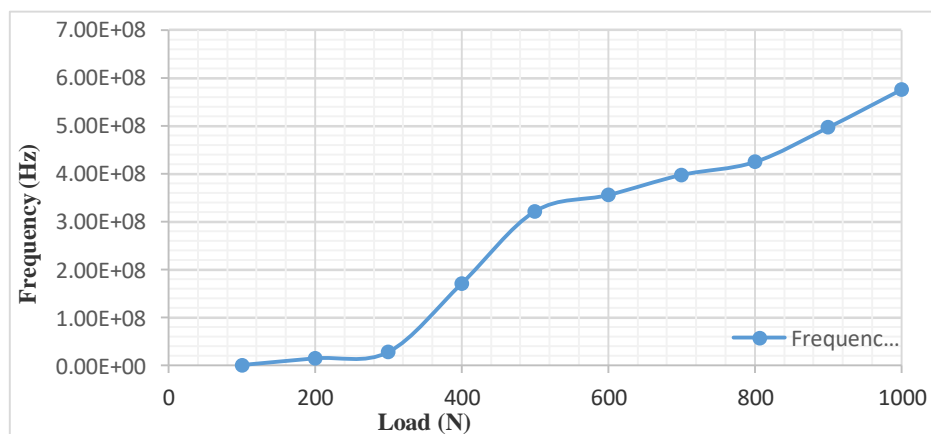


Figure 4.12: Line curve of Frequency vs Load

According to Figure 4.12, we find that, at a cracked point, the frequencies of beam increase proportionally to applied load. So, the changes of the natural frequency is directly influenced by the different location of the crack and applied loads.

4.6 Validation of the study

Table 4.5: Comparison among Priyadarshini , Kisa and Present Analysis

Serial no	Distance between cracks (m)	Crack position of first crack (m)	Crack position of second crack (m)	Priyadarshini A Frequency (Hz)	Kisa <i>et al.</i> Frequency (Hz)	Present analysis FEA Frequency (Hz)
1st	0.05	0.01	0.06	6465.83	6458.34	6356.1
2nd	0.05	0.02	0.07	6470.53	6457.4	6423.6
3rd	0.05	0.03	0.08	6465.81	6454.48	6485.5
4th	0.05	0.04	0.09	6451.41	6448.18	6442.3
5th	0.05	0.05	0.10	6397.71	6436.01	6398.3
6th	0.05	0.06	0.11	6211.68	6174.71	6233.2

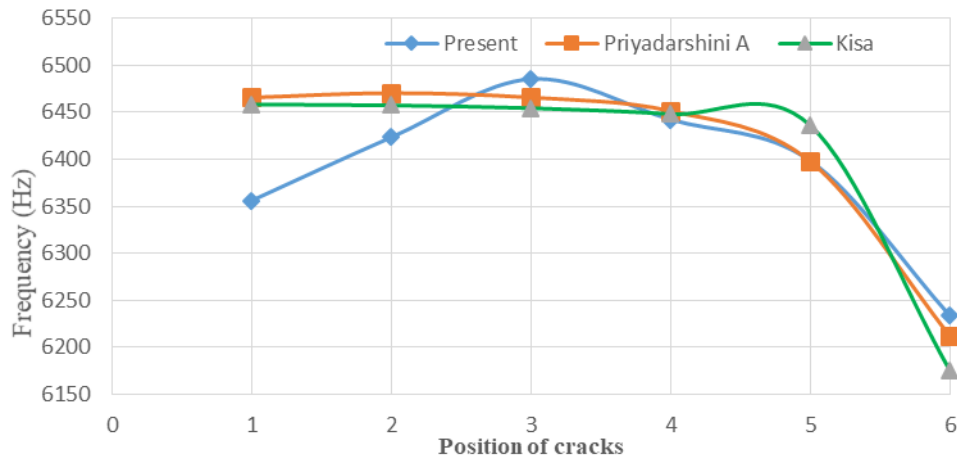


Figure 4.13: A Comparison of the frequencies in different positions of the crack of present analysis with Priyadarshini A[6] and Kisa et al.[7] experiments.

According to the Figure 4.13 it is observed that when the position of the crack moves from the fixed end towards the free end of the beam, the effect of the crack also decreases gradually. In order to check the accuracy of the present analysis, we tried to compare our experiment with the experiment done by Priyadarshini A [6] and Kisa et al. [7] the case is considered to validate the program. The presence and position of the crack are typically detected from the comparison of the basic modes of cracked beam. It should be mentioned here that they have used different models and different computational method for their experiments.

By comparing with the study of Priyadarshini A [6] and Kisa et al.[7] our results shows an agreement with their results though initially different approach for first two cracks. The analysis was performed on the first six mode shapes. Results of this research on the effectiveness of the damage detection technique applied to higher vibration modes lead to the conclusions that, in practical the presence of crack affects the natural frequency of the structure. The changes of the natural frequency is directly influenced by the different location of the crack.

4.7 Conclusion

The results of simulations and experiments of this study show that the considered beam enhances the small changes in the natural frequencies resulting from a crack. To explain physically why the concrete beam enhances the dynamics of a system at the crack location, first and foremost, it is necessary to know the physical meaning of modes, which are used as a simple and effective tool to characterize resonant vibration. It is essential to understand the accurate realistic behavior of cracked body phenomena to predict something in industry for proper production. In such case to get an approximation we need to solve some Initial and Boundary Value Problem by using a proper computational model with the help of computer. In this work, we developed a model and the simulation was done using the COMSOL Multiphysics Software [8].

We found that the magnitude of frequencies is higher at the cracked portion of the beam and lowest at the boundary of the domain. Modes are defined as inherent

material properties of a structure. In principle, the material properties (mass, stiffness and damping properties), and boundary conditions govern (or determine) the resonances of a structure during vibration. That is, a natural (or resonant) frequency, modal damping, and a mode shape are the intrinsic factors that define each mode. Thus, modes of a structure will change if either material properties or the boundary conditions of the structure change. We also observed the pressure and shear rate distribution of load. A linear pressure drop is found from the inlet to the outlet and the shear rate is decreased with a small fluctuation along the beam. There are different change in the behavior of the beam due to different locations of cracks.

References

- [1] Rao S. D., Rao K.M., and Raju G.V., "Crack Identification on a Beam by Vibration Measurement And Wavelet Analysis", *International Journal of Engineering Science and Technology*, Vol. 2(5), pp.907-912, 2010.
- [2] Subramani T., Manivannan R., Kavitha M, Subramani T., "Crack Identification in Reinforced Concrete Beams Using Ansys Software", *Int. Journal of Engineering Research and Applications*, ISSN : 2248-9622, Vol. 4(6), pp.133-141, 2014s.
- [3] Kocharla R. P. B., Bandlam R. K., Kuchibotla M.R., "Finite Element Modelling of a Turbine Blade to Study The Effect Of Multiple Cracks Using Modal Parameters", *Journal of Engineering Science and Technology*, Vol. 11(12), pp.1758 – 1770, 2016.
- [4] Jena P.C., Parhi D. R., Pohit G., "Theoretical, Numerical (FEM) and Experimental Analysis of composite cracked beams of different boundary conditions using vibration mode shape curvatures, *International Journal of Engineering and Technology (IJET)*, Vol 6 (2), pp.509-518,2014.
- [5] Hu H. and Cheng Y. F., "Modelling by Computational Fluid dynamics simulation of pipeline corrosion in CO₂-containing oil-water two phase flow," *Journal of Petroleum Science and Engineering*, Vol. 146, pp. 134-141, 2016.
- [6] Priyadarshini A., "Identification of Cracks in Beams Using Vibrational Analysis", *Thesis Paper*, (2013), *Department of Civil Engineering*, National, Institute of Technology, Rourkela.
- [7] Kisa M., Brandon J. and Topcu M., "Free vibration analysis of cracked beams by a combination of finite elements and component mode synthesis methods", *Computers and Structures*, Vol. 67, pp.215-223, 1998.
- [8] COMSOL Multiphysics Software. www.comsol.com.

CHAPTER V

CONCLUSIONS

CHAPTER V

CONCLUSION

The significant achievements and major conclusions of our work are summarized in this chapter and recommendations are given for future research in the field. In this work, we presented a mathematical model considering the natural frequencies by using the Finite Element Method based on a non-destructive method namely the vibration analysis method to detect the crack in the industrial application sector. We found that, the presence of crack affects the natural frequency of the structure distinctly. The changes in the natural frequency are directly influenced by the crack depth and crack location.

A vertical load about 500N applied on the crown edge of the domain and is considered to simulate the dynamical flow of load. The crack survey was performed on the computational domain is considered as a concrete beam with a length of 0.12m, width of 0.015m and thickness of 0.008m. The simulation has been running for 30 minutes using the COMSOL Multiphysics package. Relative natural frequency was calculated varying the crack locations. Finite element analysis in COMSOL was used to extract natural frequency and mode shapes of various end supports. The dynamic behavior including stress profiles, deformations, shear rates and load distributions at different times were investigated.

This thesis provides a correlation between cracking in beam, age and sustainability of beam structure and concrete properties. Also, the actual crack widths from the crack survey at different locations were compared. The load and cracking applications are complex phenomena and difficult to find a solution analytically. Due to many variables involved, sometimes it becomes difficult to point out one specific concrete property, mix design, construction practices or curing method that increased the likelihood of cracking, we depend on computational fluid

dynamics which uses different numerical methods. Out of those methods, the finite element method gives better approximation and so we have used the finite element method based on the non-destructive method to get a standard result. As the COMSOL Multi-Physics software is based on structural mechanisms, we used that software to validate our model.

In Chapter II, we have described a details overview of different types of cracks in structure, reasons of creating cracks, several types of crack detection methods specially focus on a non-descriptive method by using different modern tools. The functional and technical overview of deformation and load distribution is given detail. With some previous studies, some important computational methods and basic essential terminologies are also given.

Chapter III presents the development of a mathematical model for vibration of a beam under load. The equations are developed based on the Finite Element Method (FEM).

The details of our main studies are described in chapter IV. In this work, we present vibration analysis based model by considering the natural frequencies of the domain. The geometry of a real structure is complex. In my study, a simplified model of a subdomain of the concrete beam has been constructed. In view of the geometry's complexity, we used FEM to evaluate frequencies under load for better approximation. Using COMSOL Multiphysics Program, the simulation was carried out. We have investigated deflection, shear rate, load distribution, damage location and thickness of the cracks which are important to understand to increase the average life of any structural body.

From our simulation, the frequency and load were found higher at the cracked point of the domain. The presence and location of the crack have been detected from the comparison of the fundamental modes between the cracked and uncracked beam. The frequency of the cracked beam decreases with an increase in the crack depth for all modes of vibration. The shear stress and load distribution was

investigated for the entire domain and observed the shear rate decreases gradually with small fluctuations and maximum load absorbs in the fatigue points. Also the frequency line raises at the highest point at the cracked point.

On the basis of the model and the simulation the dynamic behavior of concrete beam the following conclusion can be made:

The model can be implemented to detect very small sizes (near 0.05 mm) hidden or visible crack in the structural beam and will provide us about the sustainability of a structural beam which plays a vital role in our daily life. The technique is also applicable to any linear structure that can be accurately modeled using the Finite Element Method.

SUGGESTIONS FOR FUTURE WORKS

In the present study, a mathematical model is developed to analyze the crack detection and structural health monitoring of a concrete beam is assumed for the computation. There are options to consider a Column Structure and different types of metallic bodies to our model and make a comparison of the behavior of the metal among them. One can also work by changing the geometry of the computational domain. With our current model, we intend to research steel and iron as a computational material by increasing parameters.

This method can be used extensively-

- to conduct periodic inspections for the automatic inspection of remote structure systems or for those operating under extreme conditions.
- to monitor crack growth, taking the initially undamaged structure as the foundation for further observations.

OUTPUT FROM THIS RESEARCH WORK

- [1] Rajib Karmaker¹ and Ujjwal Kumar Deb², **Crack Detection of Iron and Steel bar using Natural Frequencies: A CFD approach.** *3rd International Conference on Intelligent Computing & Optimization 2020 (ICO'2020)*, Proceedings published by SPRINGER, Hua Hin, Thailand. AISC 1324, Paper ID No.93, Chapter No: 23, pp. 1–13, 2021.
https://doi.org/10.1007/978-3-030-68154-8_23.

- [2] Karmaker R., Deb U.K. and Das A., **Modeling and Simulation of a Cracked Beam with Different Location Using FEM.** *Computational Water, Energy, and Environmental Engineering*, 9, 145-158, 2020.
<https://doi.org/10.4236/cweee.2020.94010> .

- [3] R Karmaker, M I Monir , S Das, U K Deb, **Comparison of Frequency and Deflection for Iron and Steel due to load: A Finite Element approach.** *21st International Mathematics Conference 2019*, Organized by Department of Applied Mathematics, University of Dhaka, Dhaka-1000, Bangladesh, pp. 33, 06-08 December, 2019.

APPENDIX

APPENDIX

CONSTRUCTION OF THE COMPUTATIONAL MODEL

To study the dynamic behavior of a concrete beam, we created a computational model in COMSOL Multiphysics for our simulation. At first the geometry of the domain is constructed which is a rectangular beam of 0.12 m length, 0.015m width and 0.008 m height.

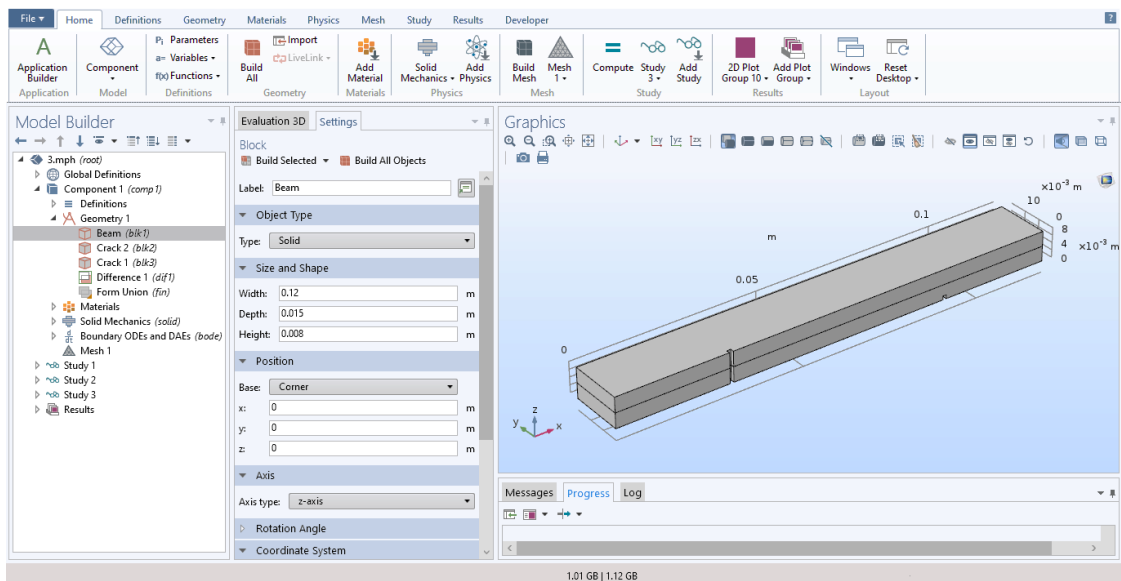


Figure i: Geometry of Computational domain

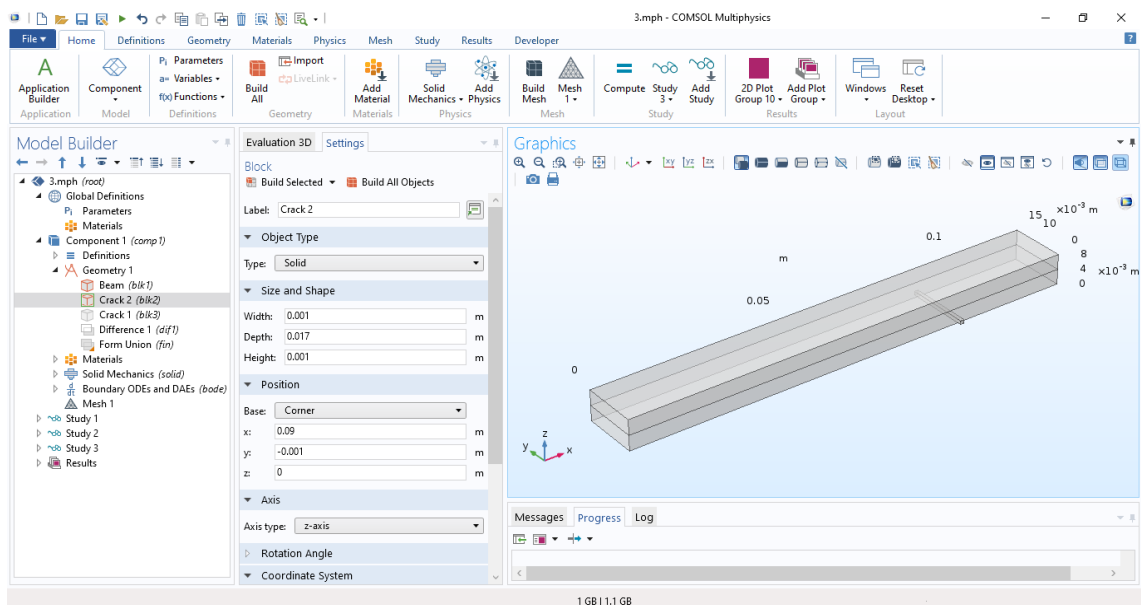


Figure ii: Internal Geometry of Computational Domain

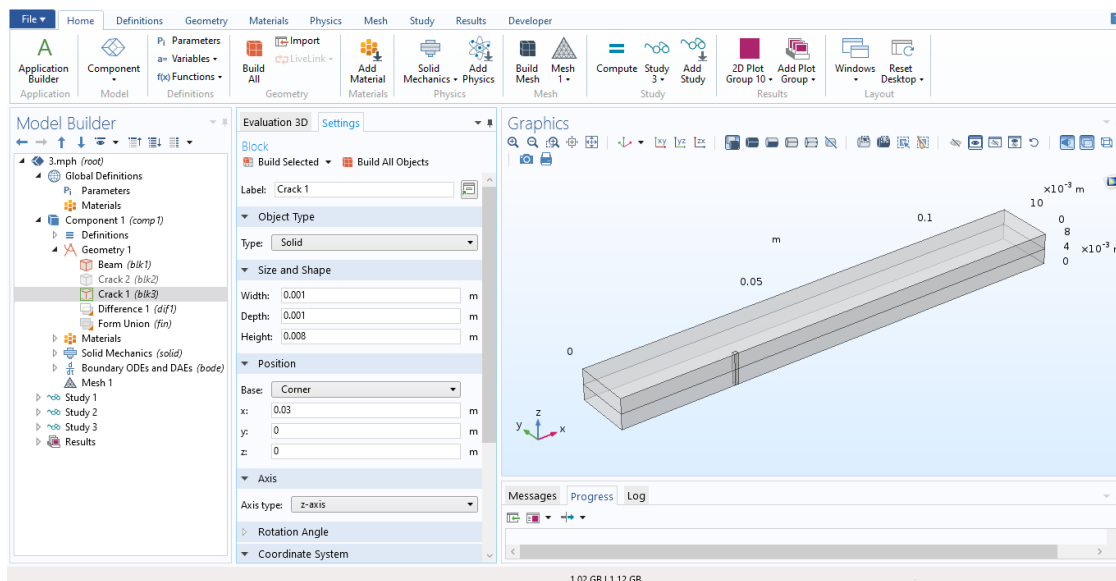


Figure iii: Internal Geometry of Computational Domain

Then input the materials by right clicking the materials icon and left click to the desired materials. It is repeated for two or more materials and rename the materials as needed. Then input the basic properties of the materials. Here the materials are concrete and iron.

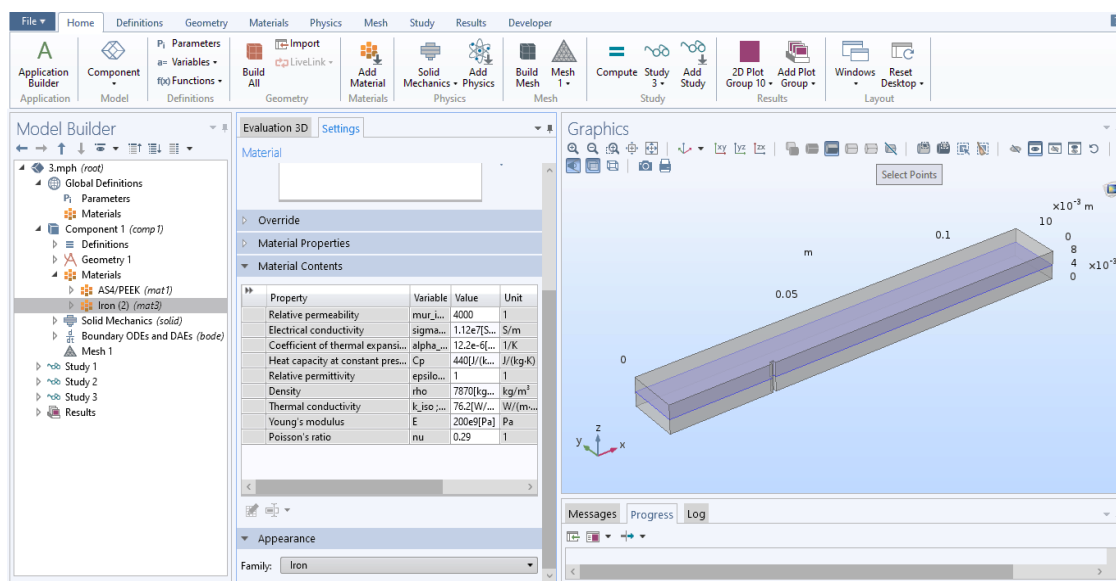


Figure iv: Inlet layer of Computational Domain

After that click on the Solid Mechanics, Load on edge and put the required data value in structural properties and initial value sections After completing those steps, the boundary conditions are set up for wall, inlet and outlet portion respectively. Then the load are applied vertically on the crown edge of the domain.

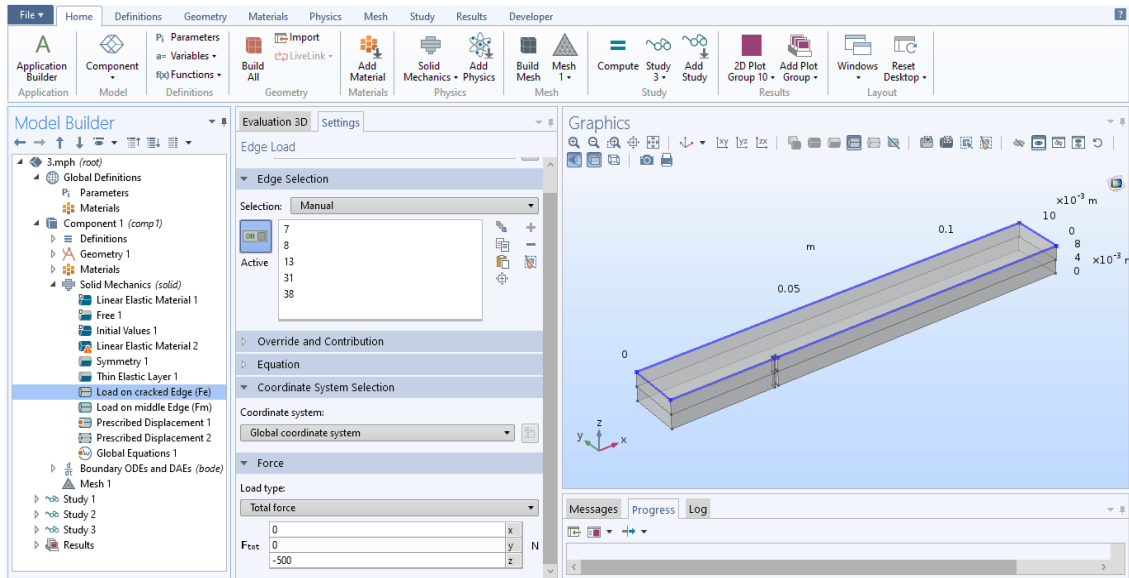


Figure v: Selection of crown edge of Computational Domain

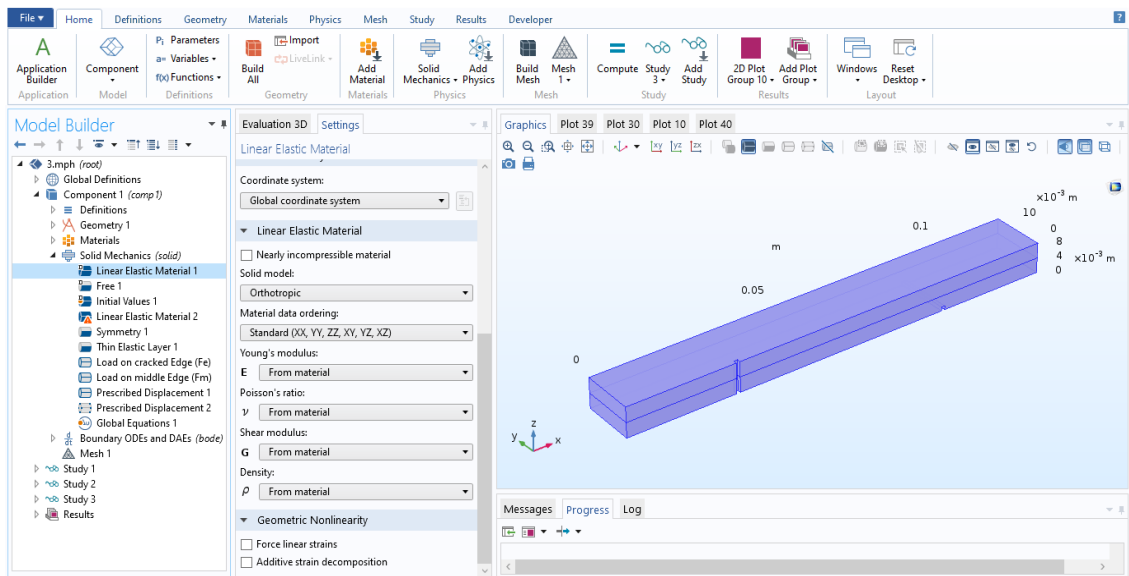


Figure vi: Selection of elastic layer in Computational Domain

After completing the above steps, it is essential to design the mesh of the domain which may be physics controlled or user defined.

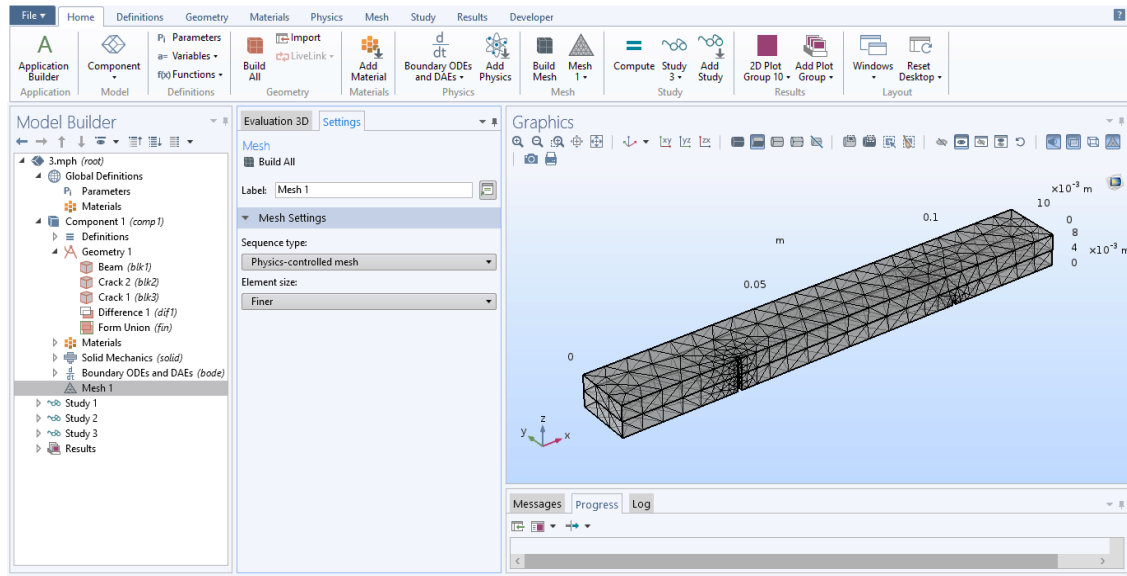


Figure vii: Meshing

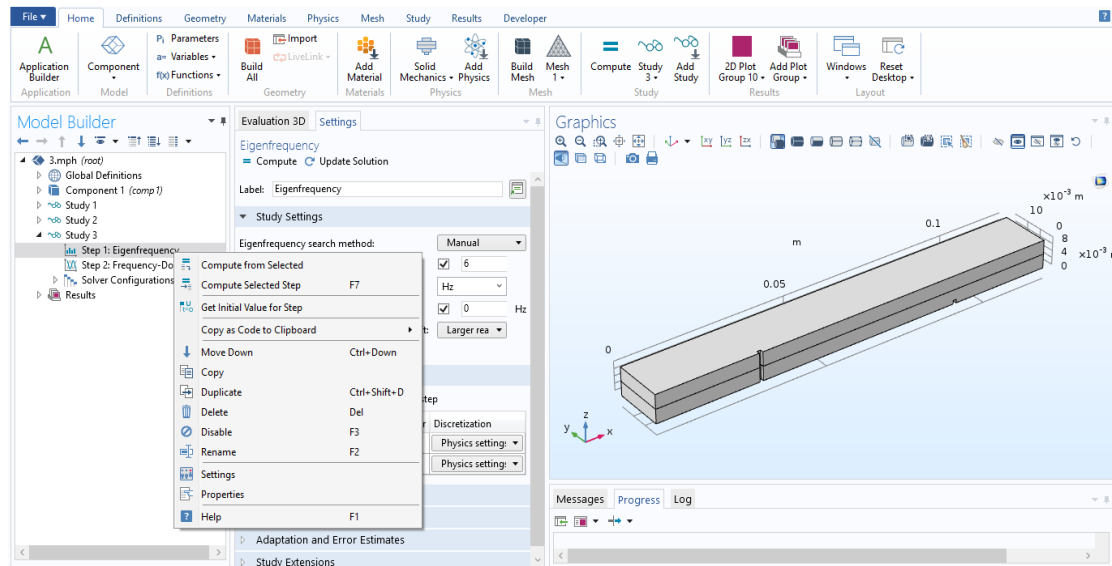


Figure viii: Selection of Eigen frequency

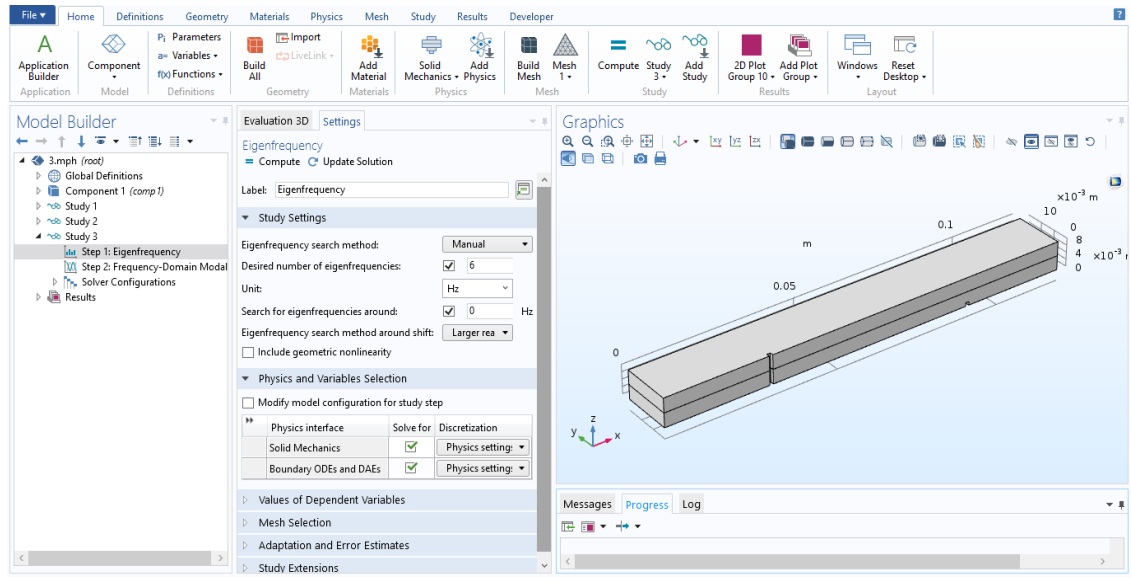


Figure ix: Selection of Eigan frequency modal

Now its time to place the time range and relative tolerance in time dependent portion in study 2 for the computation and click on the compute button.

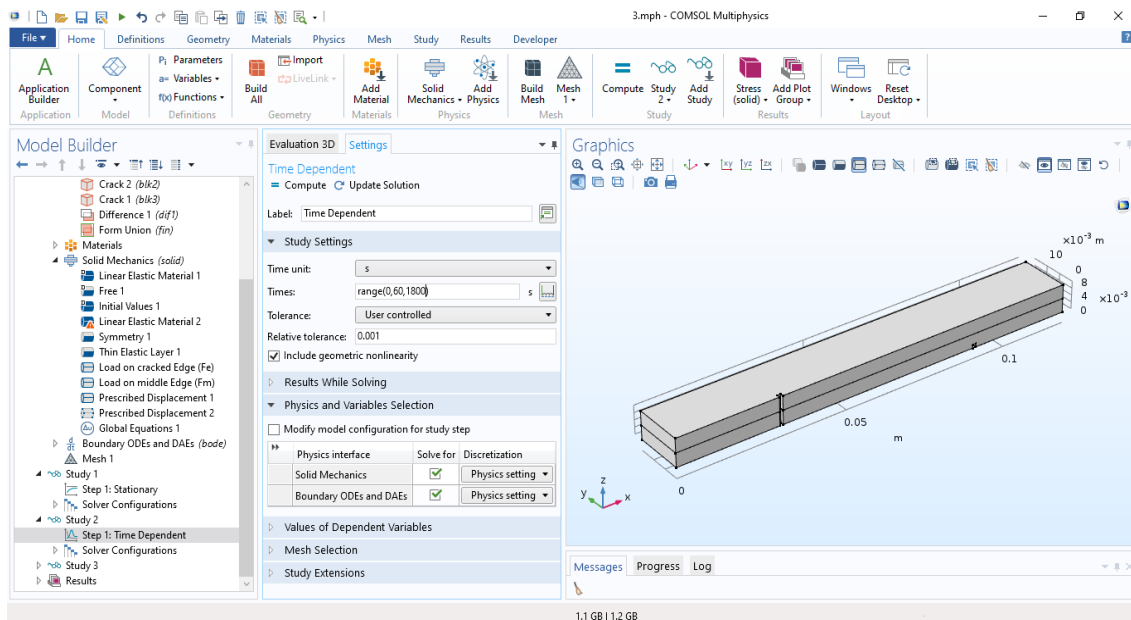


Figure x:Time selection of simulation

Therefore, we have got our expected results after computing the simulation successfully for the specified time.

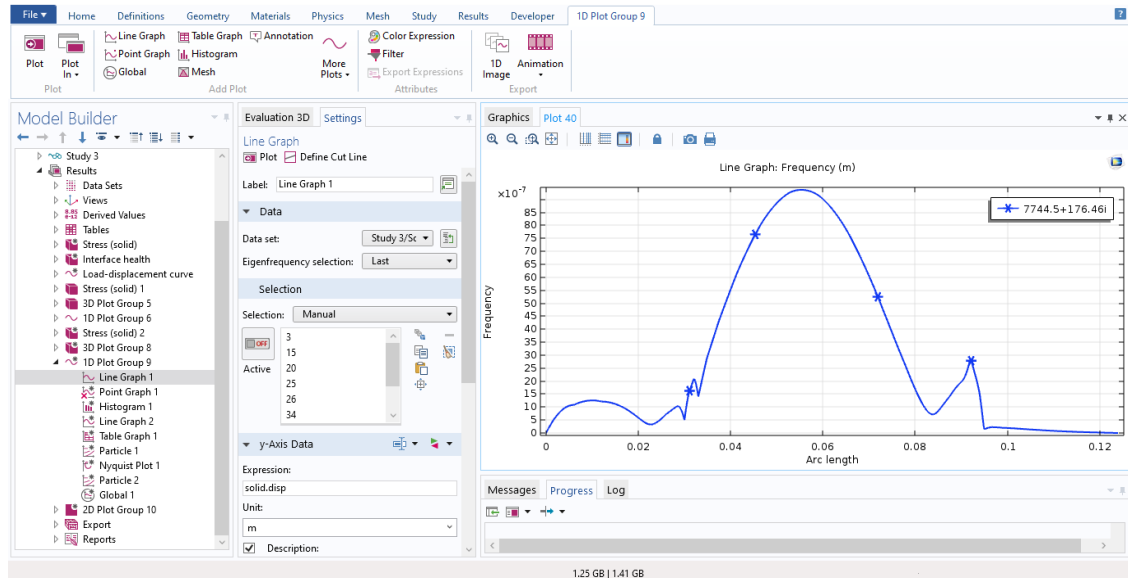


Figure xi: Line graph of the relative position of crack v/s Frequency

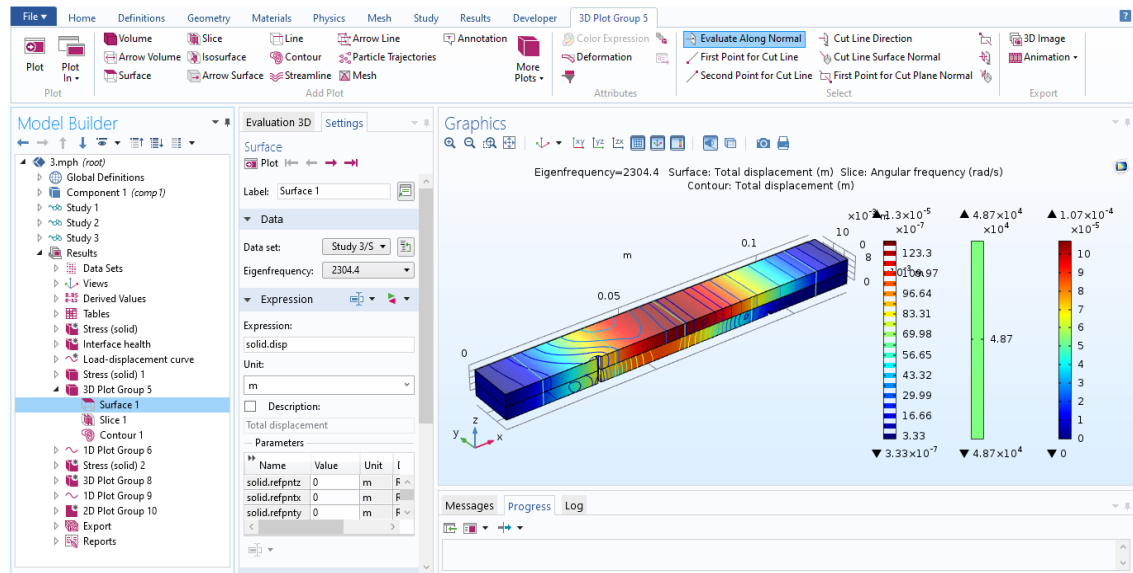


Figure xii: Contour Graph

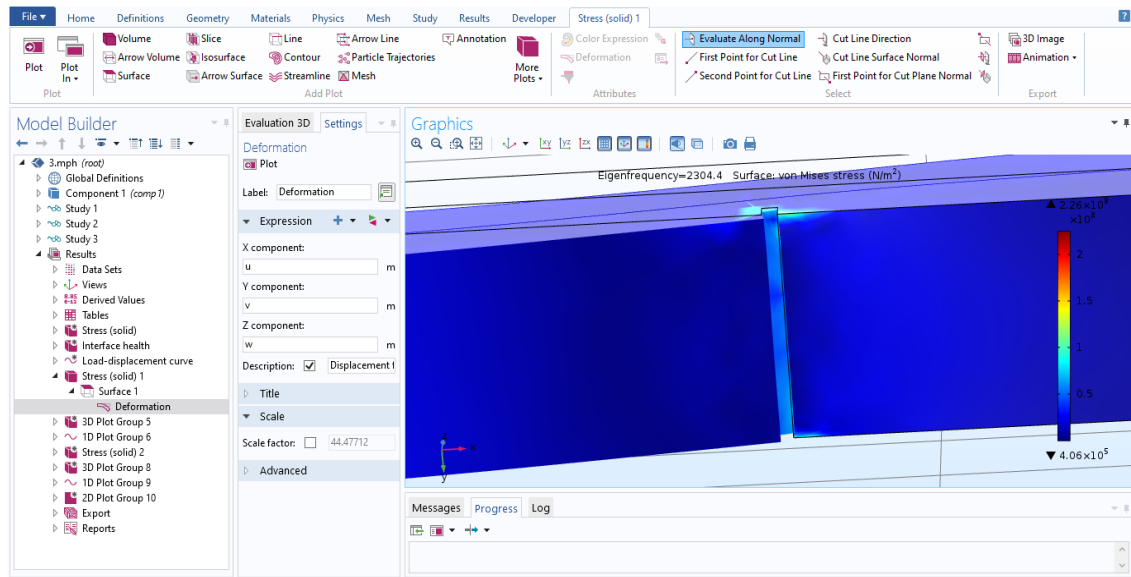


Figure xiii: Load on Horizontal Crack

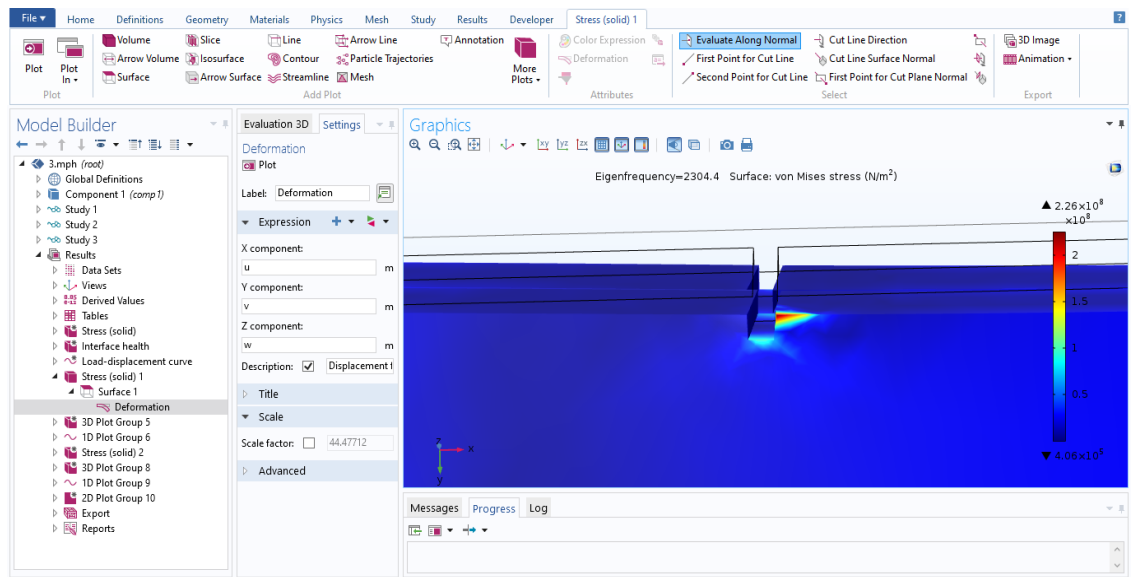


Figure xiv: Load on Vertical Crack

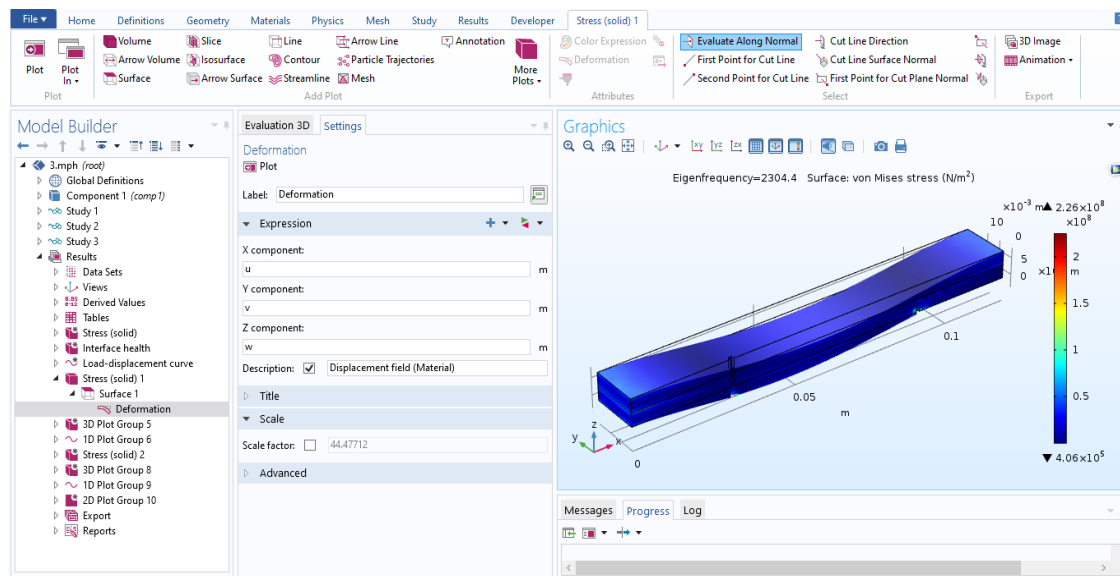


Figure xv: Deformation of Domain after applying transverse load

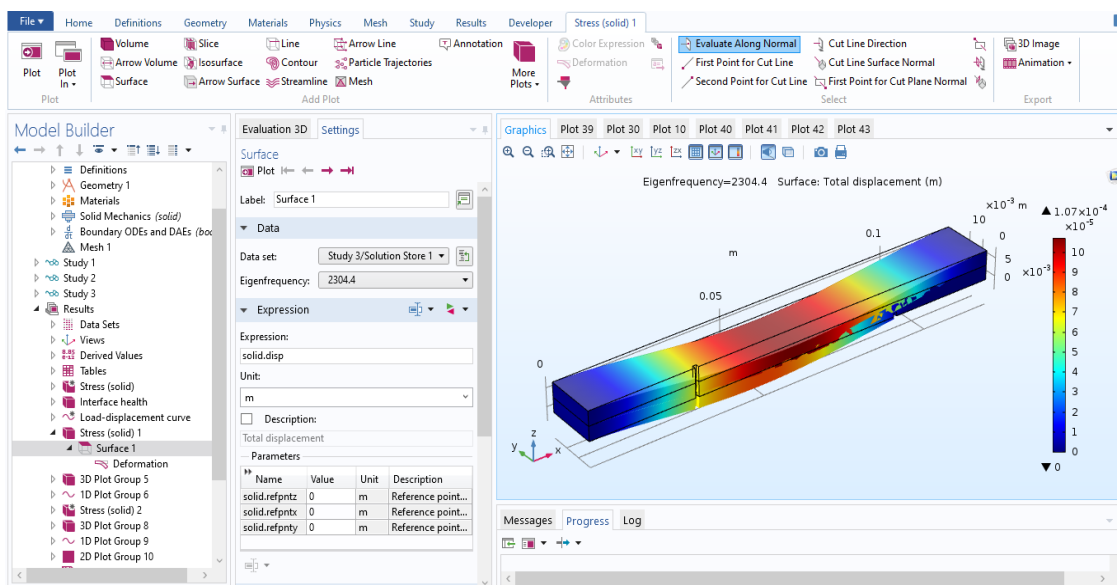


Figure xvi: Deflection of beam with load absorbtion

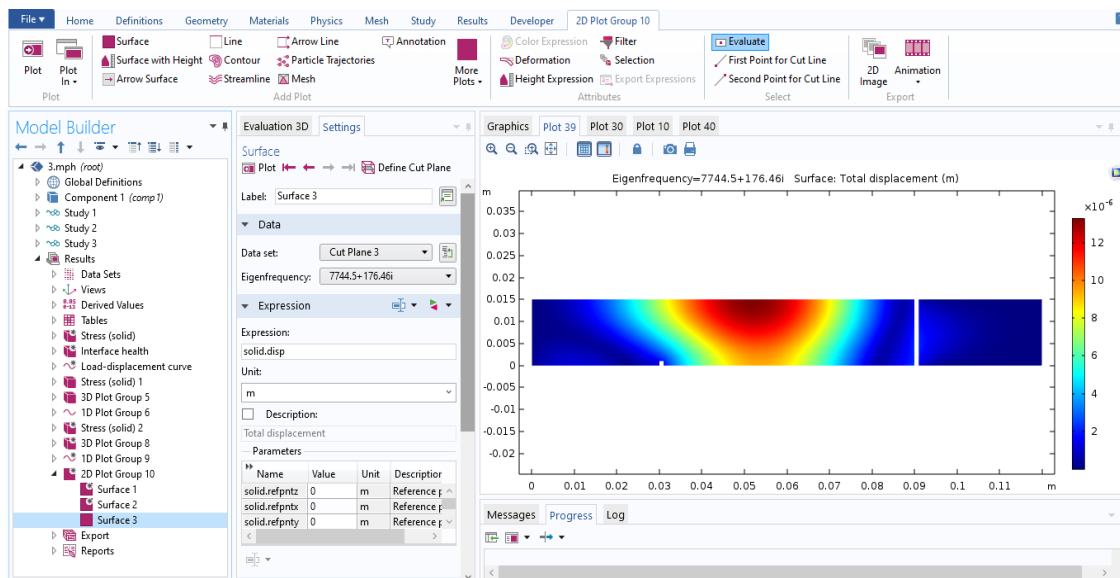


Figure xvii: Cross section of the load distributions at different position of the domain

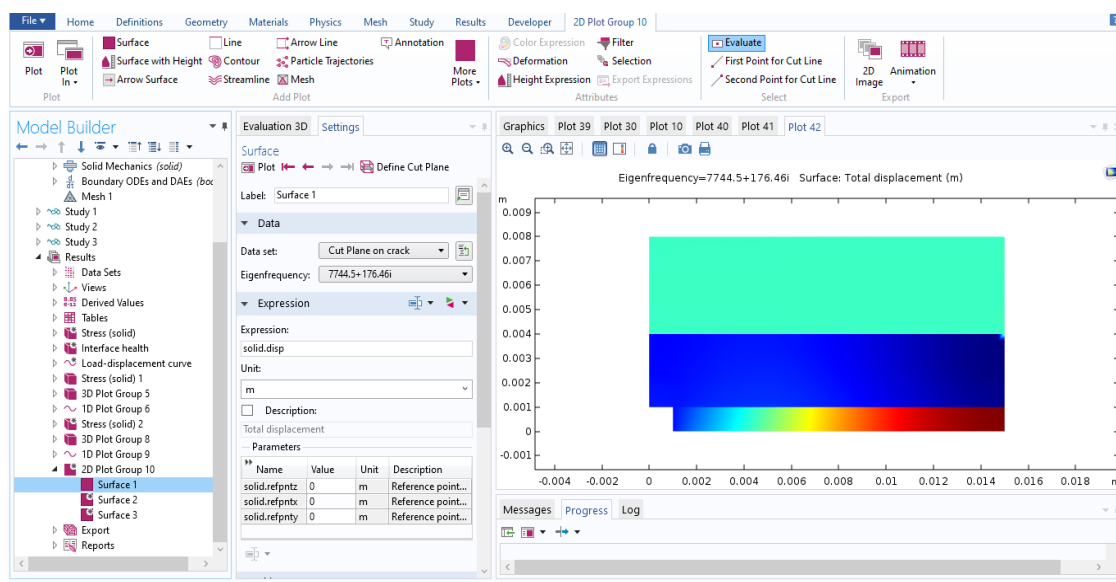


Figure xviii: Slices of the load distributions at different position of crack